Modelling the Influence of Vegetation, Soil Moisture and Aerosols on Early Summer Southern African Climate

Report to the
WATER RESEARCH COMMISSION

by

Mark Tadross
Igor Oliveira, Marshall Mdoka,
Fiona Tummon, Genito Maure,
Neil MacKellar, Babatunde Abiodun,
Nana Browne, Oliver Crespo,
Sepo Hachigonta, Bruce Hewitson

Department of Environmental and Geographical Science,
University Of Cape Town

WRC Report No. 1681/1/10
ISBN 978-1-77005-976-4

MAY 2010

DISCLAIMER

This report has been reviewed by the Water Research Commission (WRC) and approved for publication. Approval does not signify that the contents necessarily reflect the views and policies of the WRC, nor does mention of trade names or commercial products constitute endorsement or recommendation for use.

Executive summary

Background

This project focussed on the links between early season (September-January) rainfall and local antecedent conditions of vegetation, soil moisture and atmospheric aerosols. The primary reasons for choosing these foci were: a) early season rainfall is hard to forecast, yet its interannual variability can have important impacts in many sectors; b) these antecedent conditions to date have received little attention and are currently assumed to have a small influence on forecasts at a range of timescales.

The majority of the project has focussed on using Regional Climate Models (RCMs) to simulate the impact of changes in these antecedent conditions on rainfall. Given this is a computationally demanding task and that it was necessary to use several different RCMs (due to structural constraints some RCMs cannot be used for simulating particular changes), the modelling requirements of this project were high and took up the majority of the available time and work. The RCMs used in this work include the Weather Research and Forecasting (WRF) model, the Mesoscale Model 5 (MM5) and the Regional Climate Model 3 (RegCM3).

Modelling experiments

Even though there existed extensive demands in undertaking the RCM experiments, several key experiments were performed, each of which required time-consuming preparation of the models and boundary conditions. The experiments consisted of the following:

- Simulating the effect of changing land surface parameterisations (LAI, minimum stomatal resistance, soil porosity and soil wilting point) for a domain over South Africa using WRF. This work was undertaken in collaboration with IBM, USA, using grid computing;
- Simulating changes in vegetation fraction over southern Africa using WRF;
- Simulating the effect of changing land use over southern Africa using MM5;
- The indirect effects of biomass burning on southern African regional climate using WRF-Chem;
- The direct effects of biomass burning and dust aerosols on southern African climate using RegCM3
- The effect of soil moisture perturbations on southern African climate using RegCM3

Some of these simulations required high end computing facilities which were supplied by the new Centre for High Performance Computing (CHPC); the WRF fractional vegetation change was run at 15km for the period 2000-2006, and the indirect effects of biomass burning aerosols using WRF-Chem required the computing facilities of the CHPC even when simulating only short periods of 3 months at 50km resolution (due to extensive atmospheric chemistry calculations).

Primary findings and experimental results

All the experiments demonstrated that changes in antecedent conditions affected rainfall as well as other aspects of surface climate, particularly surface temperature. The main findings can be summarised as:

- Soil moisture perturbations affect the atmospheric boundary layer, more so in early spring than later in summer. Dry/wet soil moisture conditions have positive feedbacks with similar (wet/dry) synoptic forcing of the regional climate. These experiments indicate that a dry synoptic forcing persists for longer and promotes a larger change in the regional circulation; a dry soil surface induces an anticyclonic atmospheric circulation anomaly which has a positive feedback when the synoptic forcing is similarly anticyclonic;

- Interannual changes in vegetation also have a larger effect (increased variability) on atmospheric conditions when the synoptic forcing is for drier (anticyclonic) conditions.
- Moving from a natural to human influenced land surface induces an anomalous anticyclonic circulation, which promotes any similar synoptic forcing.
- The representation of vegetation in regional climate models is biased wrt observations and changing these parameters to be more realistic (e.g. reducing LAI) can reduce latent heat fluxes and the transfer of moisture to the atmosphere.
- Including the radiative effect of aerosols in the modelling of the regional climate during winter and early summer reduces incident shortwave radiation and consequent heating of the surface landmass. This and heating of the lower troposphere results in a more stable atmospheric vertical profile and induces an anomalous anticyclonic circulation.

In all experiments the resulting changes in rainfall are heterogeneous and tied to changes in the atmospheric circulation, rather than a direct consequence of changes in the local antecedent conditions. Changes in atmospheric circulation induce changes in convergence/divergence and consequently rainfall. Changes in surface temperature, however, were clearly tied to changes in latent/sensible heat fluxes with clear links to changes in surface properties and energy budget.

Implications for feedbacks between the local and regional climate

These experiments suggest that changes in soil moisture, vegetation and aerosols have positive feedbacks with the large scale circulation when they act in concert i.e. when the surface or aerosol changes induce anticyclonic circulations in the presence of large-scale anticyclonic circulations. It was more difficult to see a similar positive feedback between locally and large-scale induced cyclonic circulations, though this may be due to several factors:

- the experimental resolution and setup;
- RCM model biases;
- dominance of the large-scale circulation.

Even so these results suggest that these previously ignored components of the climate system contribute to the simulation of the local climate, and particularly extremes associated with drought and dry conditions. This observation is borne out by simulations during the early summer when anticyclonic circulations dominate the large-scale forcing and feedbacks with anticyclonic-inducing antecedent changes are often stronger. Given that climate change simulations from the Inter Governmental Panel on Climate Change suggest an increase in these large-scale circulations in a future climate, stronger feedbacks with these antecedent conditions are implied in the future, especially during early summer.

Implications for forecasting southern African climate

In parallel with these RCM experiments, seasonal forecasts using GCMs have been operationalised at CSAG. These forecasts use a range of GCMs, including HadAM3, HadAM3P (both from the UK Meteorological Office) and CAM (Community Atmospheric Model from the US). These forecasts are downscaled using a statistical downscaling technique which is conditioned on the large-scale synoptic circulation. In essence, the statistical downscaling associates a probability density function (PDF) of surface rainfall and temperature with each daily synoptic state or weather type.

The original suggested approach to forecasting using antecedent conditions was to use an Artificial Neural Network (ANN), however there was little time and human resources to pursue this approach. Furthermore the modelling results suggest that any forecasting scheme utilising antecedent conditions should account for the dependence of the resulting changes in climate on the large-scale circulation, i.e. the feedbacks highlighted from the modelling. The current forecast system, which uses the GCMs to forecast changes in the large-scale circulation and the statistical downscaling stochastically samples from the PDF of the response variable (rainfall and temperature), is one potential way forward for incorporating these antecedent conditions in a forecast system. The suggested approach would use the RCM simulated changes in the PDFs of the response variable (as simulated in the experiments conducted in this project) to perturb the PDFs used in the statistical downscaling. These perturbations would be different for each synoptic or weather archetype.

It still, however, remains to be seen if these changes in antecedent conditions will have an appreciable effect on forecasts. Whilst this work has shown that the effects are likely to be more easily observed during conditions of large-scale subsidence (anticyclonic circulation), there are still several factors which need to be considered. In particular, the residence time of any perturbation in antecedent conditions will vary:

- initial perturbations in soil moisture and vegetation are slowly evolving over weekly-monthly timescales and may prove useful for forecasting on these timescales;
- aerosol concentrations can change quickly and are to a large degree dependent on the large-scale circulation – potentially less so if the source is removed from the region.

Suggestions for further work

Given the findings of this project and the potential for improving climate forecasts several further avenues of exploration are considered potentially fruitful:

- Continue the current suite of modelling experiments, concentrating on the effects of these antecedent conditions on simulating the variability of the climate, particularly extremes and especially droughts. How do these antecedent conditions contribute to the frequency with which particular drought (or flood) thresholds are crossed?
- Further experiments to determine the primary factors which affect the residence time of aerosols in the atmosphere. How do the different aerosol components respond and contribute to the localised changes in circulation?
- Incorporate these factors into current seasonal forecasting schemes and climate change projections. In particular, when should these factors be considered and when can they be largely ignored.

The overarching goal of this work would be to improve current forecasting schemes and to lead to better forecasts which will benefit society at large.

Acknowledgements

The authors would like to thank the Reference Group for the assistance and the constructive discussions during the duration of the project. In particular we'd like to thank Professors Sue Walker and Roland Schulze, as well as Dr Warren Tennant for their help and encouragement.

This work would not have been possible without the computing support provided by the Centre for High Performance Computing and especially Chris Jack and Jeremy Main of the Climate Systems Analysis Group.

Dr S Adams	Water Research Commission (Chairman)
Dr R Dube	Water Research Commission
Prof H Rautenbach	University of Pretoria
Prof A Thomas	University of the Western Cape
Mr T Lumsden	University of KwaZulu-Natal
Dr M Tadross	University of Cape Town
Prof S Walker	University of the Free State
Dr J Olwoch	University of Pretoria

Table of contents

List of Figures

List of tables

List of abbreviations

AAO	ANTARCTIC OSCILLATION
AMIP	ATMOSPHERIC MODEL INTERCOMPARISON PROJECT
ANN	ARTIFICIAL NEURAL NETWORK
AOD	AEROSOL OPTICAL DEPTH
ARW	ADVANCED RESEARCH WRF
BATS	BIOSPHERE-ATMOSPHERE TRANSFER SCHEME
CAM3	COMMUNITY ATMOSPHERE MODEL
CCN	CLOUD CONDENSATION NUCLEI
CFCS	CHLORO FLUORO CARBONS
CHPC	CENTRE FOR HIGH PERFORMANCE COMPUTING
CLWP	CLOUD LIQUID WATER PATH
CNRS	CENTRE NATIONAL DE RESEARCHES SCIENTIFIQUE
CRU	CLIMATE RESEARCH UNIT
CSAG	CLIMATE SYSTEMS ANALYSIS GROUP
CSIR	CENTRE FOR SCIENTIFIC AND INDUSTRIAL RESEARCH
ECMWF	EUROPEAN CENTRE FOR MEDIUM RANGE WEATHER FORECASTING
ENSO	EL-NINO SOUTHERN OSCILLATION
ERA	EUROPEAN REANALYSIS
GCM	GENERAL CIRCULATION MODEL
GFED	GLOBAL FIRE EMISSIONS DATABASE
GPH	GEOPOTENTIAL HEIGHT
GVF	GREEN VEGETATION FRACTION
HADAM3	HADLEY CENTRE ATMOSPHERIC MODEL
KPP	KINETIC PRE PROCESSOR
LAI	LEAF AREA INDEX
LHFLUX	LATENT HEAT FLUX
LSM	LAND SURFACE MODEL
MADE	MODEL AEROSOL DYNAMICS FOR EUROPE
MAXSMC	MAXIMUM SOIL MOISTURE CONTENT
MM5	MESOSCALE MODEL 5
MRF	MEDIUM RANGE FORECASTING
NCAR	NATIONAL CENTRE FOR ATMOSPHERIC RESEARCH
NCEP	NATIONAL CENTRES FOR ENVIRONMENTAL PREDICTION
NDVI	NORMALISED DIFFERENCE VEGETATION INDEX
NMM	NON-HYDROSTATIC MESOSCALE MODEL
NOAH	LAND SURFACE SCHEME USED IN MM5
NPP	NET PRIMARY PRODUCTIVITY
NWP	NUMERICAL WEATHER PREDICTION
PBL	PLANETARY BOUNDARY LAYER
PDF	PROBABILITY DENSITY FUNCTION
PFT	PLANT FUNCTIONAL TYPE
PRECIP	PRECIPITATION
Q2M	2M SPECIFIC HUMIDITY
RCM	REGIONAL CLIMATE MODEL
REFSMS	REFERENCE SOIL MOISTURE STRESS
REGCM3	REGIONAL CLIMATE MODEL 3
RSMIN	MINIMUM STOMATAL RESISTANCE
SAWS	SOUTH AFRICAN WEATHER SERVICE
SDGVM	SHEFFIELD DYNAMIC GENERAL VEGETATION MODEL
SHFLUX	SENSIBLE HEAT FLUX
SOA	SECONDARY ORGANIC AEROSOLS
SOM	SELF ORGANISING MAP
SORGAM	SECONDARY ORGANIC AEROSOL MODEL
SST	SEA SURFACE TEMPERATURE
SSW	SURFACE SHORTWAVE RADIATION
T2M	2M SURFACE TEMPERATURE

UCT	UNIVERSITY OF CAPE TOWN
UKZN	UNIVERSITY OF KWAZULU-NATAL
USGS	UNITED STATES GEOLOGICAL SURVEY
WRF	WEATHER RESEARCH AND FORECASTING MODEL
WRF-CHEM	WEATHER RESEARCH AND FORECASTING MODEL WITH ATMOSPHERIC CHEMISTRY
WSI	WATER SATISFACTION INDEX
Z (GMT)	ZULU (GREENWICH MEAN TIME)

1 Introduction

The early part of the rainfall season is a critical period for water resources in South Africa. Initial rainfall and its characteristics (frequency and intensity) determine the saturation of soils, contribution to runoff, streamflow and farmers' preparations for planting. The time taken for soils to reach near-saturation determines the effective period before rainfall can be meaningfully harvested via dams and rivers, directly affecting the water available to metropolitan areas of South Africa. Crops (e.g. maize) are particularly vulnerable to the depletion of soil moisture during the early stages of the crop-growth cycle, which typically occurs during this critical period. It is the character of the climate (rainfall and temperature) that largely determines soil moisture levels e.g. infrequent, intense rainfall may lead to drier soils than frequent, light rainfall, mostly due to higher runoff and evaporation. Determining which antecedent conditions (e.g. local SST, vegetation, aerosols and pre-season soil moisture) contribute to these aspects of rainfall, during this crucial period, will enable a clearer understanding of factors affecting secondary impacts such as runoff and crop planting times.

Little is currently known regarding global and regional controls of the early part of the rainfall season. Tadross et al. (2005), with particular reference to the moisture required for growing maize, found that the start of the rains (onset) had been, on average, arriving later over South Africa since the mid-1970s. The largest changes in onset were over the coastal regions of KwaZulu-Natal and the Limpopo valley, with onset arriving as much as 47 days later in the late 1990s than in the mid 1970s. Positive 500 hPa geopotential height anomalies to the south-east, which promote the advection of moisture from the Indian Ocean, were found to be associated with early onset and El-Nino was suggested as a cause of late onset. Results noted by Reason et al. (2005), however, indicate that over the Limpopo region onset is inversely related to Nino3.5 SSTs, whereas further north over Zambia Hachigonta et al. (2008) found that early onset was dependent on ridging highs and moisture advection from the southeast, with ENSO impacts via the Pacific South America (PSA) pattern.

Together these results indicate that onset is at least partly controlled by large-scale atmospheric circulations. However, Tadross et al. (2005) also showed that before early onsets moisture is advected over the continent and pre-season soil moisture and land-surface characteristics (e.g. vegetation) play an as yet unquantified role. A study by Martiny et al. (2005) demonstrated relationships between annual rainfall during previous years and vegetation (as measured by NDVI) in the semi-arid region of the Karoo; positive (negative) rainfall anomalies leading to increased (decreased) vegetation. More recent work by Richard et al. (2008) suggests that these effects are detectable in the early summer (September – December) period, though the effect on rainfall is only detectable when rainfall and vegetation anomalies were negative.

It is clear therefore that an enhanced understanding of the controls of early-season rainfall characteristics are required to enable the design of new forecasting methodologies, which in turn may offer practical benefits to water managers and under-served members of the South African population e.g. subsistence farmers. New forecasting methodologies will require knowledge of which antecedent conditions (vegetation, aerosols, soil moisture and SST) are important and be able to use this information to predict early-season rainfall, given likely non-linear interactions. Such knowledge will also enable a clearer assessment of the impact of other human-induced changes (besides changing greenhouse gas levels), currently unknown factors in the development of scenarios of regional climate change.

1.1 Sectoral impacts of onset variability

Here we briefly summarise some of the impacts of changes in early season rainfall that have been noted. They are taken from the proceedings of an initial workshop held at the beginning of the project, a summary of the most pertinent information is provided in Appendix B.

1.1.1 Fire

Fire depends on a several factors including: density and composition of vegetation, canopy and soil moisture levels, as well as atmospheric winds, humidity, temperature and rainfall. Rainfall affects all these factors (perhaps with the exception of winds); vegetation is dependent on rainfall perhaps as much as 1 season – 1 year previously, soil and canopy moisture levels are directly impacted by rainfall, as is humidity and temperature (both influenced by the amount of soil moisture and consequent latent heat fluxes). Over the eastern rainfall regions of South Africa a delay in the onset of rains results in a longer dry season, which depletes soil moisture levels and results in heightened temperature levels at this, the hottest time of year. The result is a hotter and drier land surface that is more susceptible to the outbreak of fire.

1.1.2 Agriculture

Effects of early rains on agriculture are varied and are summarised for each agricultural sector.

Impacts on maize farming are dependent on location:

- *Highveld:* start of the rains is earlier in the east (October-December) with the potential to plant a short-season cultivar in January but too late if rains come after 10th January. Heat units are also important as is the frequency and intensity of the rainfall;
- *Lowveld:* if no frost can plant in September but too late after 10th January
- *Eastern seaboard:* earliest in September and latest end of December. Heat units are important when planting late;
- *Northwest:* plant later than rest of highveld (November-December) with latest being 10th January. Heavy storms are a problem for getting equipment into the field and creating large runoff. Farmers like to plant after 15th September when 2+ days of general rainfall occur.

Impacts on Sugar are mostly minimal as it is an irrigated crop and more dependent on rain at the end of the season for getting equipment etc. into the field

Impacts on livestock are related to fire i.e. when to move stock between winter and summer pastures. Angora goats are susceptible to wet and cold periods during winter (e.g. early rains), whereas other livestock can suffer heat stress due to a delay in the start of the rains

1.1.3 Water resources

Much of the interest in the start of the rains relates to the catchment management areas run by the Department of Water Affairs and Forestry. Whilst individual extreme years are important, many catchments can carry over water storage for 4-5 years. Changes in onset are then mostly important after long periods of drought when water resources reach critically low levels. Information on the coming start of the rainfall season is mostly useful for planning purposes and scheduling water releases etc.

1.1.4 Savanna ecosystems

Impacts of early season rainfall on savanna ecosystems depends on whether it is in an arid or moist (east of Thabazimbi) region:

- *Arid:* similar to water resources - not so important for indigenous plants and systems not providing resources. Savanna systems have on average 9 mm per event - moist savanna such as kruger. Potential importance for fire risk - dependent on biomass and fuel load
- *Moist:* need approximately 170 mm of moisture penetration in the soil (dry in 4-5 days) to define the start of the season. 400 mm of soil wetting dries in approximately 5-10 days but very dependent on the type of soil. Trees and grasses green at very different rates. Greenup of grass keeps getting higher to maximum in February. LAI in trees maximises earlier but doesn’t depend on the amount of rainfall.

1.2 Rationale for project

The rationale for this project is that regional antecedent conditions, especially of vegetation, soil moisture and aerosols, could alter the subsequent regional climate and that these antecedent conditions could provide information that could be utilised to improve current seasonal and climate forecasts.

The focus on the early summer season was partly due to the difficulty in predicting rainfall during this season (ENSO provides more predictability during the JFM season), as well as the interaction with stakeholders, especially subsistence farmers for whom the prediction of the start of the rains is a key forecast requirement.

1.2.1 Seasonal forecasts

In terms of seasonal forecasts the relative unpredictability of OND or early season rainfall using observed SST fields suggests that there is a large noise component relative to any signal due to SSTs. It is currently not clear if this 'noise' is due to chaotic atmospheric variability or whether a component of this noise is due to other antecedent conditions that can potentially provide some predictability. Furthermore, it is presently unclear how changes in these regional conditions will interact with changes in the large-scale circulation e.g. forced by ENSO. This is also potentially a non-linear problem - regional changes may interact with and promote particular aspects of synoptic change, leading to say a dry extreme but not a wet extreme. The problem, as will be discussed later, is how to include any such information in a forecasting scheme.

1.2.2 Climate change

Current climate change projections (even regional or downscaled projections) assume that the main forcing of any change comes from anthropogenic emissions of greenhouse gases (with a relatively simple treatment of global aerosols). Similar to the issue discussed for seasonal forecasting, we currently do not know if other regional changes (e.g. land use, biomass burning etc) will promote and exacerbate – or counteract – changes induced through anthropogenic climate change. Again the potential is that these changes may promote particular extremes in climate leading to quicker regional change in climate than those suggested by current GCM and downscaled scenarios.

1.3 Aims and objectives

The following aims (and their associated priorities) were identified in the original proposal and formed the underlying basis for the work undertaken within this project:

- Aim (priority) 1: Understand the interactions of vegetation and soil moisture with the large-scale atmospheric circulation, during the early part of the rainfall season (September-December);
- Aim (priority) 2: Identify regions where characteristics of early seasonal rainfall may be influenced by vegetation and soil moisture.
- Aim (priority) 3: Understand the implications of land-use change for the early season climate of the region.
- Aim (priority) 4: Test the feasibility of enhancing current early season rainfall forecasts

The work plan for the project therefore followed a path from Aim 1 through to Aim 4. As will be shown later a subjective assessment of whether these aims were achieved can be summarised as:

- Aim 1: This aim was achieved and even added to; during the course of the project aerosols were added to the list of antecedent conditions that were modelled

- Aim 2: This aim proved difficult as changes in rainfall were often dependent on changes in atmospheric circulation which promoted rainfall changes remote to the location of the perturbation in antecedent conditions. Effects on surface temperature were however more localised.
- Aim 3: This aim was achieved through modelling the effect of historical land use change
- Aim 4: This aim was not achieved because time and human resources did not allow it. We discuss the implications for future forecasting efforts.

2 Regional climate modelling experiments

The modelling focus has been on three different aspects of the climate and environment that could have a measurable effect on early season rainfall: soil moisture; vegetation; and atmospheric aerosols (particularly those due to biomass burning). We use Regional Climate Models (RCMs) to investigate the effects of these antecedent conditions on the subsequent climate and for this purpose there are currently a number of existing RCMs. However, not all RCMs represent the different components of the climate system in the same manner. For instance, some RCMs allow for a monthly varying Leaf Area Index whilst others do not. Similarly some RCMs have an atmospheric chemistry module that allows the impact of aerosols to be modelled whilst others do not. Therefore considerable effort has been made to utilise the appropriate RCM that can best run the experiments needed to answer the identified scientific questions. Even so the physical structure of each RCM places limits on what experiments can be performed and hence scientific questions that can be answered.

In this regard there has been a significant shift away from the MM5 model, which has traditionally been the model of choice at CSAG, and the uptake of its successor the WRF model. We also continue to use the RegCM3 model developed at the International Centre for Theoretical Physics (ICTP) in Italy. There have been several new initiatives that have fed into and been informed by this process and both revolve around the theme of high performance computing:

- the use of grid technology (networks of computers distributed around the world) in collaboration with IBM, US.
- the use of South Africa's Centre for High-Performance Computing (CHPC)

Soil moisture experiments have demonstrated that when the MM5 RCM is initialised at the beginning of the rainfall season with excessive soil moistures, this results in increases in rainfall throughout the remainder of the summer season. This clearly demonstrates that the model is sensitive to soil moisture and that the effects are persistent long after it has commonly been assumed that the soil moisture initial perturbation dissipates.

Experiments to understand the effect of inter-annual variations in Green Vegetation Fraction (GVF) have been implemented on the CHPC system and this will form the basis for further modelling to understand the effect of a changing Leaf Area Index (LAI). Whilst these experiments form the basis for understanding changing vegetation-climate interactions, further large-ensemble multi-parameterisation experiments (using grid technology) are taking place to better understand the role of other vegetation parameters such as minimum stomatal resistance and soil hydrology.

There have been significant developments related to the modelling of aerosols, with the PhD student undertaking these studies (and his institute in Mozambique) collaborating with the CSIR to write a project proposal to the African Laser Centre. If funded the project will utilise a LIDAR system to measure aerosol optical properties over South Africa, which will then be used to model the effect of these aerosols on the regional climate. In the meantime the work has progressed and has largely involved developing methods to import fire inventory databases into the WRF model and enable the chemistry scheme within the model. Another PhD student is working collaboratively in Toulouse, France (though registered at UCT) using RegCM3 and the aerosol chemistry module developed there.

2.1 WRF and WRF-chem

The Weather Research and Forecasting (WRF) model is a numerical weather prediction (NWP) and atmospheric simulation system designed for both research and operational applications. WRF is supported as a common tool for the university/research and operational communities to promote closer ties between them and to address the needs of both. The development of WRF has been a multi-agency effort to build a next-generation mesoscale forecast model and data assimilation system to advance the understanding and prediction of mesoscale weather and accelerate the transfer of research advances into operations.

The WRF Software framework provides the infrastructure that accommodates the dynamics solvers, physics packages that interface with the solvers, programs for initialization, WRF-Var, and WRF-Chem. There are two dynamics solvers in the WSF: the Advanced Research WRF (ARW) solver (originally referred to as the Eulerian mass or "em" solver) developed primarily at NCAR, and the NMM (Non-hydrostatic Mesoscale Model) solver developed at NCEP. Community support for the former is provided by the MMM Division of NCAR and that for the latter is provided by the Developmental Testbed Center (DTC). For all the simulations used in this research, the ARW solver was the dynamic solver chosen.

Features of ARW Solver:

- Equations: Fully compressible, Euler non-hydrostatic with a run-time hydrostatic option available. Conservative for scalar variables.
- Prognostic Variables: Velocity components u and v in Cartesian coordinate, vertical velocity w, perturbation potential temperature, perturbation geopotential, and perturbation surface pressure of dry air. Optionally, turbulent kinetic energy and any number of scalars such as water vapour mixing ratio, rain/snow mixing ratio, cloud water/ice mixing ratio, and chemical species and tracers.
- Vertical Coordinate: Terrain-following, dry hydrostatic-pressure, with vertical grid stretching permitted. Top of the model is a constant pressure surface.
- Horizontal Grid: Arakawa C-grid staggering.
- Time Integration: Time-split integration using a 2nd- or 3rd-order Runge-Kutta scheme with smaller time step for acoustic and gravity-wave modes. Variable time step capability.
- Spatial Discretisation: 2nd- to 6th-order advection options in horizontal and vertical.
- Turbulent Mixing and Model Filters: Sub-grid scale turbulence formulation in both coordinate and physical space. Divergence damping, external-mode filtering, vertically implicit acoustic step off-centring. Explicit filter option.
- Initial Conditions: Three dimensional for real-data, and one-, two- and three-dimensional for idealized data. Digital filtering initialization (DFI) capability available (real-data cases).
- Lateral Boundary Conditions: Periodic, open, symmetric, and specified options available.
- Top Boundary Conditions: Gravity wave absorbing (diffusion, Rayleigh damping, or implicit Rayleigh damping for vertical velocity). Constant pressure level at top boundary along a material surface. Rigid lid option.

Model Physics:

- Microphysics: Schemes ranging from simplified physics suitable for idealized studies to sophisticated mixed-phase physics suitable for process studies and NWP.
- Cumulus parameterizations: Adjustment and mass-flux schemes for mesoscale modelling.
- Surface physics: Multi-layer land surface models ranging from a simple thermal model to full vegetation and soil moisture models, including snow cover and sea ice.
- Planetary boundary layer physics: Turbulent kinetic energy prediction or non-local K schemes.
- Atmospheric radiation physics: Longwave and shortwave schemes with multiple spectral bands and a simple shortwave scheme suitable for climate and weather applications. Cloud effects and surface fluxes are included.

The treatment of aerosol chemistry within WRF (WRF-Chem) is the most comprehensive available and consists of the following components (in addition to resolved and non resolved transport):

- Dry deposition, coupled with the soil/vegetation scheme
- Four choices for biogenic emissions
- Three choices for anthropogenic emissions
- Several choices for gas-phase chemical mechanisms
- The use of the Kinetic Pre-Processor, (KPP) to generate the chemical mechanisms. The equation files (using Rosenbrock type solvers) currently available for RADM2, RACM, RACM-MIM, NMHC9 chemical mechanisms as well as others
- Three choices for photolysis schemes
- Three choices for aerosol schemes
- Aerosol direct and indirect effect through interaction with atmospheric radiation, photolysis, and microphysics routines
- A tracer transport option in which the chemical mechanism, deposition, etc. has been turned off. The user must provide the emissions data for their own domain in the proper WRF data file format for this option.
- A plume rise model to treat the emissions of wildfires

2.1.1 MADE/SORGAM Aerosol Chemistry Package

The aerosol module is based on the Modal Aerosol Dynamics Model for Europe (MADE) (Ackermann *et al.*, 1998) which itself is a modification of the Regional Particulate Model (Binkowski and Shankar, 1995). Secondary organic aerosols (SOA) have been incorporated into MADE by Schell *et al.*, 2001, by means of the Secondary Organic Aerosol Model (SORGAM).

This package is subdivided into two subsets: one for solving inorganic chemistry and the other for organic chemistry. The inorganic chemistry part is based on MARS (Saxena et al., 1986) with further modifications by Binkowski and Shankar (1995). This is where the chemical composition of a sulphate-nitrate-ammonium-water aerosol is calculated according to equilibrium thermodynamics. Two regimes are considered depending upon the molar ratio of ammonium and sulphate. For values less than 2, the code solves a cubic polynomial for hydrogen ion molality, and if enough ammonium and liquid water are present, it calculates the dissolved nitrate. For modal ionic strengths greater than 50, nitrate is assumed not to be present. For molar ratios of 2 or greater, all sulphate is assumed to be ammonium sulphate and a calculation is made for the presence of water.

The organic chemistry is based on SORGAM (Schell et al., 2001). SORGAM assumes that Secondary Organic Aerosols (SOA) compounds interact and form a quasi-ideal solution. The gas/particle portioning of SOA compounds are parameterized according to Odum et al. (1996). Due to the lack of information, all activity coefficients are assumed to be unity. SORGAM treats anthropogenic and biogenic precursors separately, and may be used with a chemical mechanism such as RACM (Stockwell et al. 1997) that provides the biogenic precursors. Since in WRF/chemistry we currently use the RADM2 mechanism (Stockwell et al., 1990), the biogenic precursors and their resulting particle concentrations are set to zero.

2.2 RegCM3

RegCM3 is a primitive equation, vertical sigma-coordinate, grid point limited-area model with compressibility and hydrostatic balance. The non-local boundary layer scheme of Holtslag et al (1990) is used, as well as there being several options for convective parameterisations: Anthes-Kuo type (Anthes, 1977), the mass flux cumulus scheme of Grell (1993) and the cumulus convective scheme of Emanuel (1991). The radiative package of CCM3 (Kiehl et al, 1996), which accounts for the effects of H_2O, O_3 , O_2 , CO_2 and clouds, and uses a delta-Eddington approach to treat solar radiative transfer. N2 O, CFCs), cloud ice and atmospheric aerosols. Cloud radiation is calculated in terms of cloud fraction and cloud water content, and a fraction of cloud ice is diagnosed by the scheme as a function of temperature.The model also includes an algorithm for reducing horizontal diffusion in the presence of steep topography (Giorgi et al 1993a,b). RegCM3 uses the ocean surface flux scheme of Zeng et al (1998), a new large-scale cloud and precipitation scheme (Pal et al, 2000) which accounts for sub-grid variability of clouds as well as the BATS1E scheme (Dickinson et al, 1993), which is used to represent the surface processes. A mosaic-type parameterisation of subgrid-scale topographical and land-use heterogeneity is also used (Giorgi et al, 2003b). NCEP-I and -II, ERA40 and ECMWF reanalysis data can be used as boundary conditions. The USGS Global Land Cover Characterisation and global 30 arc-second elevation datasets have also been included to create the terrain files.

2.2.1 Dust and aerosols

Dust emissions are calculated using the soil aggregate saltation and sandblasting parameterisations of Marticorena and Bergametti (1995) and Alfaro and Gomes (2001). These processes depend on the wind conditions, soil characteristics and the particle size. the main steps in dust emission calculation include: the specification of soil aggregate size distribution for each model grid cell, calculation of a threshold friction velocity leading to erosion/saltation, calculation of the horizontal saltating soil aggregate mass flux and lastly, the calculation of the vertical transportable dust particle mass flux. In relation to the BATS interface, these parameterizations become effective in the model for cells dominated by desert and semi desert land cover.

The sulfur model consists of prognostic equations for SO_2 and SO_4, which include transport by resolvable scale circulations and cumulus clouds, turbulent diffusion, dry deposition, wet removal by resolvable-scale and cumulus precipitation, and chemical conversion from SO_2 to SO_4. Parameterisation of wet removal is based on the schemes of Giorgi and Chameides (1986) and Giorgi (1989) and depends on the local cloudwater-to-rainwater conversion rate, which is explicitly calculated for resolvable-scale clouds and is specified for cumulus clouds. Below-cloud scavenging of SO_2 is also incorporated. Dry deposition of both SO_2 and SO_4 is parameterized using a constant deposition velocity with different values for land and ocean. Both gas-phase and aqueous phase SO_2 to SO_4 chemical conversion pathways are included as described in Qian et al. (2001). RegCM3 also includes the effect of fossil fuel soot following the parameterization of Haywood et al. (1997) and Myhre et al. (1998).

The calculation of aerosol direct radiative forcing is based on the delta-Eddington representation used in the CCM3 radiation package (Kiehl et al. 1996), in which the aerosol radiative properties are described in terms of specific extinction, single scattering albedo, and an asymmetry parameter. Sulfate and fossil fuel soot are treated as an external mixture, i.e. the optical properties for each aerosol type are treated separately. Optical properties for the sulfate are from the CCM3 radiative transfer scheme (Kiehl et al., 1996) while the fossil fuel soot optical properties are from Haywood and Shine (1997). The aerosol specific extinction also depends on the environmental relative humidity.

2.2.2 Land Surface Scheme

The soil-vegetation-atmosphere interactions are parameterized through BATS1E (Biosphere-Atmosphere Transfer Scheme), described in detail by (Dickinson et al., 1993). BATS is designed to describe the role of vegetation and interactive soil moisture in modifying the surface-atmosphere exchanges of momentum, energy and moisture. It has a vegetation layer, a snow layer, a surface soil layer (10cm thick), a root zone layer (1-2mthick) and a third deep soil layer (3 m thick). Prognostic equations are solved for the soil layer temperatures using a generalization of the force-restore method of Deardoff (1978). The soil hydrology calculations include predictive equations for the water content of the soil layers. These equations account for precipitation, canopy foliage, evapotranspiration, surface runoff, snowmelt, infiltration below the root zone and diffusive exchange of water between soil layers. The scheme also has functions accounting for soil water movement, surface runoff, sensible heat, water vapour and momentum fluxes. BATS has 20 vegetation types; soil textures ranging from coarse (sand), to intermediate (loam), to fine (clay) and different soil colours (light to dark) for the soil albedo calculation (Dickinson et al., 1986). Additional modifications have been made to BATS in order to account for subgrid variability of topography and land cover using a mosaic-type approach (Giorgi et al., 2003b). This parameterization showed a marked improvement in the representation of the surface hydrological cycle in mountainous regions. A more detailed description of RegCM3 and refereed articles can be found in Pal et al. (2007).

2.3 MM5

The fifth-generation Pennsylvania State University-National Center for Atmospheric Research Mesoscale Model (MM5; Grell *et al.*, 1994) is used to simulate the effects of land use change. The domain was set to cover approximately 0-40 ºS in latitude and 5-57 ºE in longitude at a grid resolution of 50 km and 23 vertical sigma levels.

Land surface processes are represented by the NOAH land surface scheme (Chen and Dudhia, 2001). NOAH consists of 4 soil layers and a single plant canopy layer. Vegetation parameters such as albedo, roughness length and minimum stomatal resistance are defined according to the dominant vegetation class in each grid cell. Green vegetation fraction (fG) – defined as the "grid-cell fraction for which midday downward solar insolation is intercepted by photosynthetically active green canopy" (Chen and Dudhia, 2001) – is provided independently as a separate spatially continuous monthly climatology. Produced by Gutman and Ignatov (1998) from satellite-derived normalized difference vegetation index (NDVI), it assumes that the leaf area index (LAI) – the total area of leaves in all layers of a canopy divided by the area of the ground beneath the canopy – is fixed at a value of 4. It is clearly unrealistic to fix LAI to represent a dense canopy for all vegetation classes, but this is done because it is difficult to derive both LAI and fG simultaneously from a single NDVI product (Gutman and Ignatov, 1998; Matsui *et al.*, 2005). It can be argued that natural variability in fG is generally higher than for LAI (Chen and Dudhia, 2001; Matsui *et al.*, 2005), so the assumption made in NOAH is to leave LAI fixed, but allow fG to vary. Green vegetation fraction is used as a weighting coefficient in the calculations of evaporation and transpiration, while LAI is a factor in the calculation of canopy resistance, and hence plant transpiration. All other vegetation parameters are independent of LAI and fG. Soil data is provided by the United Nations Food and Agriculture Organization global classification. In the NOAH LSM, soil parameters determine hydrological properties such as field capacity and wilting point, which affect direct evaporation for the soil as well as plant transpiration. Surface albedo is defined according to land-use and is not altered by soil properties.

Planetary boundary layer (PBL) processes are computed using the MRF PBL scheme (Hong and Pan, 1996). The Betts-Miller convective adjustment scheme was chosen to represent moist convection and precipitation (Betts and Miller, 1993). This is a semi-empirical approach whereby profiles of temperature and moisture computed by the atmospheric model are relaxed toward predetermined reference profiles. In MM5 simulations for southern Africa, Tadross *et al.*, (2006) found that the combination of the MRF PBL and Betts-Miller convection schemes tended to overestimate the magnitude of precipitation events, but better captured the phase of the diurnal cycle and inter-annual rainfall variability. Lateral boundary conditions, initial conditions and sea-surface temperatures are taken from the National Centers for Environmental Prediction-National Center for Atmospheric Research (NCEP-NCAR) reanalysis (Kalnay *et al*.,1996).

2.4 Soil moisture experiments

These experiments have been undertaken as part of 2 PhD studies by Neil MacKellar (graduated) and Marshall Mdoka. The first set of experiments utilised the MM5 model, whereas the second set of experiments utilised the RegCM3 model – and were initially focussed on the later January period, usually considered the mid-summer period.

2.4.1 Experiments undertaken using MM5

At the start of the project it was noted that the RCM soil moisture climatology differs significantly from that of the NCEP-NCAR reanalysis (typically used to initialise RCMs) and that the RCM takes significantly longer than 1 month to revert to an equilibrium state with the overlying atmosphere. An experiment to test the implications of this observation, given potential errors in initialising the soil moisture fields was therefore undertaken.

2.4.1.1 Experimental setup

MM5 simulations are run to test the sensitivity of the model to the same perturbation in initial soil moisture at a) the beginning of Nov and b) the beginning of Aug. Two sets of simulations are carried out, named NOV_INIT and AUG_INIT. Each set consists of 3 pairs of MM5 integrations. Each pair consists of 2 simulations initialized on the same date, but using different initial soil moisture conditions. For NOV_INIT, the three pairs are initialized on 1, 2 and 3 Nov 1991 and run through to 28 Feb 1992. The differences in atmospheric fields between the initial dates introduce perturbations that can contribute to the RCM's internal variability (see Giorgi and Bi, 2000; Christensen *et al*., 2001; Caya and Biner, 2004), so by using these different starting dates we account for some of the noise associated with the RCM's internal variability. For the NOV_INIT simulations the first member of each pair, irrespective of starting date, takes its initial soil moisture from the NCEP-NCAR reanalysis as at 1 Nov 1991, whereas the second member takes initial soil moisture from the 1 Nov conditions of a separate MM5 integration initialized on 1 Aug 1991. These two initial soil moisture fields are named, respectively, NOV_SOIL_A and NOV_SOIL_B. For AUG_INIT, three pairs of simulations are initialized on 1, 2 and 3 Aug 1991 and run through to 28 Feb 1992. Once again, three pairs of simulations are run to account for internal variability. The first member of each pair, irrespective of starting date, takes its soil moisture initial conditions from the NCEP-NCAR reanalysis at 1 Aug 1991 (hereafter AUG_SOIL_A). The initial soil moisture conditions of the second pair (AUG_SOIL_B) represent the volumetric difference between NOV_SOIL_A and NOV_SOIL_B, imposed on AUG_SOIL_A. In this way the same volumetric soil moisture anomaly is applied at the start of both the NOV_INIT and AUG_INIT sets of simulations.

2.4.1.2 Persistence of spatial anomalies

Figure 1 – (a) shows the initial soil moisture anomaly field and (b) the spatial correlations of selected surface variables with this field for each month in the 4-month simulation started on 1 November. The spatial correlations decrease throughout the simulation but are still significant (except for precipitation) in January. This highlights that looking for a soil moisture signal in simulated precipitation is hard to detect, but the signal in other surface variables is more persistent.

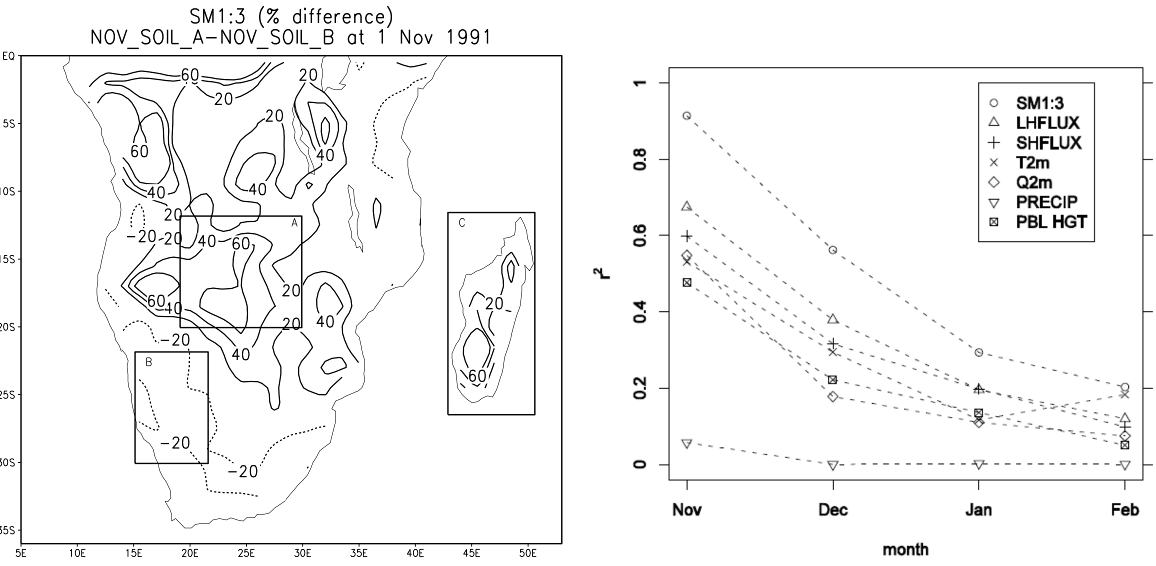

(a) (b)

Figure 1: (a) Initial soil moisture anomaly field applied to RCM climate simulations; (b) spatial correlations with initial soil moisture anomaly applied on 1 November, of simulated latent heat flux (LHFLUX), sensible heat flux (SHFLUX), 2m temperature (T2m), 2m specific humidity (Q2m), precipitation (PRECIP) and boundary layer height (PBL HGT)

Figure 2 presents the results of an initialisation with the same soil moisture anomaly as used to initialise on 1 November, except that in this case the run was initialised on 1 August. A similar decay in the spatial correlation is observed for all variables, except it is noticeable that the values of r^2 remain higher during the first 2-3 months of the simulation, than during the first 2-3 months of the simulation started on 1 November. This indicates that the spatial patterns associated with the initial soil moisture anomaly and the corresponding surface climate variables persist for longer during the late winter than during early summer, suggesting a positive feedback that maintains the initial anomaly.

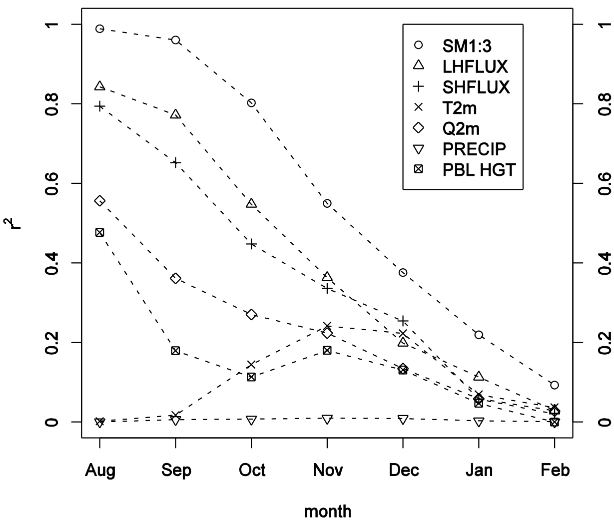

Figure 2: Same as Figure 1b, except for simulations started 1 August 1991.

It is important to note that these experiments span the period leading into the peak summer months and in the context of this project it is important to understand how these interactions develop during spring – these results suggest that feedbacks may be stronger at this time of year. These results also demonstrate that initialisation of soil moisture in an RCM is an important consideration that may affect seasonal forecasts made with an RCM. The utility of soil moisture as a predictor in an empirical seasonal forecasting scheme remains largely unknown, mostly because it is so hard to measure or model. However, new satellite-based measurements may offer this possibility in the future.

2.4.2 Experiments undertaken using RegCM3

The aim of the soil moisture experiments was to use the RegCM3 model to determine how soil moisture and surface fluxes affect the boundary layer climate of Southern Africa. The state of soil moisture, as described by the level of saturation in the soil levels, is regulated by rainfall and potential evaporation. Both of these atmospheric forcings exert significant control on the evolution of the soil moisture state. To investigate these underlying processes a series of experiments utilizing wet, dry and normal soil moisture conditions were designed. Soil moisture perturbation experiments focus on January for dry (1992) and wet (1996) years with the respective control simulation being driven by initial boundary conditions from NCEP. Perturbation experiments are based on changing the soil moisture field capacity in the RegCM3 at percentages of 25% and 75% of the field capacity.

RegCM3 FORTRAN code within the BATS scheme was altered so that the model simulates with soil moisture fixed or interactive for all selected capacities. For fixed simulations, the surface impacts the atmosphere, but the soil moisture does not respond to the atmosphere. Whilst for the interactive simulations, the soil moisture does respond to the atmosphere but starting the initialization at chosen soil moisture perturbations of either 25 or 75%. These one month simulations are performed with a 15 days spin up (from 15th December) period using the Emanuel convective scheme.

2.4.2.1 Temporal analysis of top-layer soil moisture conditions

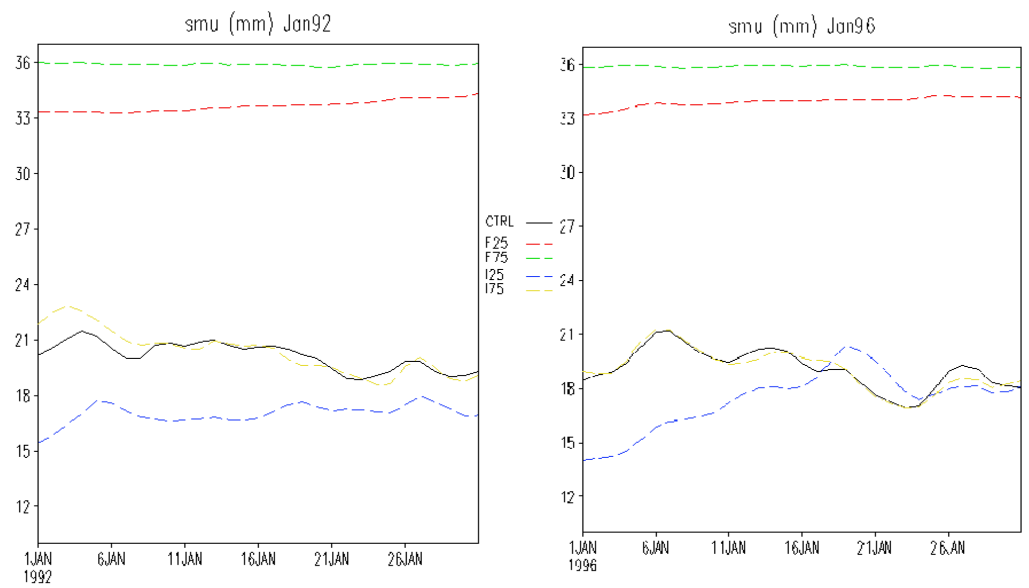

Figure 3: Top soil moisture conditions (mm) for control, fixed and interactive simulations during January 1992 and January 1996.

Figure 3 shows top soil moisture conditions for the control, fixed and interactive simulations. For the fixed cases of 25% and 75% field capacities and the model being not allowed to be interactive with surface the top soil moisture layer is represented as shown by the red (F25) and green (F75) respectively. Whereas for the control experiment the model is enforced with prescribed data and allows interaction with the model's climate and the response is depicted by the solid black line. The interactive cases required the model to be initialized at the 25% and 75% field capacity within the scheme and be allowed to interact with the climate thereafter. There appears to be a problem with the fixed initialisations (both being higher than the interactive initialisations) – this problem is currently being investigated and the experiments with fixed soil moisture will be ignored in the following discussion.

The control and interactive at 75% (yellow colour) tend to keep almost same amounts of top soil moisture for both January 1992 and 1996. Whilst the interactive dry experiment (denoted by blue colour) accumulates its soil moisture as the month progresses beginning with 15.5 mm and 13.8 mm on the first day of the month respectively. Between 17 and 24 January 1996 it overshoots both control and interactive wet simulation to reach almost 21 mm on 22 January 1996. Also worth noting is that by end of January 1996 both interactive and control experiments show similar top soil moisture conditions.

2.4.2.2 Model precipitation

Figure 4 shows total daily precipitation for January 1992 as simulated in RegCM3 using the Emanuel convection scheme and CRU data (observations). In RegCM3, total precipitation comprises of the non-convective and convective rainfall. RegCM3 precipitates more than CRU data in the central parts of southern Africa especially over Angola, Zambia, southern Mozambique, Lesotho, southeastern South Africa and some high precipitation spots are also observed in isolated areas. RegCM3 shows the west–east rainfall gradient over southern parts of the region and fairly represents the precipitation distribution over the northern parts of the region in comparison with CRU data. Some grid point storms were observed in the simulations for tropical areas especially near lakes and high terrain. This can possibly be associated with some local effects or the lake model scheme. Although not presented here, the results indicate a similar precipitation distribution when using the other convection schemes (Grell) in RegCM3.

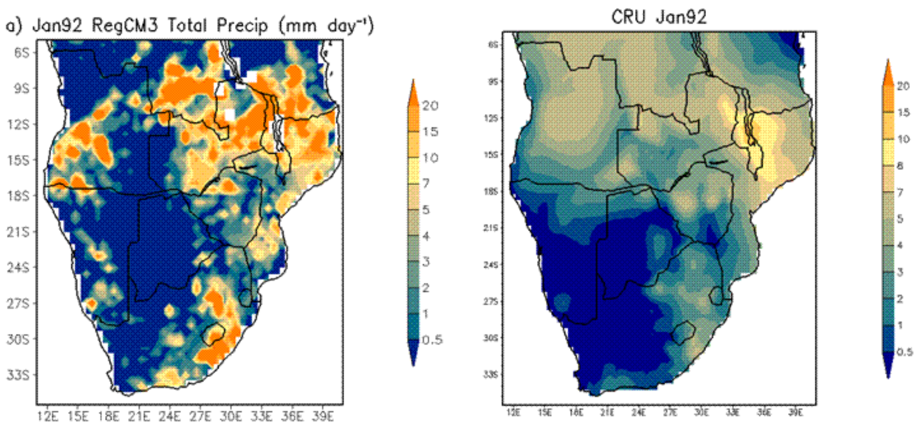

Figure 4: Total daily precipitation for January 1992 (a) RegCM3 simulation and (b) CRU data.

Figure 5 shows the precipitation simulated for January 1996 in comparison to January 1996 CRU dataset. The model overestimates the precipitation over much of central parts of the region. The peak observed over eastern Zimbabwe in CRU is slightly displaced to northwestern Zimbabwe. However, the precipitation distribution over the western parts of the region was well captured. A west to east precipitation gradient over South Africa was well captured in the model as observed in CRU. Over the north of the region, RegCM3 highly underestimates total daily precipitation by as much as 8-10 mm/day.

Whilst RegCM3 simulates variability in precipitation between 1992 and 1996, and to some degree captures the spatial distribution of this interannual variation, it has a tendency to overestimate rainfall, which partly results in lower simulated temperatures.

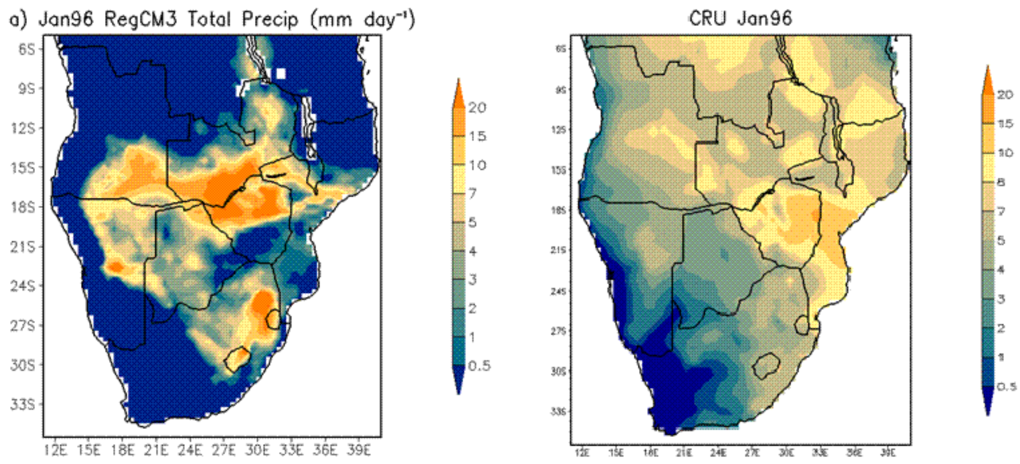

Figure 5: Total daily precipitation for January 1996 (a) RegCM3 simulation and (b) CRU data.

2.4.2.3 Model comparison to air temperature

In RegCM3, air temperature is measured at 2 metres above surface level. Figure 6 shows air temperature for January 1992 from RegCM3 simulation and CRU reanalysis data. RegCM3 does poorly in simulating the temperature as compared to CRU. RegCM3 underestimates by as much as 12°C over the hot and dry parts of the region during the summer rainfall season especially Botswana, Namibia and Limpopo or Lowveld areas. However, the model does well in simulating temperature over high terrain such as Lesotho and the central high watershed of Zimbabwe as well as northwestern Angola, northern Zambia and coastal areas.

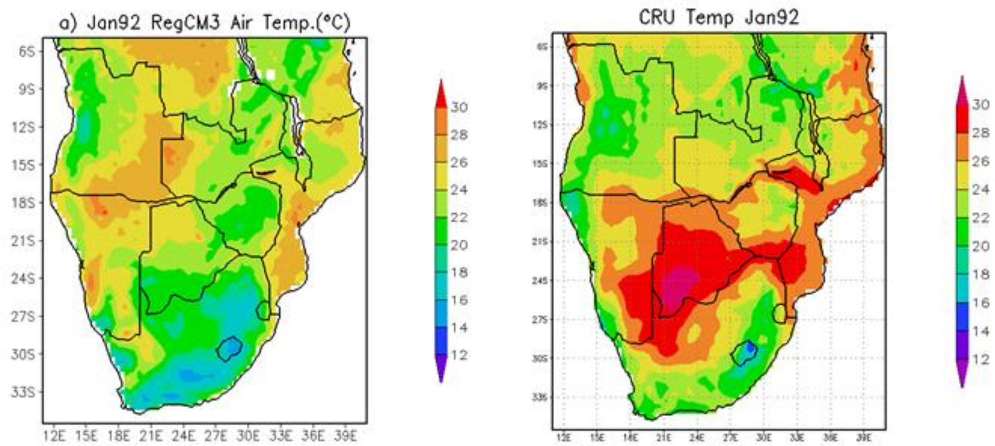

Figure 6: 2m air temperature for January 1992 RegCM3 simulation and CRU reanalysis data.

For January 1996 simulation of air temperature in RegCM3 and from CRU dataset are shown in Figure 7. The model does fairly well in capturing the spatial distribution in temperature over southern Africa except for central Mozambique and DRC. RegCM3 manages to capture the peak to the southwestern of the region and the magnitude of above 26°C within the vicinity of that area. Again, high altitude, Limpopo/Lowveld and coastal areas temperatures are well simulated to within ±2°C.

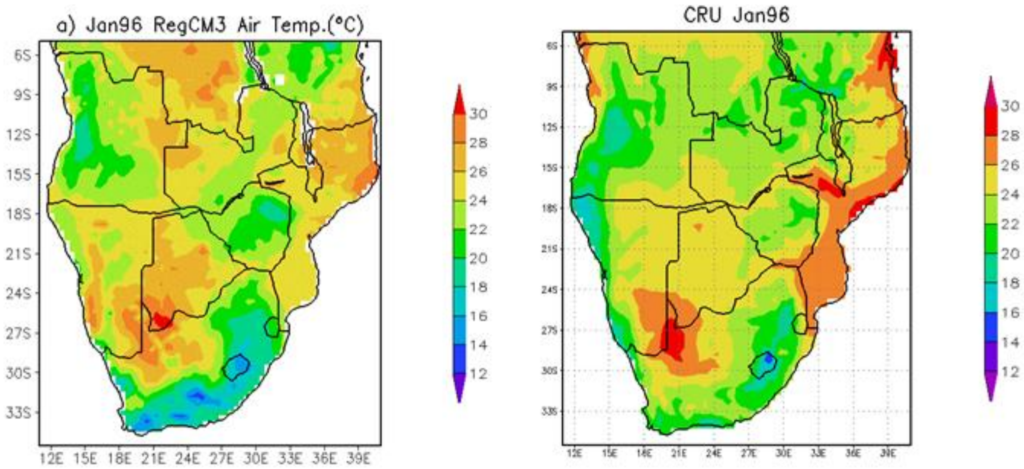

Figure 7: 2m air temperature for January 1996 RegCM3 simulation and CRU reanalysis data.

2.4.2.4 Diurnal Cycles

One aspect of climate that rarely receives attention in model evaluation is the diurnal cycle. Lin et al. 2000, explains that the diurnal cycle is one of the prominent cycles in the water and energy exchanges within the climate system and can be considered to be an ideal test-bed for GCMs and RCMs as well as their parameterisations.

The diurnal cycle of precipitation shows peaking after midday for both years (Figure 8). This is anticipated as most of southern African rainfall is of convective form and falls during daytime into night time after the surface warms up. The average peak magnitude is higher for January 1996 for all experiments, which should be anticipated for the simulated wetter year than for January 1992. The interactive simulation for the wet runs tends to be similar in pattern to the control whilst the interactive dry run has the lowest peak. As anticipated, the peak in surface temperature occurs in the afternoon (Figure 8) with coldest temperatures occurring at night. The diurnal pattern for the surface temperature depicts higher peaks for the interactive dry run which was shown to have a lower peak for the total rainfall. This implies drier surfaces result in higher surface temperatures. Coherently with rainfall patterns, the peaks decrease through control simulations and the interactive wet run.

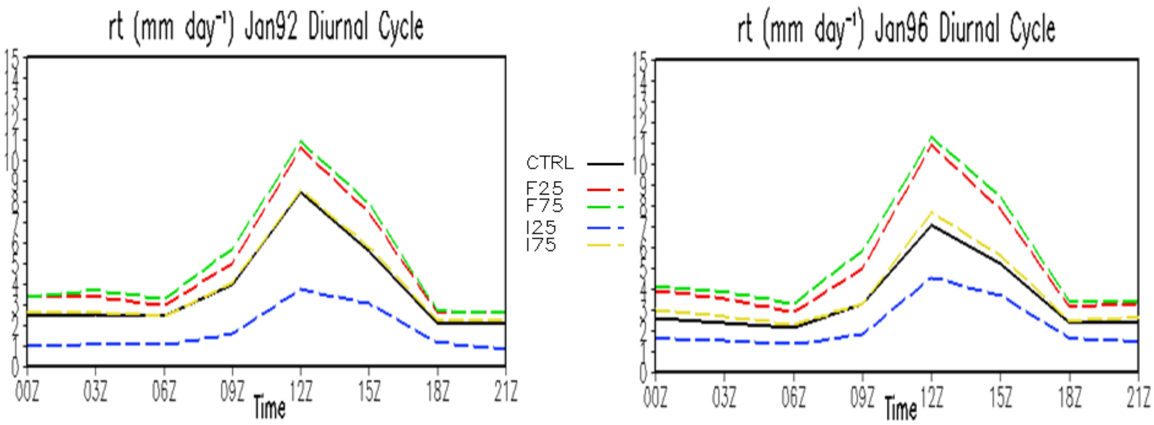

(a)

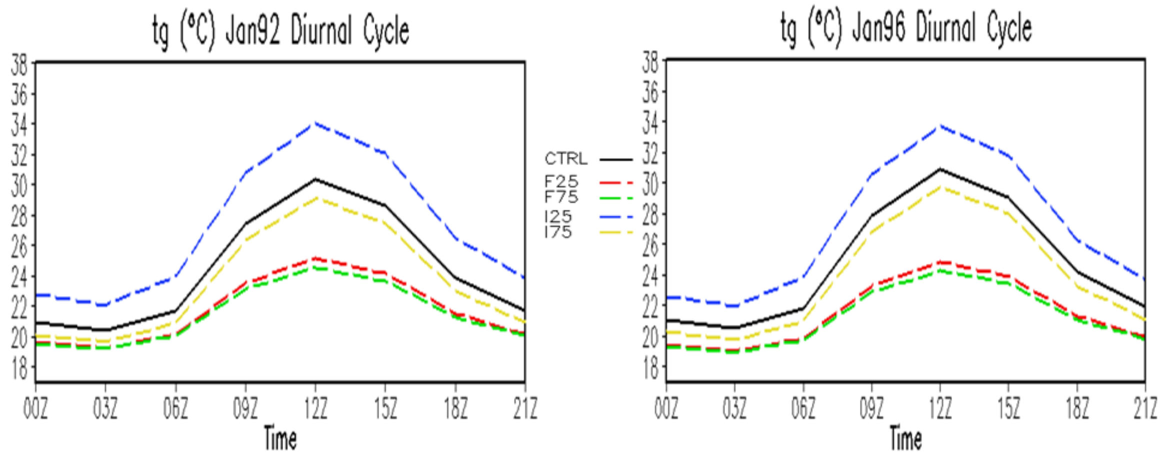

(b)

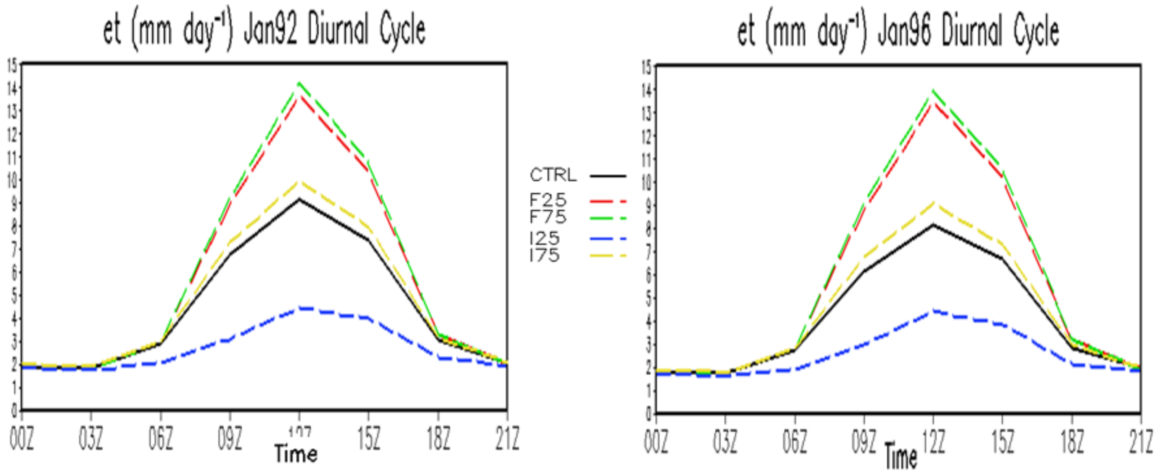

(c)

Figure 8: Diurnal cycles of (a) Total precipitation, (b) surface temperature and (c) Evapotranspiration for January 1992 and 1996.

Evapotranspiration diurnal cycles show similar patterns to the total rainfall cycles with evaporation rates peaking up in the afternoon and less rate from around midnight to 5am. The highest peak in evapotranspiration rate is observed with fixed wet simulation experiments where the peak rises from a rate of 9 mm/day in the control simulation to about 14 mm/day in January 1992 and doubling up in January 1996 to 14 mm/day from 7 mm/day. Interactive simulation initialized at 25% field capacity shows a reduction in the rate to 4 mm/day for both years. There is no marked difference from the interactive experiment at 75% capacity and the control run.

In contrast, the interactive dry run set up depicts a higher peak in sensible heat than the control experiment (Figure 9) due to low evapotranspiration rate, low rainfall rates and high surface temperatures as shown in the earlier diurnal patterns. The diurnal cycle for sensible heat shows similar patterns to the surface temperatures discussed earlier for all experiments. A marked drop in sensible heat is shown to occur between control run at about 200W/m^2 and the fixed wet run experiment at 50W/m^2. No marked difference in diurnal patterns occurs with incident solar radiation for all experiments as the peaks are almost similar. However, highest peak occurs with the interactive dry run which would imply the model simulating less cloud and thus allowing more incoming solar radiation to reach the surface than for the other experiments.

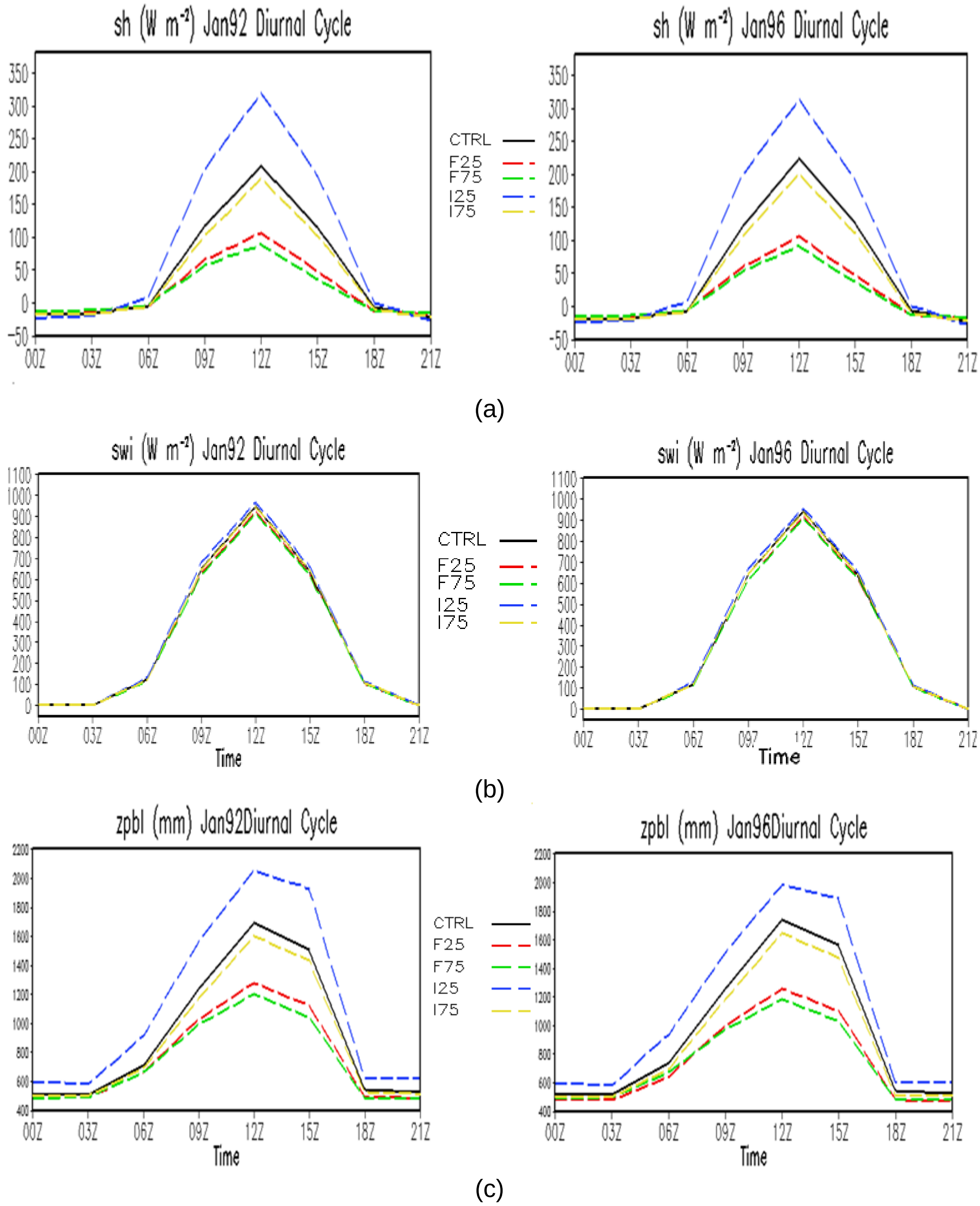

Figure 9: Diurnal cycles of (a) Sensible heat, (b) incident solar radiation (c) Planetary boundary layer for January 1992 and 1996.

The planetary boundary layer diurnal cycle increases in height to reach a peak in afternoon at around 2pm and a gradual decrease in layers until around 5pm then sharp decreases till 8pm then the layers become constant. During the day incident solar radiation results in the warming of the surface air which destabilizes the vertical profile of air above. This leads to a daytime convective boundary layer. Mixing in the mixed layer occurs through turbulence and thus the height increases during the day. At night, there is no incident solar radiation so the surface begins to cool through outgoing longwave radiation. Less mixing occurs at night time and thus the layer becomes stable. From these diurnal patterns, the mixed layer is lower for fixed soil moisture experiments and higher for interactive dry experiments. According to Pal and Eltahir, 2001 anomalously high soil moisture tends to reduce the PBL height thus increasing the moist static energy per unit mass air amongst other additional factors.

2.4.2.5 Total rainfall

Total Rainfall anomalies for January 1992 and 1996 are shown in Figure 10. They are a difference of the interactive simulations from the control simulation. The comparisons are made using the monthly averages of the resultant precipitation from these different soil moisture conditions expressed as an anomaly from the precipitation of the control simulation. Note that, the total precipitation is presented and no convective precipitation output is shown as it is very similar to the responses shown here. Only results for the interactive simulations are discussed due to the problems associated with the fixed simulations mentioned earlier.

For the interactive 25% experiment anomalies during 1992 a marked decrease in precipitation occurs over Zambia, northern Zimbabwe, Malawi, northern Mozambique, and parts of DRC as well as Angola. Most of western Botswana and western province of South Africa fall within the transitional zone between the increase and decrease of precipitation anomalies. Areas enclosed within white contours depict areas that are statistically significant at 95% level. Interactive experiment at 75% (Figure 10c) shows an increase over southern Zambia and Angola and marked increases in precipitation are confined to the central parts of the region and equator wards. In general, for January 1992 drier experiment (Figure 10a) results in a decrease in precipitation over most of the region whereas the wetter soil moisture experiment (Figure 10c) leads to an increase.

Figure 10b & Figure 10d show total precipitation anomalies for January 1996. For the interactive simulations, there is a northeast-southwest (NE-SW) inclination in total precipitation anomaly distribution. The interactive drier experiment of 25% field capacity (Figure 10b) depicts an increase in precipitation over the northeastern parts of southern Africa and a decrease over the southwest. The converse is true for the interactive wetter experiment of 75% field capacity (Figure 10d). There are areas that are showing a similar response for all the different perturbations. Lesotho, southeastern South Africa, and part of northeastern Namibia always result in a decrease in precipitation whilst the western coastal areas are non-responsive. Note that for total precipitation anomalies most of the area is not statistically significant at 95% level. A comparison of January 1992 and 1996 shows that marked responses are observed for dry January 1992 where the drier experiment results in mostly a decrease in precipitation over the region whilst the wetter experiment leads to an increase in precipitation. This suggests that a dry year is more responsive to soil moisture perturbations than a wet year.

2.4.2.6 Rain days and intensity

Figure 11 shows the rain days and intensity for control experiment of January 1992. Rain days were considered to be any day receiving 0.2 mm/day and intensity was then calculated from the total rainfall and the number of rain days. January 1992 reveals the greater part of the region as having more than 24 rain days. However, the southwestern areas show little precipitation with less than 12 rain days especially Western Cape areas, as well as the semi-dry or deserts areas of Botswana and Namibia with less than 3 rain days.

(a) (b)

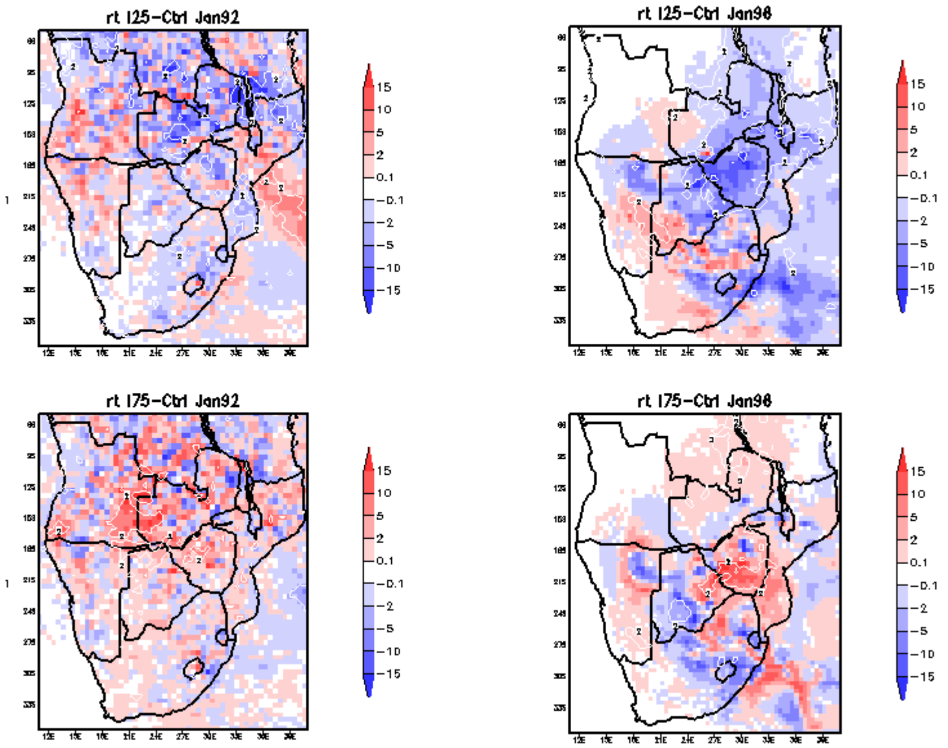

(c) (d)

Figure 10: Total rainfall anomalies between the interactive experiments from the control simulation for January 1992 (a&c) and 1996 (b&d). White contours enclose areas that are statistically significant at 95% level.

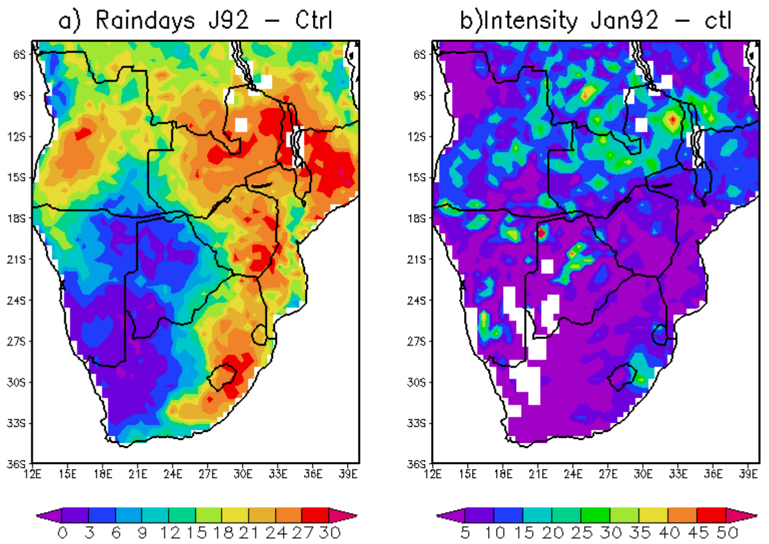

Figure 11: (a) Rain days and (b) Intensity for RegCM3 simulations of January 1992.

Less intense rain is shown over the southern parts of the region and more intense being inclined towards the tropics especially over northern Zambia. Some isolated intense storms are shown over Namibia and Botswana implying that most of the falls occurred within a 3 day period, Figure 11b. Over the eastern parts of southern Africa, less intense pattern (Figure 11b) in comparison to high number of rain days (Figure 11a) implies a fair distribution of the rainfall throughout the month.

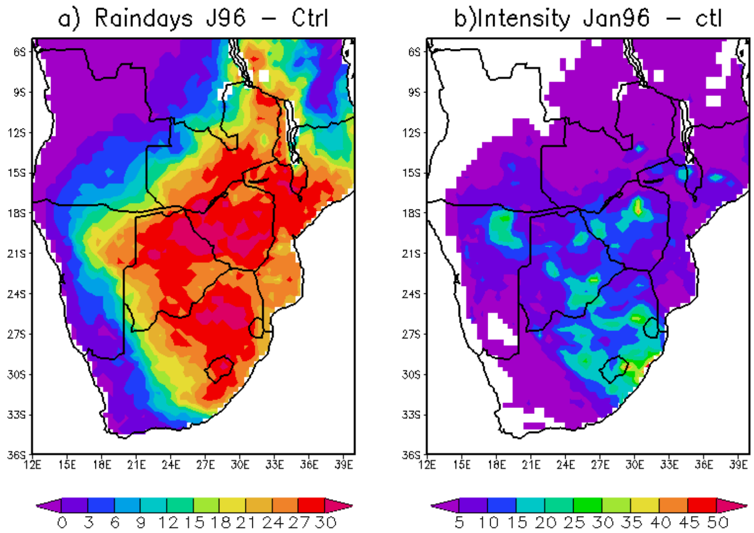

Figure 12**:** (a) Rain days and (b) Intensity for simulations of January 1996

Figure 12 displays rain days and intensity for control simulations for January 1996. Most of Zimbabwe, Botswana, northern South Africa, central Zambia and northern Mozambique depict a situation of raining daily. The rest of the region has a gradual spread of rain days increase from the west towards the east. It can be inferred that Emanuel scheme has too many rain days. The area with maximum rain days has increased for January 1996 in comparison to January 1992 (not shown). As for intense rains (Figure 12b), there are confined within the region of highest number of rain days (Figure 12a) implying that the model simulates higher intensities in the same regions it simulates the most raindays, though the intensity field is much more heterogeneous.

(a) (b)

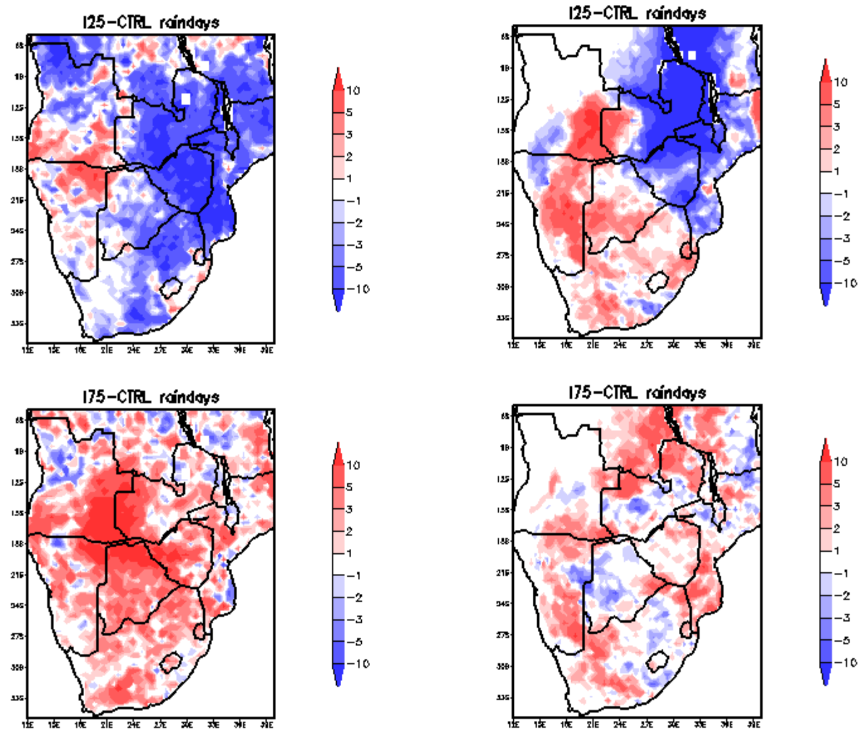

(c) (d)

Figure 13: Total rain days anomalies between the interactive experiments from the control simulation for January 1992 (a & c) and January 1996 (b & d).

Figure 13 displays total rain days anomalies in RegCM3 between the fixed and interactive experiments from the control simulation for January 1992 and 1996. Interactive dry run for 1992

(Figure 13a) depicts a decrease in rain days over the region with marked reduction of more than 5 rain days occurring over Zimbabwe, northwestern Angola, southeastern Zambia and southern Mozambique. However, a small area of southern Angola and northeastern Namibia results in an increase of up to 10 rain days. For the wet run of January 1992 (Figure 13c) an increase of 5-10 rain days is observed. In general, the distribution pattern in rain days follows a west to east for increase to decrease in the dry run whereas there is an increase in rain days over most of the region for the wet run.

Figure 13b & d illustrate rain day anomalies for January 1996 obtained from the interactive experiments wrt the control simulation. The interactive dry run (Figure 13b) has a NE-SW inclined distribution with a marked decrease over the northeastern parts of the southern African region and an increase over most of the southwestern region. There is no distinctive response for the interactive wet run (Figure 13d) but there is more of an increase in rain days and isolated areas with decreases in rain days. There is a vast area falling within the transitional zone between decreases and increases. Western coastal areas, southwestern parts of the region, southeastern South Africa and eastern Tanzania show a decrease for all forms of soil moisture perturbations, indicating that dynamical changes resulting from these experiments result in a shift of rainfall producing systems away from these regions

Figure 14 displays intensity anomalies between the interactive simulations from the control run for January 1992 and 1996. Figure 14 (a&c) shows January 1992 Intensity anomalies between the interactive simulations and the control simulation. There is no clear response shown in the rainfall intensity distribution pattern over the region for all simulations. The response is extremely heterogeneous. The interactive dry run for 1996 (Figure 14b), however, shows a NE-SW distribution with a decrease over the northeastern parts of the region and an increase over the southwestern areas. As for the wet runs (Figure 14d), the converse pattern applies with an increase over the northeastern areas and a decrease toward the southwestern areas of southern Africa. Western coastal areas, northeastern Namibia, southeastern parts of South Africa including Lesotho all show a decrease in rainfall intensity for all soil moisture initializations. This is a very interesting contrast to 1992 when the synoptic forcing is characterised by large-scale subsidence, more so than during 1996. Although this requires further investigation it implies that the spatial organisation of changes in rainfall intensity may be heavily dependent on the synoptic forcing of the regional climate.

2.4.2.7 Surface temperature

Figure 15 shows the surface temperature anomalies of interactive simulations from the control simulation for January 1992 and 1996. There is an increase in surface temperature over most of the region for both interactive dry soil moisture perturbations experiments (Figure 15a and Figure 15b) with an exception of the western areas depicting a decrease in surface temperature. Figure 15 c&d, representing wet soil initializations for the interactive simulation show a decrease in surface temperature over much of southern Africa. Exceptions are in the northeastern areas and northern areas where slight increases of 1°C occur. Marked decreases of about 6°C occur over western areas of semi-arid and desert plains Namibia, Botswana and western sections of South Africa. Regions that are statistically significant at 95% are enclosed in white contours and most of the region depicts significant change. Figure 15 b&d displays surface temperature anomalies for January 1996. For interactive soil moisture initialization at 25% field capacity, an increase in surface temperature occurs over most of the region (>2°C and as high as 4°C) except from a small area over eastern Namibia and southwestern Botswana where a slight decrease of 1°C is apparent. Statistically significant decreases in surface temperature are apparent in the interactive 75% initialisation over most of the region.

(a) (b)

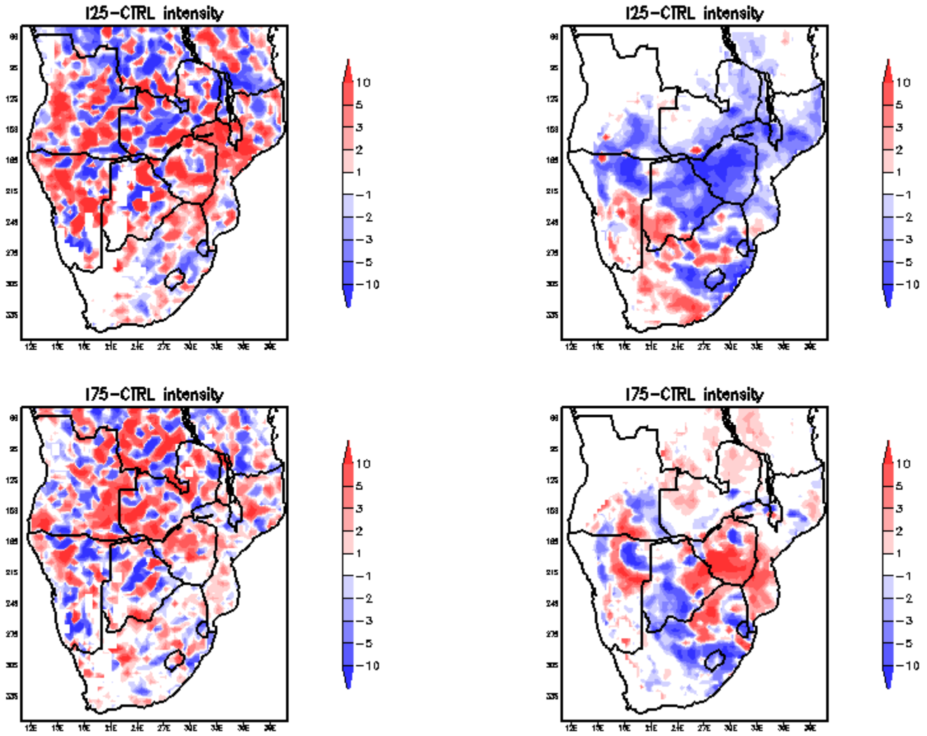

(c) (d)

Figure 14**:** Intensity anomalies interactive experiments from the control simulation for January 1992 (a&c) and 1996 (b&d).

(a) (b)

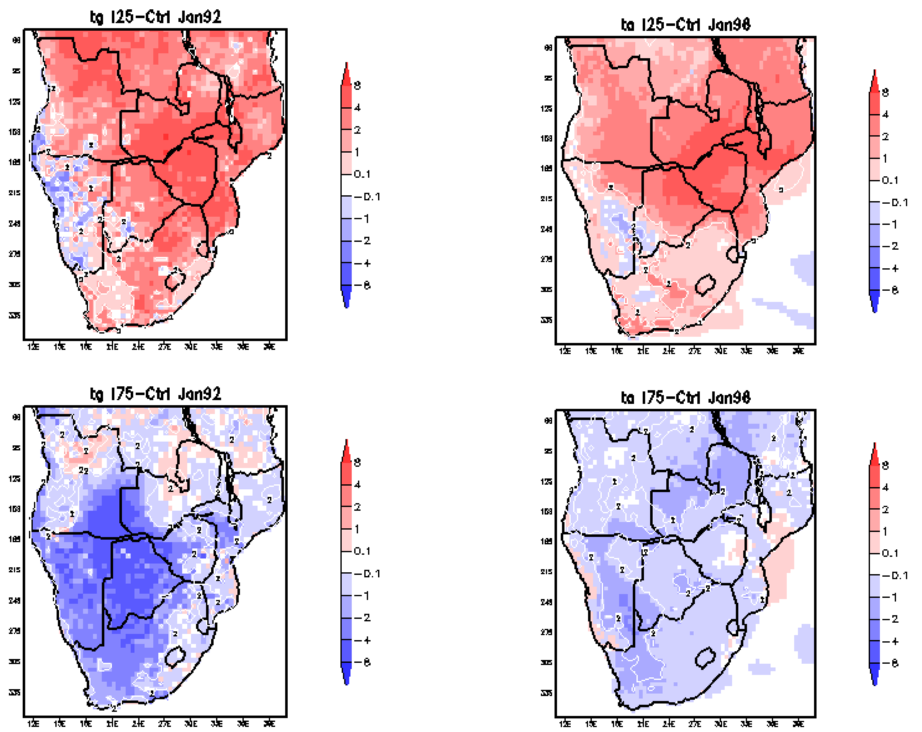

(c) (d)

Figure 15**:** Surface Temperature anomalies interactive experiments from the control simulation for January 1992 (a&c) and 1996 (b&d).

2.4.2.8 Evapotranspiration

Figure 16 shows evapotranspiration anomalies of January 1992 and 1996 calculated from the difference between the interactive simulations from the control simulation for both dry and wet soil moisture perturbations. The interactive dry soil moisture initialisation results in slight decreases over most of the region with islands of increases of evapotranspiration especially over the western parts of the subcontinent. As for interactive wet runs, evapotranspiration mostly increases over the bulk of the region except during 1992 for southeastern Angola, southwestern Zimbabwe, Botswana, eastern Namibia and western South Africa with rises of up to 3 mm/day. The rest of the region is divided between slight rises and falls in evapotranspiration rate by 1 mm/day. Figure 16 b&d displays evapotranspiration anomalies between interactive simulations from the control simulation of January 1996 for both dry and wet soil moisture perturbations. Figure 16b shows the interactive dry soil moisture perturbation from the control simulation of January 1996 where a reduction in evapotranspiration is obtained over most of southern Africa. Negative anomalies of 2 mm/day occur over eastern Namibia, southeastern Botswana and western South Africa. For all forms of soil moisture initialization i.e. dry or wet, southern Zimbabwe and northern South Africa always show with a decrease in evapotranspiration whilst east central Namibia indicates a rise in evapotranspiration. Small portions of the subcontinent show statistical significance at 95% level for the evapotranspiration rate anomalies.

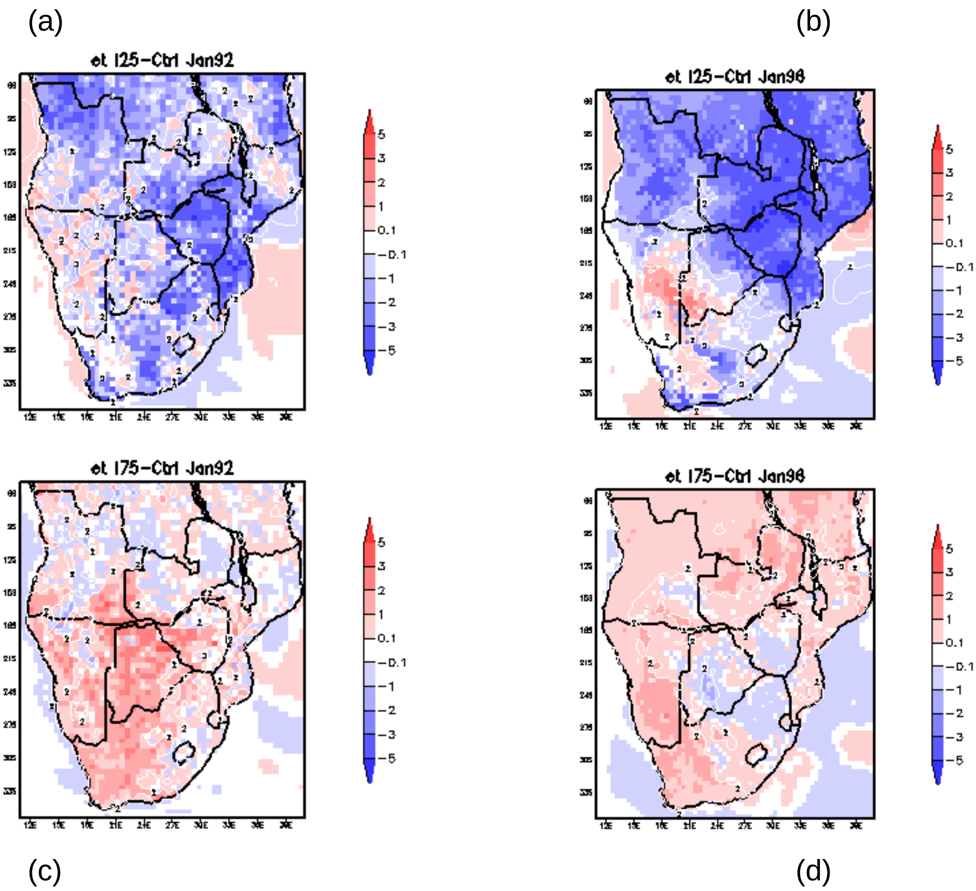

Figure 16**:** Evapotranspiration anomalies interactive experiments from the control simulation for January 1992 (a&c) and 1996 (b&d).

2.4.2.9 Incident short wave solar radiation

Figure 17 shows the incident solar radiation differences for the different soil moisture initializations from the control simulation for January 1992 and 1996. Both increases and decreases of up to 60 W/m^2 are apparent in different regions during 1992. Interactive dry soil moisture experiment from the control simulation (Figure 17a) results in an increase in incident solar radiation over eastern half of the subcontinent except for central Mozambique with some slight reduction. The most notable reduction in incident solar radiation is over Angola, Namibia and western Botswana. In the wet interactive experiment (Figure 17c), slight decreases in incident solar radiation is attained. Marked and significant decreases occurred over eastern Angola and western Zambia.

(a) (b)

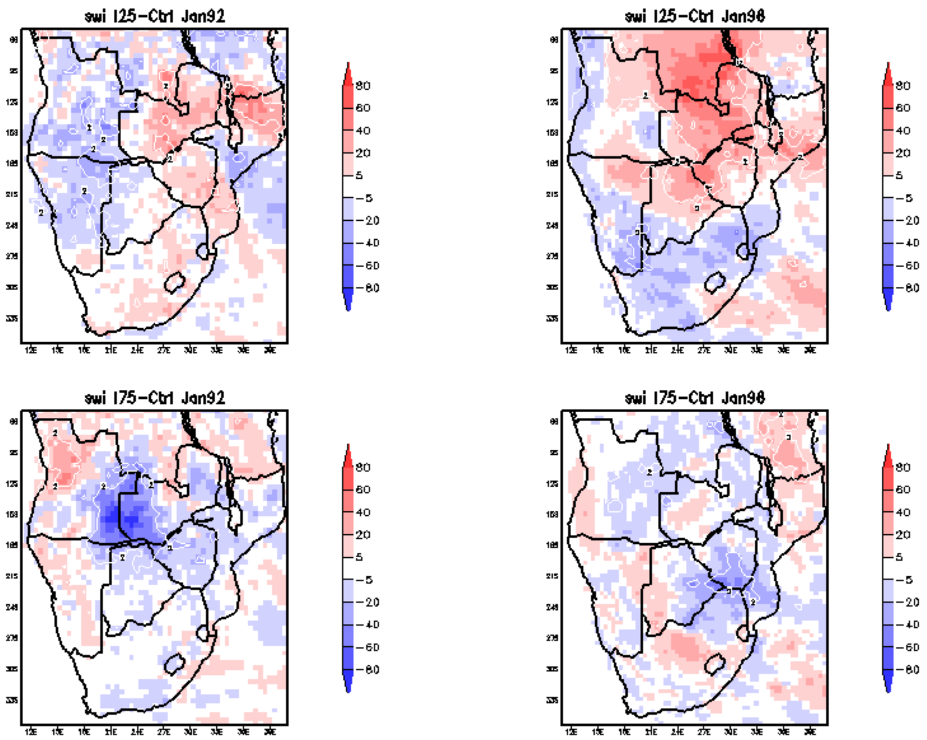

(c) (d)

Figure 17**:** Incident solar radiation anomalies interactive experiments and control simulation for January 1992 (a&c) and 1996 (b&d).

For January 1996, Figure 17 (b&d) shows incident solar radiation differences between the interactive experiments from the control simulation for both dry and wet soil moisture conditions. Figure 17b shows the interactive dry soil moisture initialization which has positive anomalies over the most of northern parts of the region with a reduction in incident solar radiation over west coast and the southern parts of region. Significantly marked increases in radiation occur over western Zimbabwe and southern DRC. For the interactive 75% field capacity for wet soil moisture conditions (Figure 17d), the incident solar radiation is showing some mixed responses. There are negative anomalies, notably especially over Zimbabwe, eastern Botswana, northern South Africa, central Mozambique as well as some slight reductions over northern parts of the region. Elsewhere, there are slight increases in incident solar radiation. Only small portions of the region exhibit statistical significance at 95% level for incident solar radiation, highlighting that this variable is significantly correlated to changes in cloud which is a spatially heterogeneous variable.

2.4.2.10 Surface sensible heat fluxes

Figure 18 shows sensible heat anomalies of interactive soil moisture experiments from the control simulation for January 1992 (a&c) and 1996 (b&d). For the dry soil moisture perturbations during 1992, Figure 18a, there is an increase in sensible heat over the subcontinent except for parts of the western areas (parts of Angola, Namibia, Botswana and western South Africa) where there is a decrease. Marked increases in sensible heat occur over southern Zambia, northern Zimbabwe, southern Malawi and northern Mozambique. Under wet soil moisture initializations (Figure 18c), there is a decrease in sensible heat for most areas except for the northern parts of the region. Notable reduction in sensible heat occurs over Namibia, Botswana and western South Africa. Slight increases in sensible heat are observable over northern parts of the region. Large portions of the region's sensible heat is statistically significant at 95% level and thus emphasise the importance of the relationship between sensible heat and soil moisture, especially during a dry season.

(a) (b)

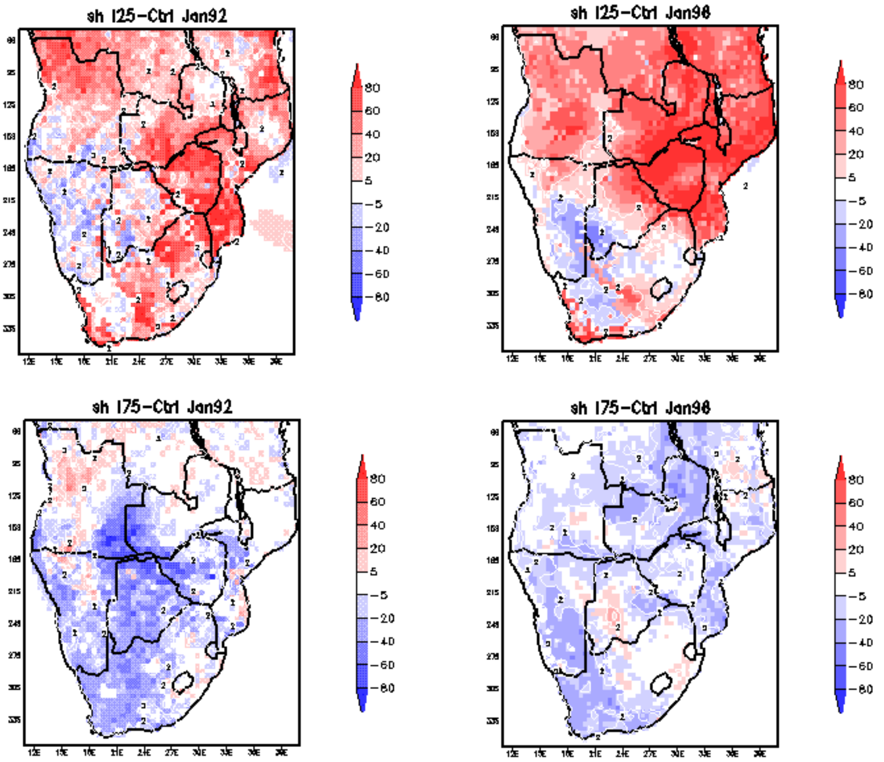

(c) (d)

Figure 18: Sensible heat anomalies interactive experiments from the control simulation for January 1992 (a&c) and 1996 (b&d).

For interactive wet soil moisture initializations during 1996 (Figure 18d), a negative anomaly is attained over southern Africa except for southeastern parts covering Zimbabwe, Swaziland, Lesotho and southeastern South Africa where no major change occurred. Marked increases in sensible heat are mostly confined to the west coastal areas, southern Namibia and western South Africa. Under interactive dry soil moisture perturbation for January 1996, Figure 18b, there is an increase in sensible heat over most of the region except for southwestern parts encompassing southern Namibia, southwestern Botswana and parts of South Africa where there is a significant decrease. Southeastern parts of South Africa and central Lesotho show no change in sensible heat. An area covering southern Namibia, southwestern Botswana and western South Africa always leads to a decrease in sensible heat for all the soil moisture perturbation setups whilst no major change in sensible heat occur over central Lesotho and southeastern parts of South Africa. The responses of sensible heat over southern Namibia, southwestern Botswana and western South Africa is to reduce during both years.

2.4.2.11 Planetary boundary layer

Figure 19 displays planetary boundary layer anomalies of interactive soil moisture initialization experiments from the control simulation for January 1992 (a&c) and 1996 (b&d). Under dry soil moisture conditions during 1992 (Figure 19a), there is a elevation of the PBL for most of the region except for the western parts especially Namibia, southwest Botswana and western South Africa where a significant lowering of the PBL occurs. Marked rises in PBL although not statistically significant occur over northern Zimbabwe and southern Zambia. Wet soil moisture perturbation experiment (Figure 19c), show a lowering in PBL over the bulk of the subcontinent especially over western areas where significant reduction of 400 m to 600 m occurs over northern Namibia, northwestern Botswana and southeastern Angola. Slight rises of less than 100 m in the PBL are mainly confined to the northern parts of the region.

(a) (b)

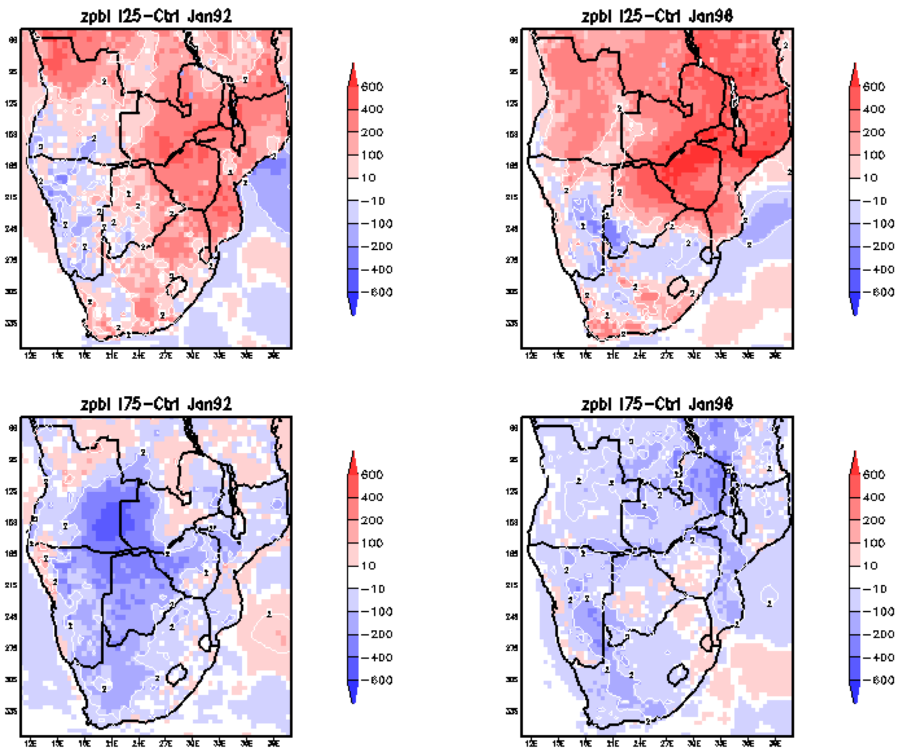

(c) (d)

Figure 19: Planetary boundary layer anomalies interactive experiments from the control simulation for January 1992.

Figure 19d shows planetary boundary layer differences for the interactive wet soil moisture experiments during 1996; a lowering in the PBL occurs over much of the region and a slight rise of less than 100 m in PBL occur over parts of Zimbabwe and northeastern portions of South Africa. Under interactive dry soil moisture conditions, Figure 19b, most of the region results in a rise of PBL, in places in excess of 400 m. Exceptions occur over to the south of the region covering southern Namibia, southwest Botswana, northern South Africa and Swaziland where the PBL lowers by about 400 m in some areas. Notable areas of west coast of Namibia, southern Namibia, southwestern Botswana and part of western South Africa have a PBL lowering for all forms of soil moisture perturbations.

2.4.2.12 Soil moisture anomalies

During the interactive 25% simulation for 1992 (Figure 20a) most of the region experiences drier soils than the control simulation. Only parts of northeastern South Africa and western coastal areas show an increase. This is a similar result to that obtained for the dry run during 1996 (Figure 20b) with the reduction in soil moisture persisting over much of the northern regions, especially southern Zambia and Zimbabwe. The main differences appear to the south where the initial soil moisture reduction becomes an increase during the 1996 season, due to the different synoptic circulations which are more conducive to the advection of moisture and rainfall. A vast portion of the area exhibiting soil moisture decreases led to unique responses for most of the variables analysed here signifying a considerable influence of soil moisture conditions within the surface-atmosphere layer. Major decreases of about 15 mm in top soil moisture occur over central Zimbabwe

(a) (b)

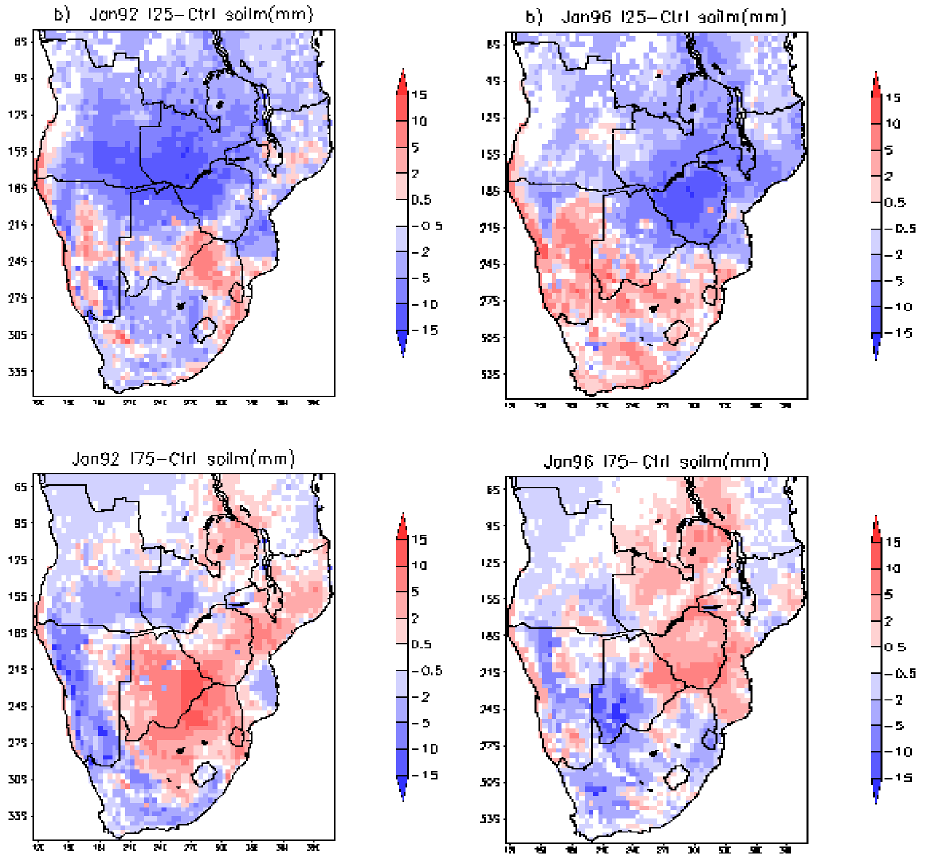

(c) (d)

Figure 20: Soil moisture anomalies from the perturbation experiments and control simulation for January 1992 (a&c) and 1996 (b&d).

The interactive wet runs (Figure 20 c&d) tend to maintain their initial positive soil moisture perturbation over the central parts of the region. The location of the central anomaly tends to be shifted in each season; it is more central during 1992 and more northerly during 1996. Marked decrease of 10 mm occurs over southwestern Botswana. Again this highlights that the maintenance of the soil moisture anomaly is dependent on the synoptic forcing of the regional climate model. These experiments also suggest there is a tendency to maintain a negative anomaly further north and a positive soil moisture anomaly further south.

2.4.2.13 Moisture Fluxes

Figure 21 displays the control run of January 1992 and 1996 depicting moisture flux (g kg^{-1} ms^{-1}) at 2mfrom the surface in RegCM3 model. Generally, the sources of moisture influx are shown to be the adjacent Indian Ocean and less being advected inland from the tropics. Very little to dry moisture is advected inland up the west coast as it is more of a southerly component. Inland, most of the moisture flux is in the easterlies passing over Zimbabwe, Zambia and Botswana. An anticyclonic circulation over north South Africa pushes some of the moisture back into the Indian Ocean and some diverging into the cyclonic circulation in the Mozambique Channel before heating landfall. Intuitively, some source of moisture must be inland waters or soil moisture already retained from the already prescribed (see figure on top soil moisture). January 1996, representation of moisture flux in the control run gives more influx from the northwesterlies down from the east coast and the easterlies from the Indian Ocean advecting more moisture inland than in January 1992. The same scenario of southerlies up the cold west coast is presented like in January 1992. Generally, there is also more moisture influx inland in January 1996 than in

January 1992. This is a very useful factor to consider on some of the weak responses to soil moisture perturbation in January 1996.

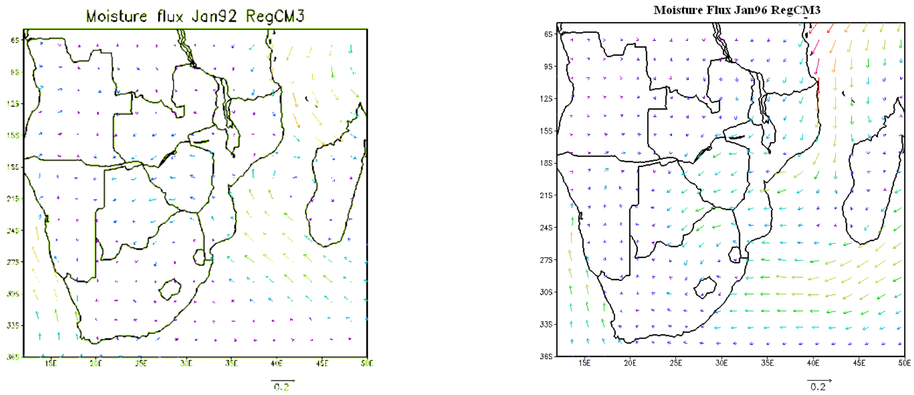

(a) (b)

Figure 21: depicts the direction and magnitude of moisture flux (g kg^{-1} ms^{-1}) for January 1992 (a) and January 1996 (b) in the RegCM3 at 2 metres above surface.

(a) (b)

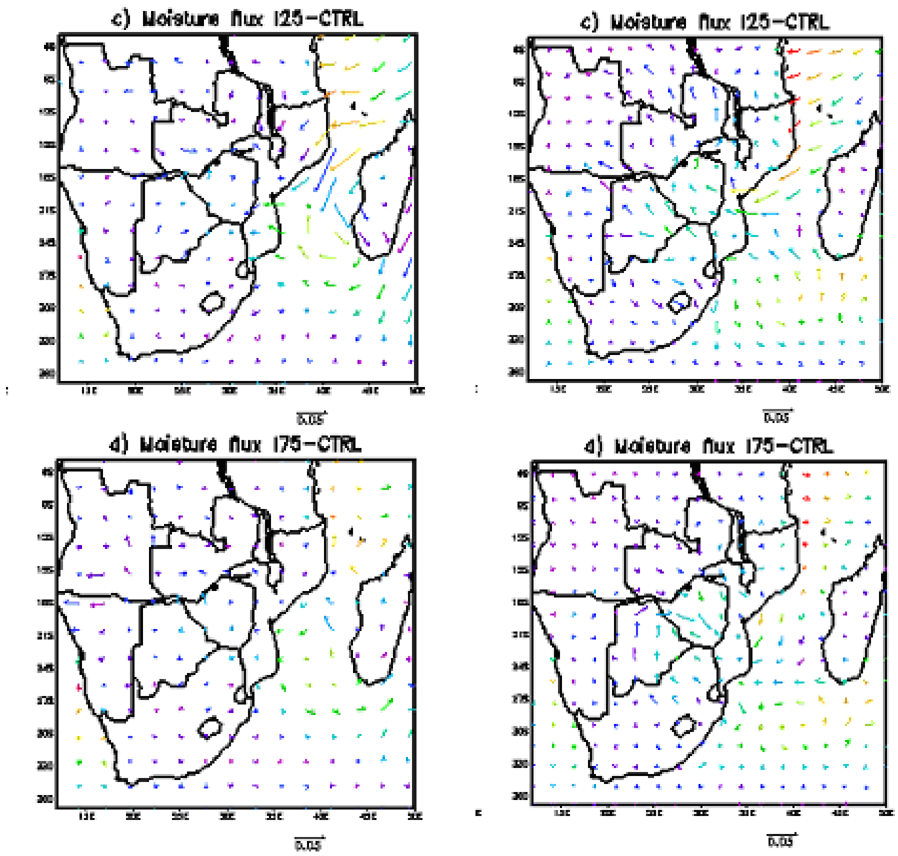

(c) (d)

Figure 22: The direction and magnitude of 2mmoisture fluxes anomalies (g kg^{-1} ms^{-1}) for January 1992 (a&c) and 1996 (b&d).

Direction and magnitude of moisture flux anomalies (g kg^{-1} ms^{-1}) of the soil moisture perturbation experiments from the control show a marked increase in moisture flux inland from the northeast during the dry experiment (Figure 22). There is also an increase in moisture flux from the Mozambique Channel for both dry soil moisture perturbation experiments, which is perhaps an indication of an enhanced north east monsoon sue to the increased heating and convection over land. A pronounced cyclonic circulation occurs over the Mozambique Channel during 1992 which could enhance rainfall in that region and draw moisture from the continent. Anomalies are generally less for the wet experiments during both years. The most notable change in moisture flux is the cyclonic circulation which develops over northern South Africa during 1996.

2.4.2.14 Geopotential height at 700 hPa

Consistent changes in 700 hPa geopotential heights are demonstrated in Figure 23 with both dry experiments inducing positive anomalies (> 25 m) over the central subcontinent. These anomalies are greater and further west during the dry year of 1992 suggesting the spatial extent and intensity are dependent on the synoptic forcing. In contrast the wet initialisations induce negative anomalies during both years, with a greater anomaly during the wet 1996 year. It is noteworthy that a negative anomaly also develops to the east of Namibia in both of the wet initialisation experiments.

(a) (b)

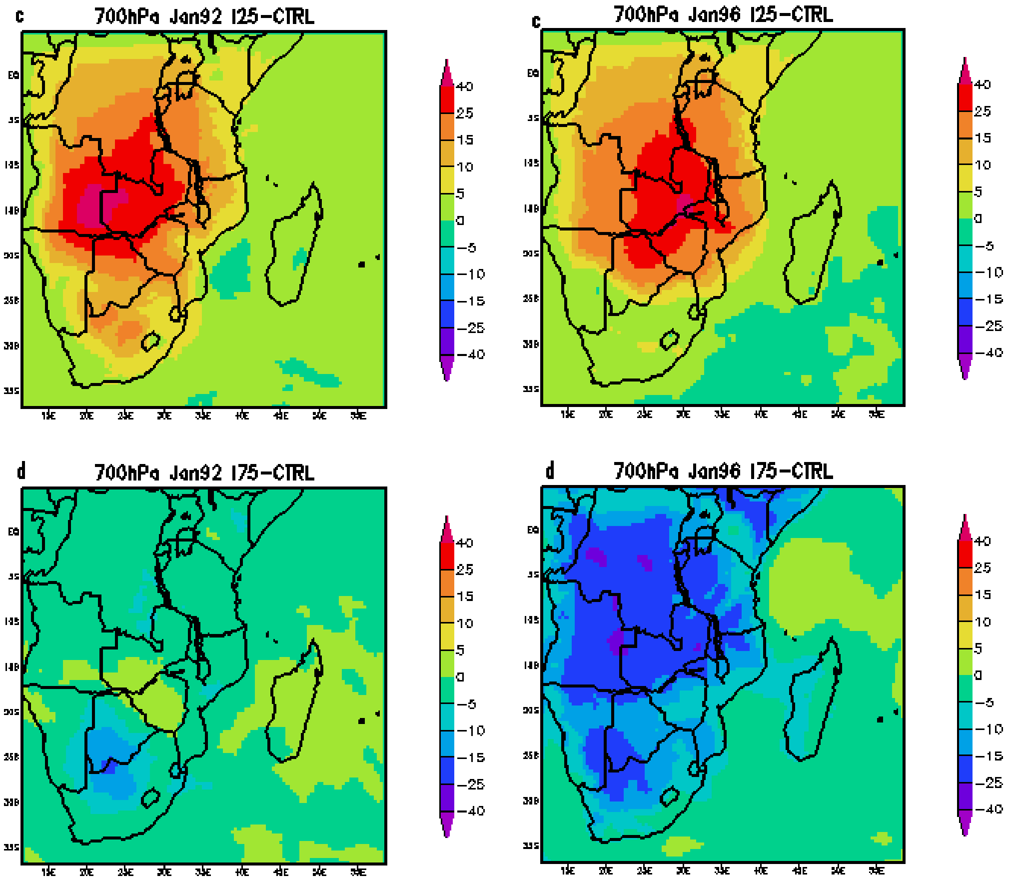

(c) (d)

Figure 23: Geopotential height anomalies at 700hPa for the soil moisture perturbations from the control for January 1992 (a&c) and 1996 (b&d)

These results clearly demonstrate that the soil moisture perturbation has a greater effect on the circulation of the lower atmosphere when the perturbation is consistent with the synoptic forcing i.e. if there are dry (e.g. anticyclonic) large-scale changes then a drier soil moisture initialisation will have a greater effect, whereas if the synoptic forcing is wetter than a wet soil moisture initialisation will interact to produce the greatest change in circulation.

2.4.2.15 Vertical Profiles

Cloud liquid water path (CLWP) is the column amount of liquid water in the cloud and is used to derive cloud optical thickness which is a very important component in the radiation scheme. CLWP plays an important role in the transport of energy (latent heat) in the earth-atmosphere system. Figure 24 shows the vertical profiles of the CLWP (g m^{-2}) for January 1992 and 1996. The control experiment (shown in solid black) is showing an almost similar profile with interactive wet anomalous experiment (yellow line) though the interactive wet run has slightly more liquid water in the upper atmosphere with a CLWP value of 14 g m^{-2}. This can support the point that these experiments have more convective rainfall activity occurring due to higher moisture contents in the vertical profile. The similarity in the top of profile CLWP values could be attributed to most of the top cloud being thin cirrus ice cloud with less influence on optical depth. The interactive dry anomalous soil moisture experiments have less CLWP than the control run throughout the profile. Importantly the level at which the profiles have their maximum CLWP, which indicates the levels at which cloud is most abundant, is most different between the control and dry interactive runs. It appears that whilst both runs reach a maximum of CLWP at level 0.9, the control run maintains higher amounts to higher levels (0.65 as opposed to 0.75). This suggests that the amount and thickness of cloud is partly determined by the soil moisture initialisation, which is also in accord with the results seen for changes in the incident short wave radiation.

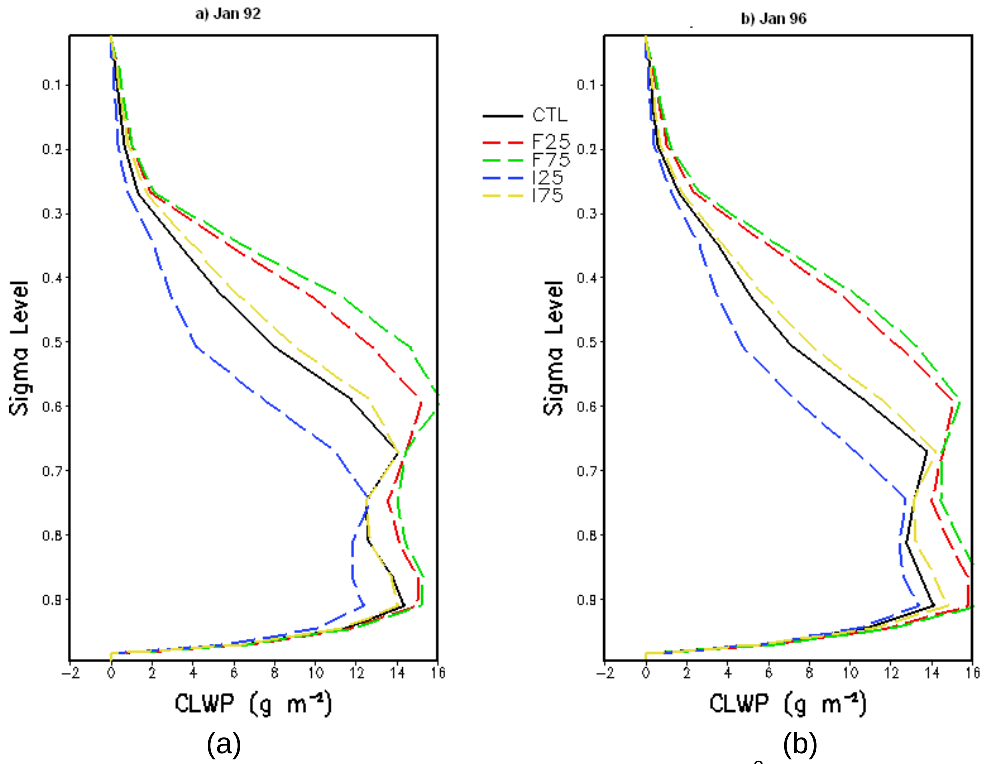

Figure 24: Vertical profiles for cloud liquid water path (g m^{-3}) for the perturbed and control simulations in January 1992 (a) and 1996 (b).

2.5 Vegetation experiments

Three experiments were developed, all of which are complimentary though focussed on different aspects of modelling climate-vegetation interactions. The first experiment utilised MM5 to study the impact of human changes in land use on the regional climate. The second experiment is designed to elucidate the sensitivity of the climate to changes in vegetation fraction (the main representation of vegetation inter-annual variability in the RCM used for these experiments). The third experiment examines more closely, and for a smaller domain over South Africa (due to computational constraints), the effect of changing land surface parameterisations (the representation of soil and vegetation in the model of the land surface).

2.5.1 Climate sensitivity to anthropogenic land use change

This work formed the basis of Neil MacKellar's PhD and was published in the International Journal of Climatology. It involved firstly simulating an idealised natural vegetation of southern Africa using a state of the art vegetation model: the Sheffield Dynamic Global Vegetation Model (SDGVM).

2.5.1.1 SDGVM and vegetation data

Two representations of spatial vegetation distribution are used. Present-day vegetation is given by the United States Geological Survey (USGS) global half-degree resolution classification, whereas an estimate of potential natural vegetation is simulated by the Sheffield Dynamic Global Vegetation Model (SDGVM; Woodward *et al.*, 1995; Woodward and Lomas, 2004a). SDGVM is designed to predict potential natural vegetation from estimates of precipitation, temperature, relative humidity and CO2. The model includes subroutines for biomass, phenology, hydrology, carbon and nitrogen cycling, and dynamics (i.e. transition between vegetation states). The resulting vegetation is predicted in terms of six possible plant functional types (PFTs), namely C3 and C4 grasses, evergreen broad- and needle-leaf trees, and deciduous broad- and needle-leaf trees, as well as bare ground. SDGVM simulations compare adequately with alternate data sources at both local and global scales (Woodward *et al.*, 1995; Cramer *et al*., 2001; Woodward and Lomas, 2004a) and the model has been deemed appropriate for applications in southern Africa (Bond *et al*., 2003; Woodward and Lomas, 2004b).

For this study, the input variables of monthly precipitation, surface temperature and relative humidity are provided by the University of East Anglia's Climatic Research Unit (CRU) land surface climatology (New *et al*., 1999, 2000). Since the smallest time step in SDGVM is 1 day, the model estimates daily values from the CRU monthly data (Woodward and Lomas, 2004a). Mean annual CO2 concentration is taken from a time series produced by the Hadley Centre for the period 1830-2100. Initial estimates of soil carbon and nitrogen are derived by integrating a simplified version of the model, consisting of the carbon and nitrogen dynamics and net primary productivity (NPP) modules, under a constant climate until an equilibrium solution is reached. The resulting conditions are then used to initialize a spin-up integration using the full SDGVM system. At the start of the spin-up, land cover is set to represent an even distribution of all PFTs. CRU climate data is taken from the period 1971-1990 and is cycled repeatedly to provide input for a 500-year integration. CO2 is set at a constant partial pressure of 29 Pa for the duration of the spin-up. The spin-up allows for vegetation structure to tend toward a steady state that can then be used to initialize a subsequent SDGVM run. Figure 1 displays the evolution of domain-averaged biomass for the four PFTs relevant to the region (i.e. C3 and C4 grasses, evergreen broad- and needle-leaf trees). After 200 years, all types are at a near-stable state. For the final simulation, SDGVM takes its initial state from the output of the spin-up and is run for a 30-year period (1971-2000) with observed climate and CO2. The mean proportions of PFTs predicted for this period are then grouped to approximate the USGS natural vegetation classes. This is done so that the same set of vegetation parameters can be used for both the USGS and SDGVM representations. The difference between the two vegetation maps thus represents a spatial shift in land surface parameters, rather than a change in the values of the parameters themselves. Previous modelling studies have identified albedo as a primary controller of surface radiative fluxes (e.g. Charney 1975; Charney *et al*. 1977; Dickinson and Henderson-Sellers, 1988; Dirmeyer and Shukla, 1994), surface roughness length (Z0) as a key parameter determining turbulent energy and moisture transfers in the boundary layer (Dickinson and Henderson-Sellers, 1988; Pitman *et al.*, 1993), and minimum stomatal resistance (RSMIN) defining the capacity for plants to transfer water vapour from their leaves to the air. The latter has not been subjected to much research, but is a potentially important parameter for forest vegetation that is not limited by soil moisture availability (Maynard and Royer, 2004). Green vegetation fraction is not specified according to vegetation type and LAI is given as a fixed value, so these are therefore not altered in this experiment. Since these are important parameters in the computation of evaporation and transpiration, the effect of vegetation change on surface moisture fluxes is likely to be underestimated.

The resulting vegetation map was them imported into the MM5 regional climate model and used to simulate the climate of southern Africa for the 1988/89, 1991/92 and 1995/96 early and late summer seasons. These simulations were then repeated with the standard USGS land use map (which includes human changes to the land surface and vegetation) and compared to those simulations using the natural vegetation.

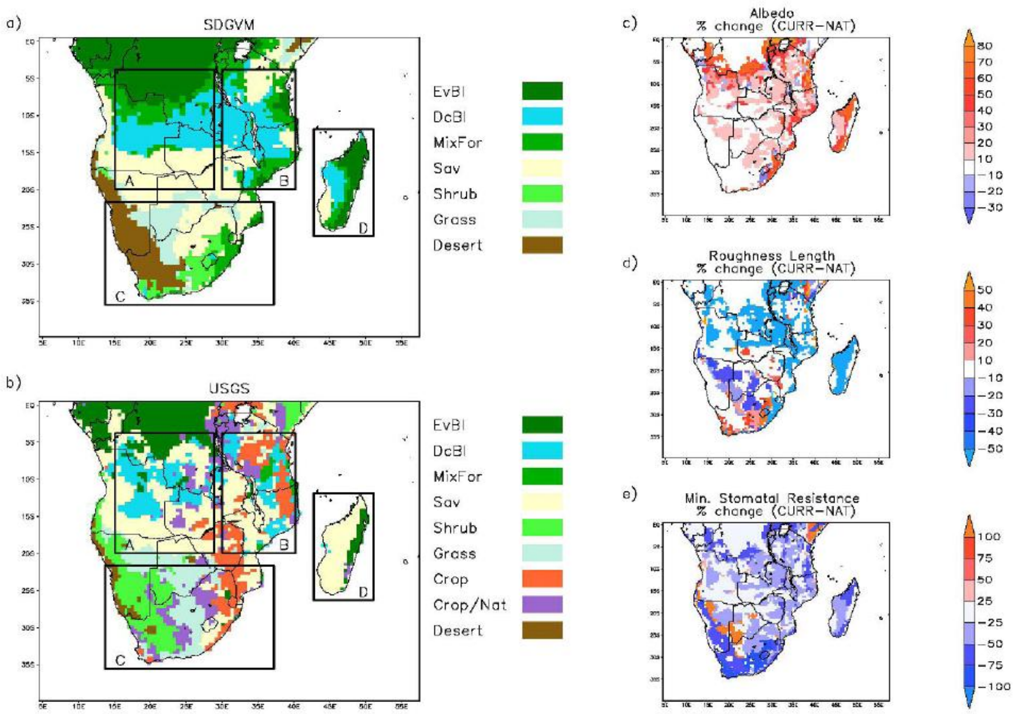

Figure 25: Vegetation maps for a) SDGVM (NAT) and b) USGS (CURR), with boxes denoting sub-regions CENT (A), EAST (B), SOUTH (C) and MAD (D). Differences in c) albedo, d) roughness length and e) minimum stomatal resistance between CURR and NAT

2.5.1.2 Modelled changes in vegetation

Figure 25 shows the vegetation classification of the southern African land surface using both SDGVM and the standard map from the USGS. One of the major differences is that the USGS classification includes crops and agricultural land which is one of the major human influences expected from anthropogenic land use change. The figure also clearly demonstrates that there are significant differences in how MM5 represents (parameterises) the land surface in each case; large differences are shown for albedo (increases up to 50%), roughness length (decreases by over 50%) and minimum stomatal resistance (reductions of over 25%).

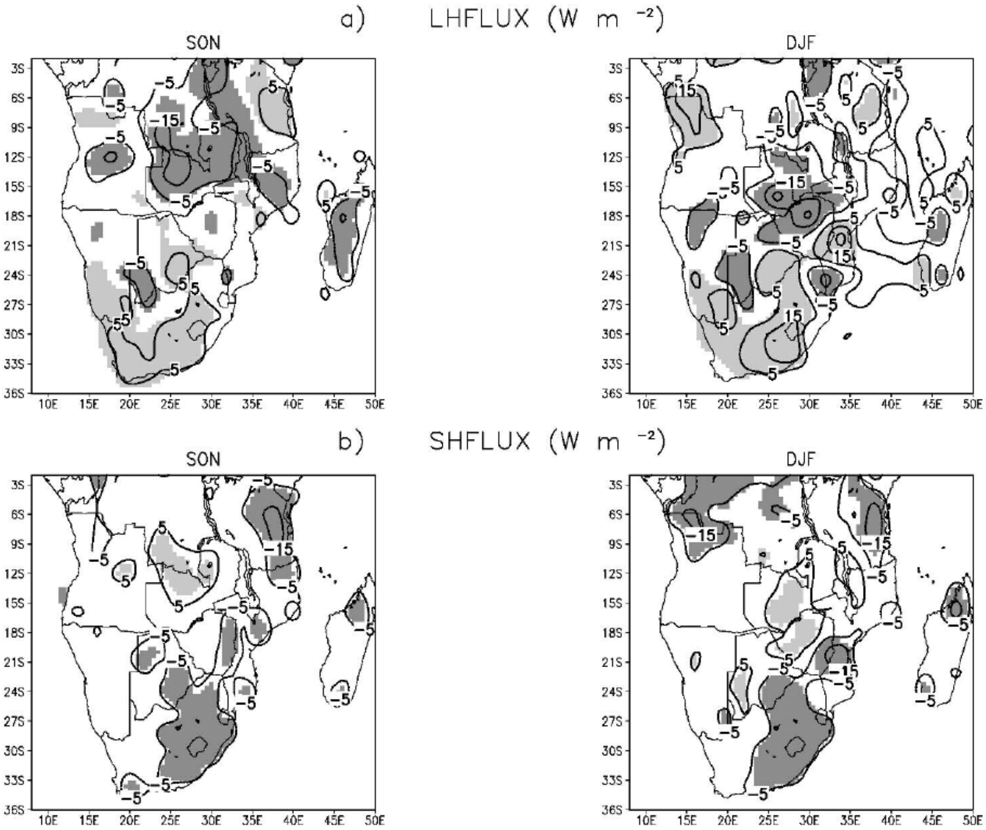

Figure 26: Difference (CURR-NAT) in simulated latent and sensible heat fluxes during SON and DJF (averaged for all 3 years). Grey shading indicates differences significant at the 95% confidence level.

2.5.1.3 Modelled changes in climate

Figure 26 clearly shows that the changes in land use result in statistically significant changes in both latent and sensible heat flues during both the SON and DJF seasons (averaged over all 3 years). Changes in LHFLUX are spatially more widespread than changes in SHFLUX in both seasons. Figure 27 indicates the resulting changes in rainfall, 700 hPa geopotential heights (GPH) and vertical profile of GPH. Rainfall changes are statistically more significant (over a wider region) during SON as opposed to DJF and this is reflected in the changes in lower troposphere (700 hPa) GPH, which are more spatially extensive during SON. The vertical profile of GPH lends further evidence to the effects being larger during SON than during DJF – increases below 500 hPa and decreases above (suggesting a geostrophic response to the surface anomaly) are greater during SON than during DJF.

Overall these results which are averaged over 3 seasons, covering an El-Niño, La Nina and neutral season, suggest that anthropogenic land use change has a greater influence on the regional climate during early spring than it does during mid-summer – at least partly due to the different synoptic forcings occurring during these different seasons, further emphasising the importance of anticyclonic circulations during spring for these land surface feedbacks.

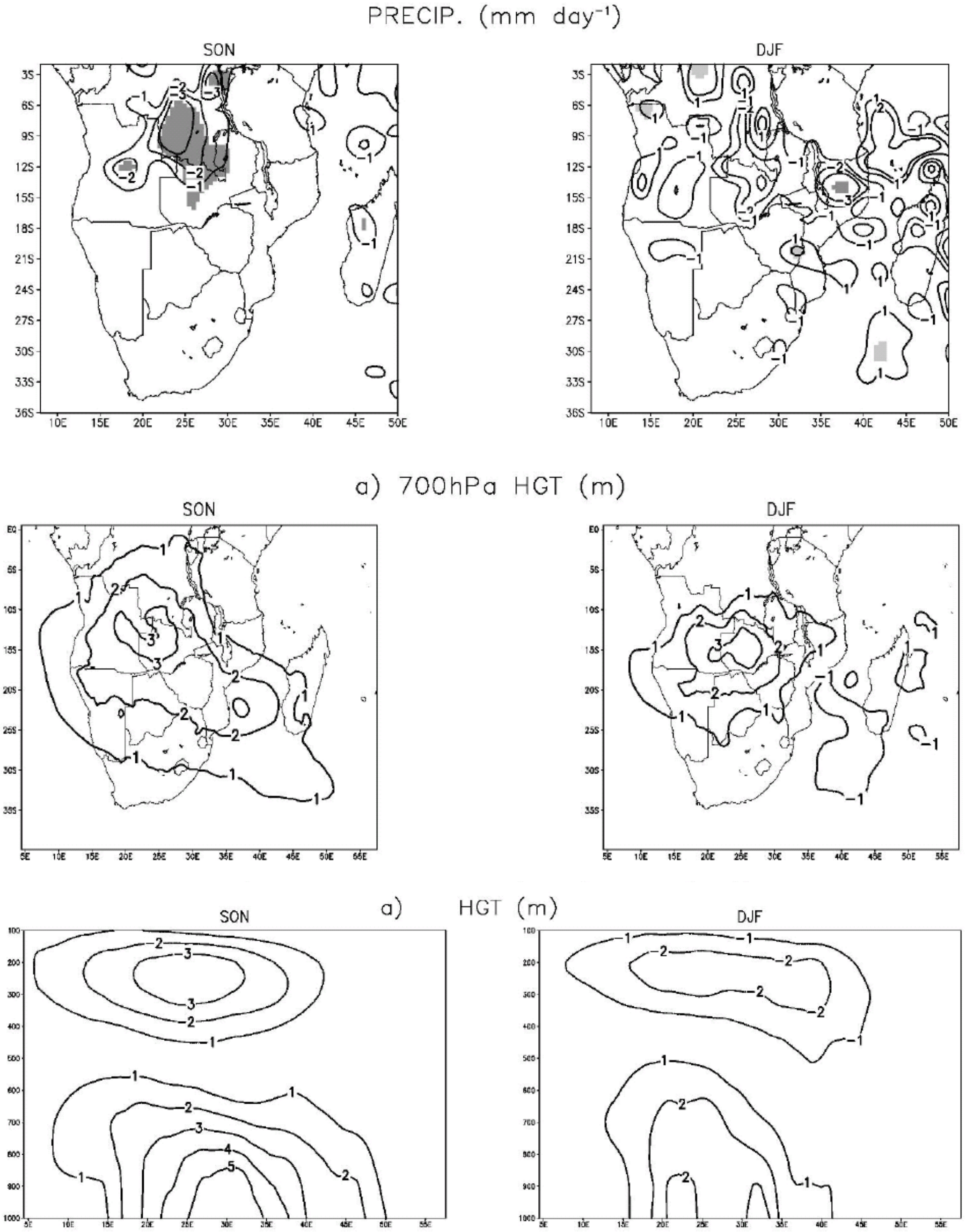

Figure 27: Changes in rainfall (shading indicates significance at the 95% level), 700 hPa geopotential height and vertical profile of changes in geopotential height for the SON and DJF seasons.

2.5.2 *Climate sensitivity to changes in vegetation fraction*

In order to understand vegetation-climate feedbacks on Southern Africa, 2 sets of simulations were performed. The modeling tool for these simulations is the Weather Research and Forecast Model (WRF, developed by NCAR). The main goal of these experiments was to simulate the role of the interannual variability of vegetation on the sub-continental climate.

2.5.2.1 Experimental setup

Except for the vegetation dataset used to represent the Green Vegetation Fraction (GVF) of each grid cell, the two simulations are identical and are described in Table 1.One of the simulations was performed using a 5-year climatology of GVF (CONTROL simulation) and the other was performed with the monthly values of GVF for each month of the integration, thus reproducing the interannual variability of vegetation (INTER simulation). The GVF dataset was generated using NDVI data after Gutman and Ignatov (1998). Note that these simulations were carried out at 15km resolution which is a significantly higher resolution than the other experiments in this report. The WRF model was run on the Centre for High Performance Computing (CHPC) which greatly speeded up the computations, allowing us to run at this higher resolution.

Table 1**:** Parameters of the interannual vegetation simulations

	CONTROL	INTER
GVF Dataset	1997/2001 Climatology of Green Vegetation Fraction	Monthly Values of Green Vegetation Fraction
Period:	Jan/1997 - Dec/2001	
Horizontal Resolution	15km	
# of vertical levels	28	
Input Data	NCEP Reanalysis I (Kalnay et al 1995)	
Parameterisations Schemes	Betts-Miller (Cumulus) - YSU (Boundary Layer) - WSM 6-Class (Microphys) - RRTM (Shortwave Radiation) - Dudhia (Longwave Radiation) - Noah Land-Surface Model	

2.5.2.2 Use of Self Organising Maps (SOMs) to disaggregate synoptic forcings

Both CONTROL and INTER simulations outputted daily data, which for the 5 years of the simulation period produced enough members for an analysis using Self Organizing Maps (SOMs, Hewitson and Crane, 2002). This analysis seeks to understand in a more objective manner one of the major issues highlighted in the previously described work; namely how the response of the local climate (to the surface perturbation) is dependent on the large-scale synoptic circulation. In the analysis applied here, the SOMs were performed on the NCEP input daily data (850 hPa geopotential heights and specific humidity). When SOMs are applied to any particular data, similar nodes will group close to each other in the self-organizing map and, consequently, different nodes will stay far of each other. A 7 x 5 SOM was applied to the NCEP daily data used as lateral boundary conditions for the simulations. Figure 28 shows the result of the 850 hPa geopotential heights SOM and its possible to see the increase of high pressure values (subsidence, dry conditions) as we look towards nodes in the lower-right corner, with the opposite conditions showing in the upper-left corner (vertical uplift, wet conditions). Figure 29 shows the same analysis applied to specific humidity data in conjunction with the geopotential height data in Figure 28. The nodes show increasingly wet conditions towards upper-left corner of the map and dry conditions towards lower right corner.

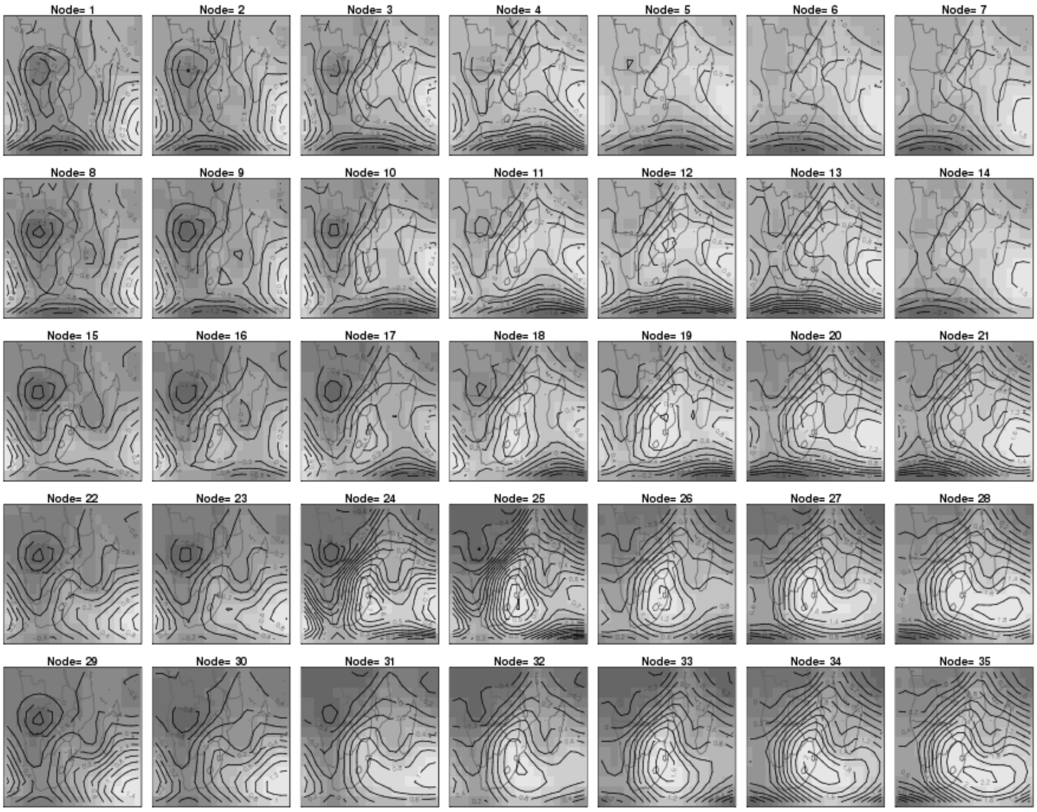

Figure 28**:** SOM analysis of 850 hPa geopotential height NCEP data.

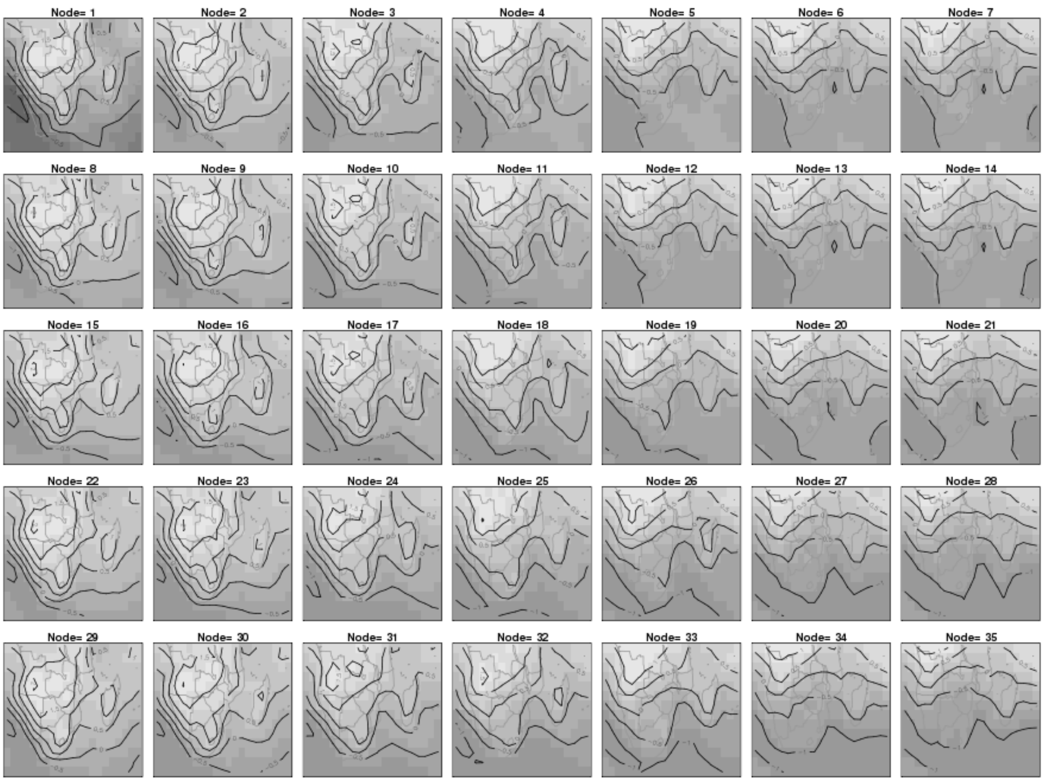

Figure 29**:** SOM analysis of 850 hPa specific humidity NCEP data.

After applying this SOM to the NCEP lateral boundary conditions for each day, the corresponding days of the CONTROL and INTER simulations were mapped to each node so that the impact of interannually-varying vegetation could be determined under different synoptic conditions i.e. different synoptic forcing of the lateral boundary conditions. Since each node represents days with different synoptic patterns, this makes it possible to produce the INTER-CONTROL differences for each of these synoptic patterns.

Figure 30, Figure 31 and Figure 32 show, respectively, the difference INTER minus CONTROL of number of rainy days, 2mspecific humidity and 2msurface temperature for the days of each node in Figure 28 and Figure 29. The three figures clearly demonstrate how the simulated impacts of interannual variability of vegetation are stronger under the dry conditions represented by nodes on the right-hand side of the SOM. Whereas wetter synoptic conditions represented by nodes on the left-hand side produce differences that are less in magnitude and spatial consistency, indicating that the impacts of biosphere-atmosphere coupling are stronger when the synoptic scale forcing is for dry conditions. It is particularly noticeable that differences in the rainfall and humidity fields are only present over ocean (and coastal regions such as Mozambique) during the wet synoptic conditions to the left of the SOM, whereas differences in surface temperatures are present over land under all synoptic forcings. This emphasises further that rainfall is influenced more by large-scale synoptic circulations, whereas surface temperature is driven more by changes in land-surface characteristics and the resulting partition of local energy fluxes into sensible and latent heat components. This also helps to explain why the results are spatially noisy for rainfall and less so for specific humidity and surface temperature, which is not surprising given the heterogeneous nature of rainfall and given similar observations for the soil moisture experiments. Note also that these vegetation experiments are conducted at a much finer resolution (15 km) than the soil moisture experiments which will result in further spatial heterogeneity.

Figure 30: Difference in number of rain days (Inter - Control) for each node (different synoptic forcing)

Figure 31: Difference in 2-meter specific humidity (Inter - Control) for each node (different synoptic forcing)

Figure 32: Difference in 2msurface temperature (Inter - Control) for each node

2.5.3 *Climate sensitivity to specification of land surface model parameterisation*

Another key aspect to be evaluated when doing atmosphere-vegetation interaction simulations is the model sensitivity to the vegetation representation. Besides the GVF dataset shown before, several vegetation parameters are featured in WRF model representing different vegetation characteristics. WRF model has as a coupled land surface model the Noah LSM (Chen and Dudhia, 2001). Noah is a comprehensive soil-vegetation-atmosphere transfer model with 4 soil layers and snow-cover effects; Figure 33 shows a schematic representation of the model.

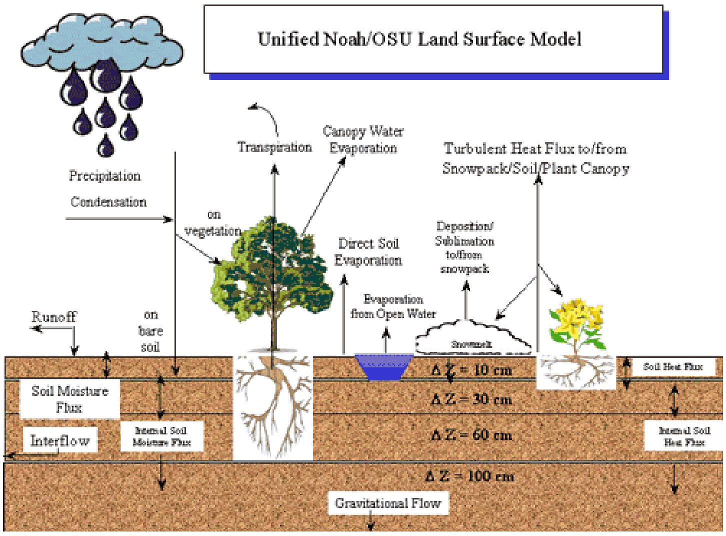

Figure 33**:** Schematic Representation of Noah LSM

Noah LSM has prognostic equations for the moisture and energy fluxes to/from the different actors in the system (soil, canopy, atmosphere and snow cover). These equations depend on a series of parameters that are statically assigned within the model code and are dependent of each plant functional types (vegetation category). These parameters, as default in WRF code, are calibrated for mid-latitude situations and may not represent realistically the vegetation in Southern Africa. Table 2 shows the soil-vegetation parameters available in Noah LSM.

Table 2**:** Noah LSM soil-vegetation parameters

Z0	Roughness length (m)
SHDFAC	Green vegetation fraction (in percentage)
NROOT	Rooting depth (layer)
RS	Minimum stomatal resistance (s m-1)
RGL	Parameters used in radiation stress function
HS	Parameter used in vapour pressure deficit function
SNUP	Threshold snow depth (in water equivalent m) that implies 100% snow cover
LAI	Leaf area index (dimensionless)
MAXALB	Upper bound on maximum albedo over deep snow
TOPT_DATA	Optimum transpiration air temperature
CMCMAX_DATA	Maximum canopy water capacity
CFACTR_DATA	Parameter used in the canopy interception calculati
RSMAX_DATA	Max. stomatal resistance
BB	B parameter
DRYSMC	dry soil moist threshold where direct evap from top soil layer ends (vol.)
F11	Soil thermal diffusivity/conductivity coef.

MAXSMC	porosity, i.e. saturated value of soil moisture (volumetric)
REFSMC	soil moisture threshold below which transpiration begins to stress (vol.)
SATPSI	SAT (saturation) soil potential
SATDK	SAT soil conductivity
SATDW	SAT soil diffusivity
WLTSMC	wilting point (volumetric)
QTZ	Soil quartz content

2.5.3.1 Experimental setup

From this list of parameters, some were chosen for sensitivity tests in a domain smaller than the one shown earlier. These tests were conducted in a project with IBM using the 'World Community Grid' system, which is a grid-computing solution provided by IBM where users can donate idle CPU time to run scientific codes. For these sensitivity tests, the simulations were designed as described in Table 3 for the domain shown in Figure 34.

Table 3**:** Description of Sensitivity Experiments

Period:	378 days
Horizontal Resolution	30km
# of vertical levels	28
Input Data	NCEP Reanalysis I (Kalnay et al 1995)
Output Frequency	3-hourly

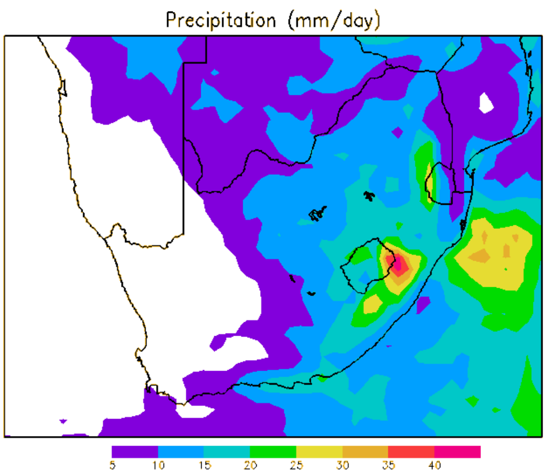

Figure 34**:** Domain used in the sensitivity tests.

Four parameters were chosen from Table 2 to be analyzed in the sensitivity tests. Leaf Area Index (LAI), Minimum Stomatal Resistance (RS), Porosity (MAXSMC) and Soil moisture threshold below which transpiration begins to stress (REFSMS). These parameters were perturbed as shown in Table 4**Error! Reference source not found.**. Each of the four parameters was tested with 3 different values (3 ** 4 = 81 simulations). An extra simulation was performed as a control simulation with all the parameters unperturbed, i.e. with the default values plus LAI equals 4, which is the Leaf Area Index values that WRF originally prescribes for all the vegetation categories.

Table 4: Description of Sensitivity Experiments

RS	-50%	default	+50%
LAI	0.47	0.97	1.48
MAXSMC	-20%	default	+20%
REFSMC	-20%	default	+20%

2.5.3.2 Initial results

Results of these sensitivity tests are still being analyzed, but some useful information could already be extracted. In particular the simulation of moisture fluxes near the surface shows sensitivity to LAI and RS. Analyzing the diurnal cycle of Latent Heat Flux (LH) we can see that the maximum simulated values of LH varies between 10 and 15% depending on the chosen value of LAI or RS (Figure 35). It is also possible to see that the original value for LAI of 4 generates a simulated maximum value of LH much higher than the more realistic values tested in these experiments. Since the values used here were chosen according to satellite-derived information for the region, this suggests that the default value of LAI may be a weak representation of Southern Africa vegetation.

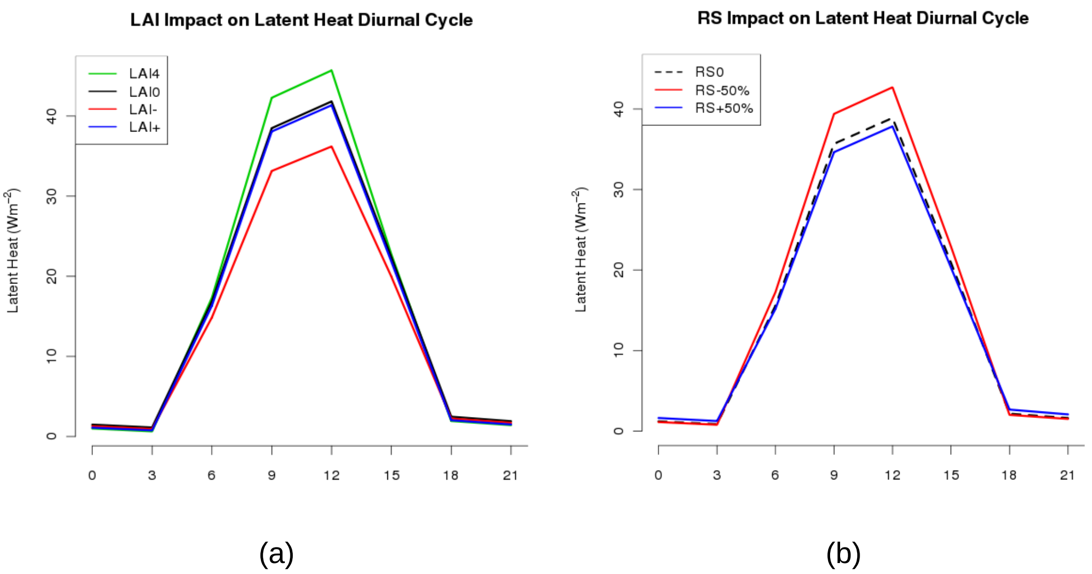

Figure 35: LH Diurnal Cycle Sensitivity to LAI (a) and RS (b)

2.6 Aerosol modelling

This is a new field within the CSAG group, though has long been recognised as important. It necessitates some collaborative work with other aerosol modellers, both locally and internationally. We have 2 PhD students working in this field; one is currently visiting the CNRS in Toulouse, France where she will stay for 6 months (she is focussing on long simulations using RegCM3 to simulate the direct effect of aerosols on the radiation budget); the other is focussing on the role of biomass burning (using the regional climate model WRF-Chem) in determining aerosol load and its effect on the regional climate (both direct and indirect effects, see Figure 36). It is important to distinguish between direct and indirect effects both because of the different physical mechanisms associated with each and the amount of computational resources each requires to be able to model them. Direct effects refer to the direct scattering and absorption of solar radiation, whereas indirect effects refer to the indirect effects on the radiation balance through changes in the formation and duration of clouds with aerosols acting as cloud condensation nuclei (CCN). Whereas a complete simulation would include both sets of effects, it is useful to simulate direct effects alone, not the least because it is less computationally intensive and allows for longer simulations. Currently, simulating both indirect and direct effects restricts simulations to the order of months (even on the CHPC).

Both of these student projects are producing results relevant to this project as the peak biomass load is generally found in late winter/early spring around September and it is known to have a significant effect on the radiation budget at the surface (both through direct and indirect effects). Some initial work detailed below demonstrates how this is likely to affect the regional circulation and stable layers within the atmosphere.

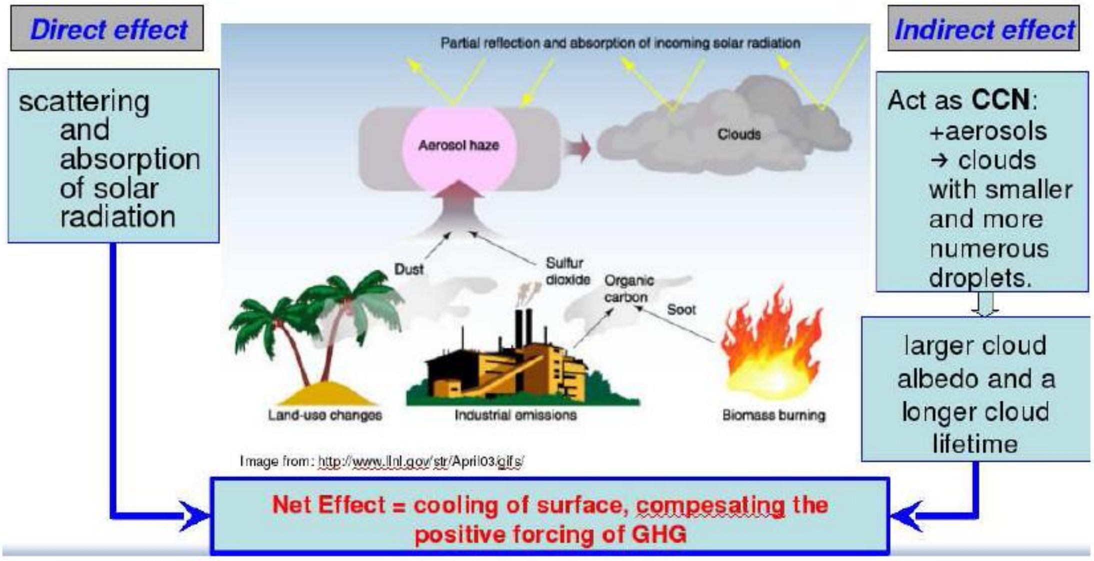

Figure 36: Effects of aerosols, via direct and indirect effects, on the climate of southern Africa

2.6.1 Biomass burning using WRF-Chem

Biomass burning is known to be a significant contributor to aerosol concentration in continental tropical regions and the corresponding radiative effects may often be much more dramatic than those attributed to greenhouse gases on local and regional scales (Rosenfeld and Feingold, 2003; Keil and Haywood, 2003). However, quantifying the impact of biomass burning aerosols on regional and/or global models is problematic, due to their physical, chemical, and optical properties; their spatial and temporal distribution in the atmosphere, difficulties in characterizing their effects, and a low level of scientific understanding of their radiative effects (Abel et al., 2005; Haywood et al., 2003). As part of common agricultural practices in southern Africa, the savanna vegetation is periodically subjected to extensive biomass burning which loads heavy amounts of aerosols into the atmosphere (Crutzen and Andreae, 1990; Helas and Pienaar, 1996; Scholes et al., 1996; Schmid, 2003; Swap et al., 2003) which are in turn kept in the region by a circulation pattern called *gyre* (Scholes et al., 2001). Approximately 50% of fine air particulate matter in the lower troposphere is composed of carbonaceous aerosols (organic and elemental carbon) (Pöschl et al., 2005). In this work, the state-of-the-art Weather Research and Forecast model coupled online with Chemistry (WRF-Chem) is being used to investigate the possible impacts of varying the rates of carbonaceous aerosols emission from biomass burning on the surface shortwave radiation (SSW) over southern Africa.

2.6.1.1 Setting up the model with the GFED database

Initially there were several problems to overcome before starting to use WRF-Chem for simulating the southern African climate. These initial steps involved:

1. "Artificial" transference of biomass emissions from the Northern America subcontinent to southern Africa to test the ability of the model to run for our region;
2. Successfully test-run WRFChem and simulate the concentrations of various aerosol types at atmospheric heights at which they may play a role in cloud formation and, therefore, in precipitation;
3. Format the data in the Global Fire Emissions Database (GFED) (Randerson et al., 2007) so that it could be read by WRF-Chem. This was successfully achieved and an example of emissions from the database for 1998 is given in Figure 37

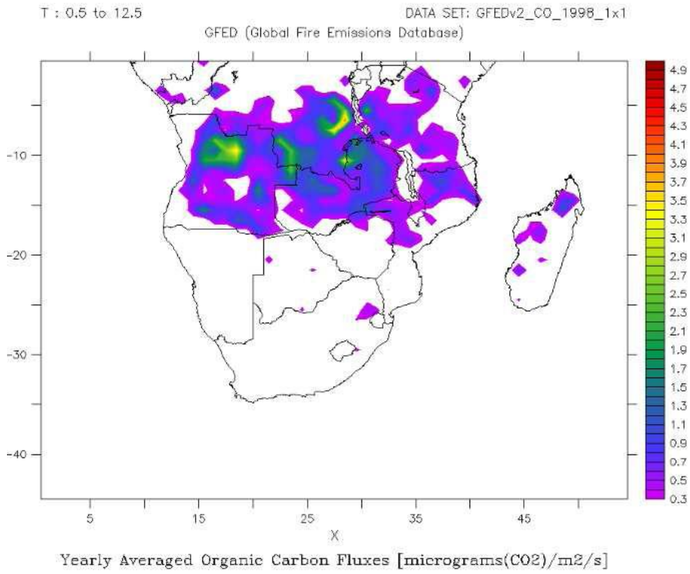

Figure 37: Annually averaged emissions for 1998 from the GFED database.

Observed emissions for the 1997-2005 period are shown in Figure 38. They indicate a clear seasonal cycle, with emissions peaking in most years during August. Some years, e.g. 2005, indicate an earlier peak in July. Also noticeable is the interannual variability, as exemplified by the difference in peak concentrations in 1998 ($1.4e^{-11}$) and 2004 ($7e^{-12}$), a factor of 2 (100%) difference.

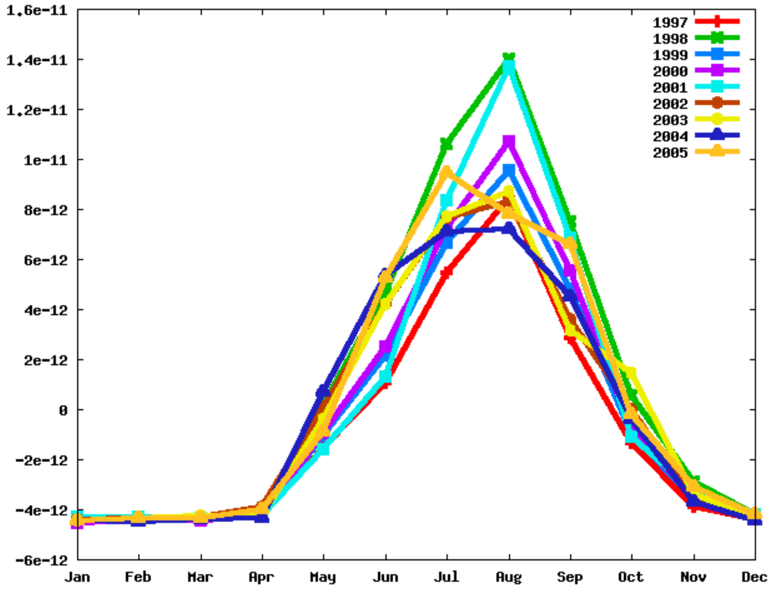

Figure 38: Observed emission anomalies from the GFED database for the 1997-2005 period.

2.6.1.2 Initial modelling results

Figure 39 demonstrates the average difference (1997-2005) in incident surface shortwave (SSW) radiation that WRF-Chem simulates when emissions are included. The average SSW decreases by -7.71 Wm-^{2}, with a maximum decrease of -34.2 Wm^{-2} during late August/September, when emissions are included. This decrease in energy cools the land surface and can reduce instability.

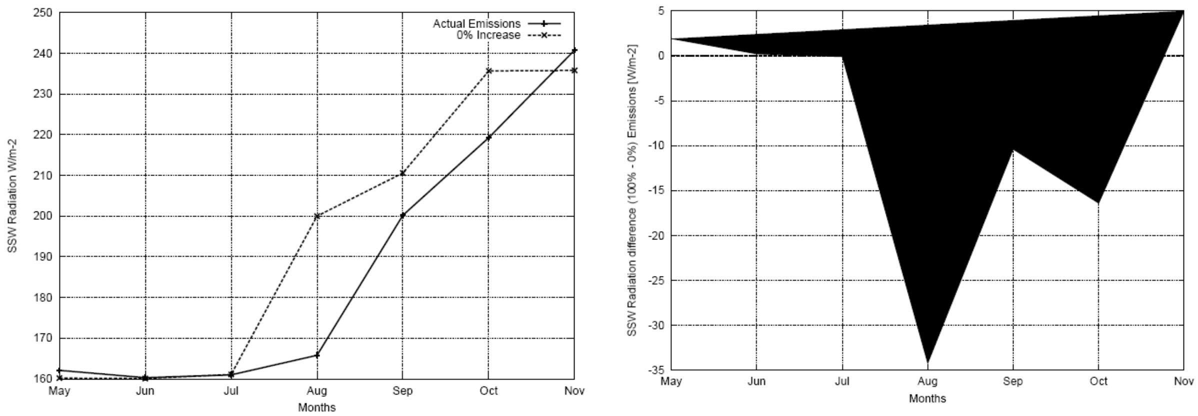

Figure 39: (a) Incident surface shortwave radiation with observed and zero emissions. (b) Difference in incident surface shortwave radiation.

Figure 40 demonstrates the changes in other chemical species which are also included in the GFED database. These chemicals also affect the radiation balance simulated by the model, as well as the distribution of cloud condensation nuclei which affect the radiation balance through indirect effects on clouds.

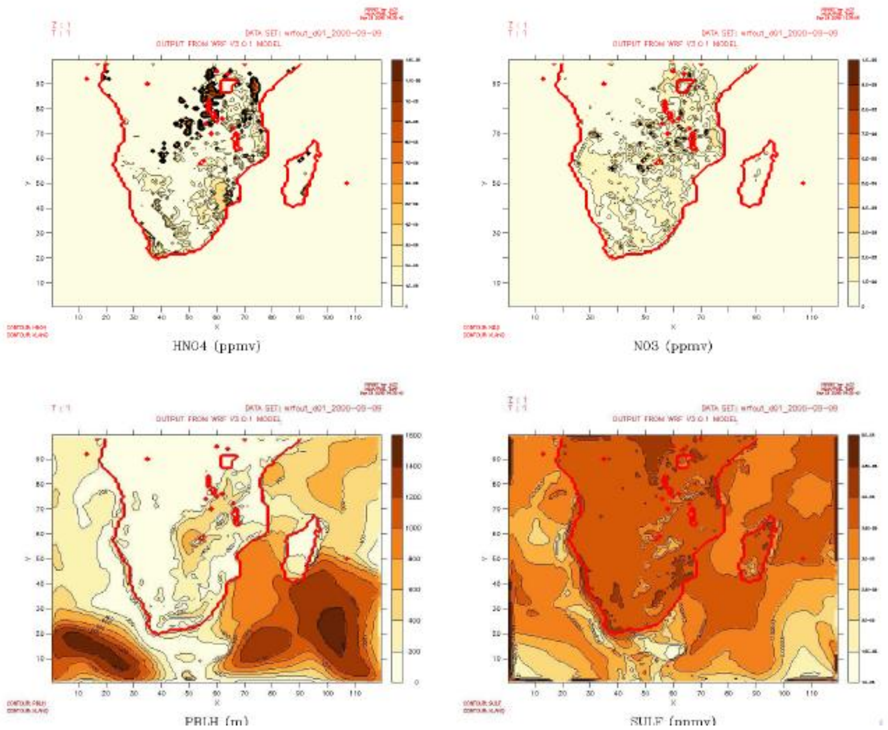

Figure 40: Changes in HNO_4, NO_3, PBLH and Sulphates included in the GFED simulations.

2.6.2 Modelling the direct effect of aerosols using RegCM3

This work has been undertaken as a collaborative effort between CSAG and the University of Toulouse. It seeks to utilise the RegCM3 regional climate model to simulate the impact of biomass burning and mineral aerosols on the radiation balance of southern Africa. Importantly, RegCM3 only includes the direct aerosol effect (a difference from the previous experiment with WRF-Chem, which includes both the direct and indirect effects). Because of this RegCM3 is computationally less expensive, allowing experiments to be undertaken for much longer periods (potentially including climate change simulations). It is also noted that the emissions source for these experiments is calculated at the University of Toulouse and may differ from the GFED database used in the WRF-Chem experiments. So far 2 simulations (one including aerosols and their radiative effect, the other without) for the April 2000 to December 2006 period have been undertaken. Both black and organic carbon aerosols (both hydrophobic and hydrophilic) are included in the aerosol simulations. The domain used for the simulations (at 50km spatial resolution) is shown in Figure 41.

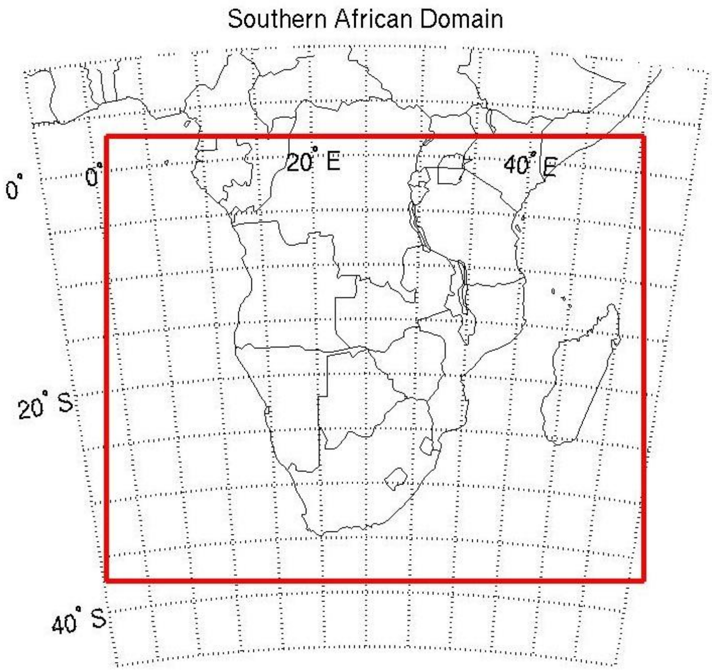

Figure 41: Domain for the RegCM3 simulations (at a spatial resolution of 50km)

2.6.2.1 Comparison of RegCM3 AOD with satellite measurements

Figure 42 shows the difference between aerosol optical depths (AOD) simulated by RegCM3 and those measured by MODIS and MISR for the June-August period between 2001 and 2006. From these comparisons it is clear that RegCM3 overestimates the AOD over Angola (which is a major source and pathway for emissions emanating over the tropical regions) and underestimates AOD over tropical regions further north.

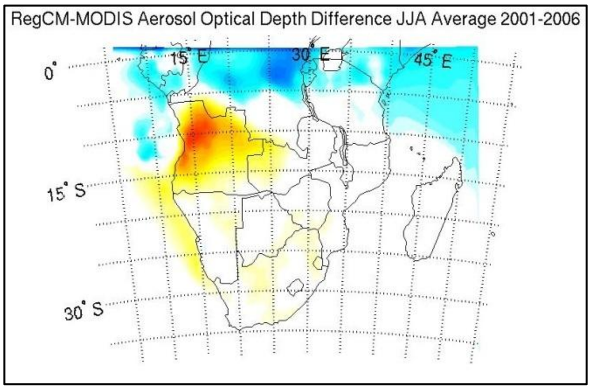

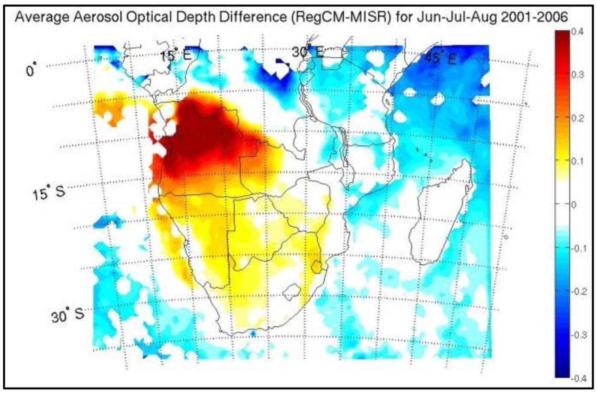

Figure 42: Difference between aerosol optical depth simulated by RegCM3 and measured by (a) MODIS and (b) MISR

Even so comparison of AOD measured and simulated at Mongu, Zambia, demonstrate a reasonable correspondence with realistic interannual and seasonal cycles (Figure 43a). There is, however, a detectable shift in the peak of simulated AODs; RegCM3 tends to simulate an earlier peak of AOD in July/August, whereas the AERONET observations suggest a later peak during August/September. This suggests that at least for this location the model is either advecting aerosols away from the region too early (due to anomalous atmospheric dynamics) or the dry/wet deposition (which removes aerosols) in the model is too vigorous or that the emission sources peak too early in the season. Figure 43b shows the same results for a different location: Skukuza, South Africa. Here there is also a more clearly a negative bias in the RegCM3 simulations during the summer periods (seen to a lesser extent at Mongu). It is likely that this is the result of not including anthropogenic aerosols in these simulations. Since Skukuza lies approximately 100km east of the Highveld, a region which produces approximately 46% of Africa's electricity, mostly through coal, the AOD is affected by the fairly high levels of SO_4 advected over the region. Similarly to at Mongu, the simulated peaks in AOD occur 0-2 months later than in the observations at this location.

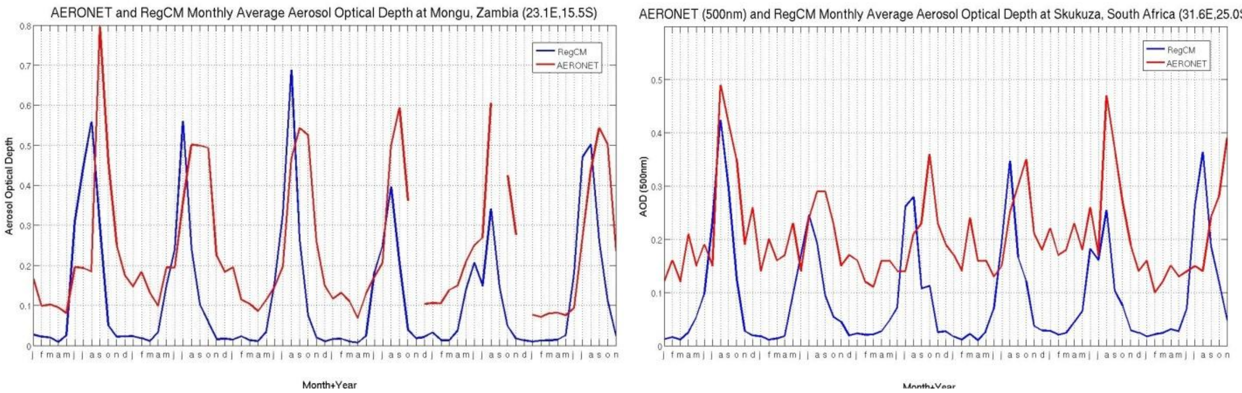

(a) (b)

Figure 43: Comparison of AOD simulated (RegCM3) and observed (AERONET) at (a) Mongu, Zambia and (b) Skukuza, South Africa.

2.6.2.2 Simulated changes in radiation and temperature

Figure 44a indicates the difference in SSW (aerosols – no aerosols) simulated during August (2001-2006). Largest decreases correspond to the same regions where AOD is greatest. This results in decreases in simulated surface temperatures during the June-August season over most of the sub-continent (Figure 44b).

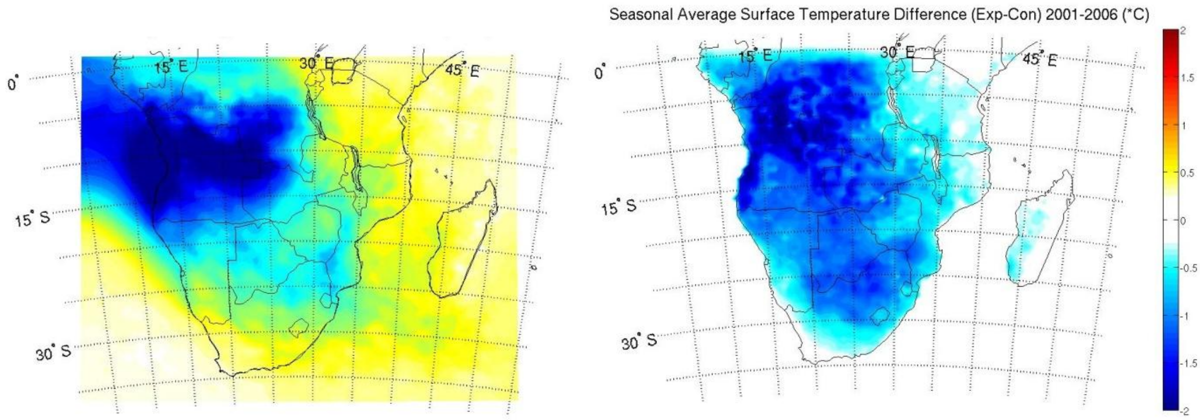

(a) (b)

Figure 44: Difference in simulated (a) SSW (aerosols – no aerosols) during August (2001-2006) and (b) simulated surface temperatures (June-August)

Besides these differences in surface temperature, aerosols also affect the vertical profile of temperature. This is largely because the dark, biomass burning aerosols within the atmosphere absorb incoming radiation (increasing the temperature of the air around them), leaving less radiation to reach the surface and lower levels of the atmosphere (and therefore cooling these lower levels). This effect is demonstrated in Figure 45 where the biomass burning aerosols can be seen to increase the temperature at 600-750 hPa and decrease the temperature in the lower levels, mostly at latitudes north of 30°S. This represents an important dynamical change in the regional atmosphere; it has the effect of stabilising the atmospheric vertical profile, inhibiting convection and potentially increasing the persistence/intensity of subsiding high pressure systems which are common at this time of year over the subcontinent.

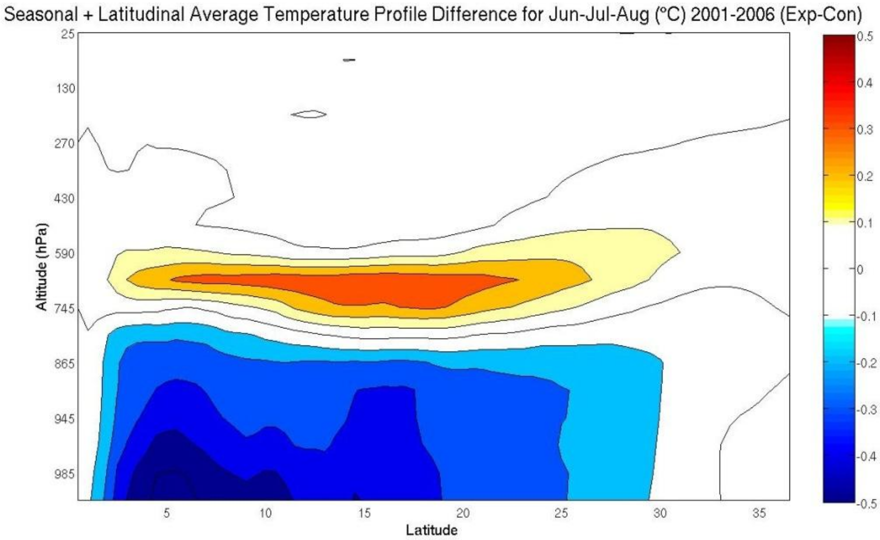

Figure 45: Vertical profile of average temperature differences (aerosols – no aerosols) for the JJA period (2001-2006)

2.6.2.3 Simulated changes in lower tropospheric dynamics and rainfall

Figure 46 shows the average difference (aerosols – no aerosols) in 510 hPa winds during September and clearly suggests an anomalous anticyclonic circulation centred over Zimbabwe. Whilst there are regions of anomalous divergence to the south and west of this circulation anomaly, there are extensive regions of convergence further north. Even so these regions do not necessarily produce rainfall as humidity levels are very low at this time of year.

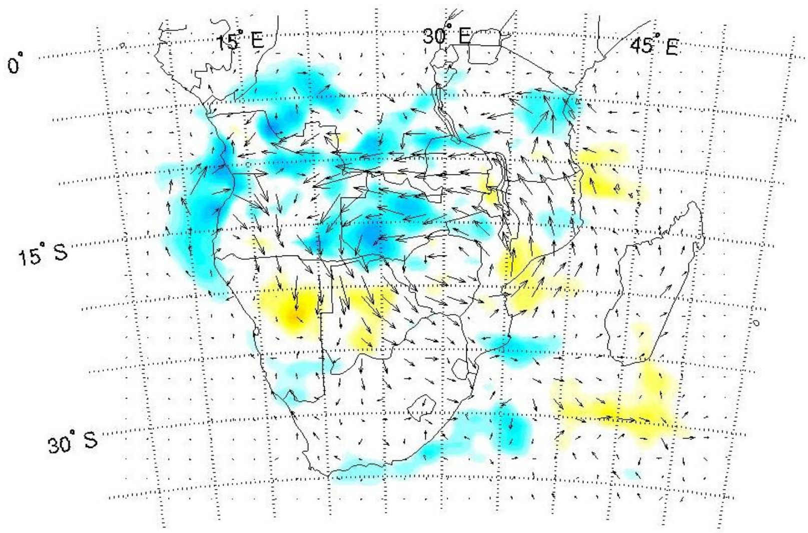

Figure 46: 510 hPa difference in winds (aerosols – no aerosols) during September (2001-2006)

Not surprisingly at this time of year the simulated effects on precipitation are small (there is little precipitation over the subcontinent during winter) as demonstrated in Figure 47a. Even so there are demonstrable changes in rainfall over regions of South Africa which receive rainfall during winter. Over the rest of the subcontinent there are clear differences in the height of the planetary boundary layer (Figure 47b), which is lower in the presence of aerosols. This is consistent with the cooling of the lower boundary layers demonstrated in Figure 45. Furthermore the changes in precipitation are accompanied by changes in clouds as represented by the cloud mixing ratio (Figure 47c) and regions of convergence in 745 hPa winds (Figure 47d). Differences in convergence and winds at these lower levels are consistent with the anticyclonic anomaly demonstrated in Figure 46, resulting in areas of divergence over Namibia and southwest South Africa.

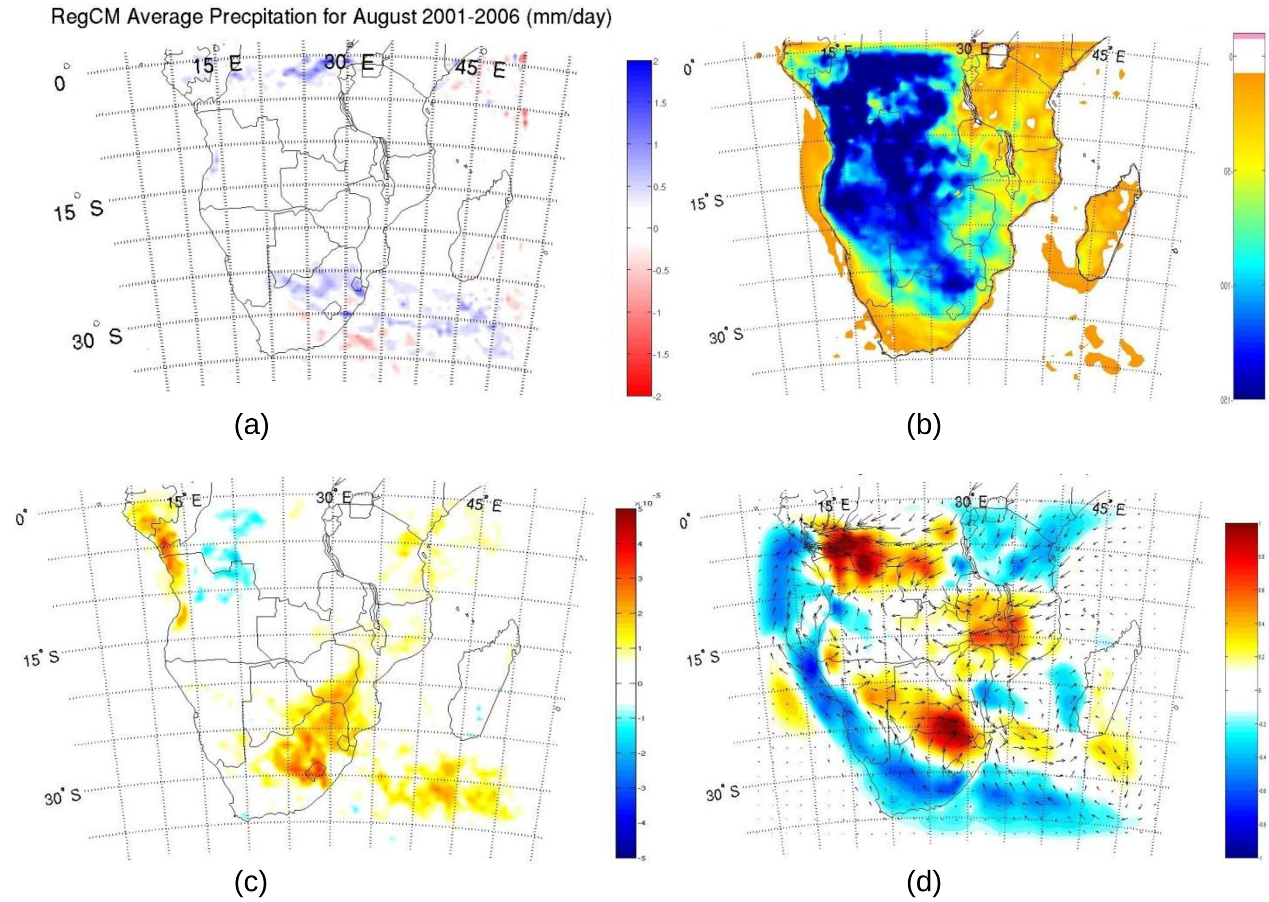

Figure 47: Simulated mean differences (aerosol – no aerosols), during August for (a) precipitation (mm day^{-1}), (b) plantary boundary layer height (m), (c) cloud mixing ratio (kg/kg) and (d) 745 hPa winds (ms^{-1}).

2.7 Summary of modelling experiments

The modelling work shown here will continue and form the basis of student research beyond the lifetime of this project. There has been great diversification in the approach to the modelling during the last 12 months. The inclusion of the aerosol modelling has made some initial inroads to fill a significant knowledge gap in our modelling of the known terrestrial forcings of southern African climate during the early summer season. Whilst all these modelling results provide a sound basis for understanding how these terrestrial forcings of climate work individually, there is plenty of scope for future work to understand how the climate may change when these forcings act together e.g. biomass burning produces aerosols but also reduces vegetation and alters the land surface at the same time.

Several clear messages are discernible from these modelling experiments:

- Soil moisture perturbations affect the lower boundary layers, more so in early spring than later in summer. Dry/wet soil moisture conditions have positive feedbacks with similar (wet/dry) synoptic forcings of the regional climate. The evidence in these experiments is that a dry forcing persists for longer and promotes a larger change in the regional circulation;

- Interannual changes in vegetation also have a larger effect (increased variability) on atmospheric conditions when the synoptic forcing is for drier (anticyclonic) conditions. Moving from a natural to human influenced land surface induces an anomalous anticylonic circulation, which would promote any similar synoptic forcing. The representation of vegetation in regional climate models is biased wrt observations and changing these parameters to be more realistic (e.g. reducing LAI) can reduce latent heat fluxes and the transfer of moisture to the atmosphere (this would be the equivalent of reducing soil moisture).
- Including the radiative effect of aerosols in the modelling of the regional climate during winter and early summer reduces incident shortwave radiation and consequent heating of the surface landmass. This and heating the atmosphere at height in the lower troposphere results in a more stable atmospheric profile and induces an anomalous anticyclonic circulation.

These experiments therefore suggest that including the effects of soil moisture, vegetation and aerosols has the potential to alter the simulated regional climate, more so in the lower troposphere. Changes are, however, dependent on the large-scale synoptic forcing and may act to enhance or mitigate those changes. The suggestion is that largest changes occur when the forcings act in concert and that the land surface will therefore influence the simulation of extreme wet/dry or hot/cold situations. In particular, such extremes are more evident when the land surface promotes hot/dry conditions under large scale dry (anticyclonic) synoptic forcing. In this manner it is not difficult to imagine increased aerosols, a dry land surface and reduced in vegetation all working in concert to promote and sustain anticyclonic large-scale forcings during winter/spring (when these circulations are common) and possibly influencing dry periods in summer – during wet periods large-scale circulations promoting rainfall and wet conditions will likely dominate any land surface forcing and will themselves eventually alter the land surface. Even so, given that one of the consistently modelled GCM climate change signals over the region is an increase in the intensity/spatial extent of anticyclonic circulations during winter/spring, interannual variability in these forcings could potentially have a greater impact in the future than at the present time.

3 Identifying locations where the local climate is dependent on antecedent conditions

Identifying locations where the local climate is dependent on antecedent land surface conditions, be it soil moisture, vegetation or even aerosol loads within the atmosphere, is extremely difficult. This difficulty has become apparent as the modelling of the effects of these different land surface forcings has progressed. The problem arises largely because the surface exchange of heat, moisture and momentum does not take place in a 1-dimensional sense with the overlying atmosphere, rather the three dimensional atmosphere responds by changing circulation patterns both laterally and in the vertical. This means that changes in the land surface at a particular location affect the climate at another location e.g. by changing circulation and moisture convergence in the overlying atmosphere. This problem is particularly significant for rainfall, which is highly dependent on regions of convergence and divergence in the atmospheric circulation, and usually occurs in the mid-troposphere at a distance from the source of the original surface change. Other climate variables, such as surface temperature are less affected by these considerations as the relevant atmospheric changes are in close proximity to and therefore more directly influenced by the surface perturbation.

3.1 Rainfall

It is therefore suggested from these results that identifying regions where rainfall is influenced by any of the antecedent conditions investigated here is exceedingly difficult. This is not to say that antecedent conditions do not influence rainfall, but that it is currently difficult to evaluate due to both its heterogeneous nature and that it is dependent on the changes in atmospheric circulation that are induced by the antecedent conditions. A further complication arises due to the choice of RCM in these experiments – different RCM simulate different baseline rainfall conditions e.g. one

RCM may simulate more raindays or less intense rainfall than another RCM. This alters the vertical distribution of changes in latent heating and therefore the simulated circulation changes, resulting in different changes in rainfall for the same change in antecedent conditions. Unfortunately we have carried out different experiments using different RCMs and so we cannot test how robust the changes in circulation/rainfall are to the choice of RCM i.e. compare the same experiment using 2 different RCMs.

3.2 Temperature

On the other hand surface temperature is more directly influenced by surface conditions; reducing (increasing) when soil moisture anomalies are positive (negative) and reducing (increasing) when aerosol anomalies are positive (negative). The influence of vegetation is more complicated as it depends on changes in several parameters e.g. albedo, roughness length, LAI and minimum stomatal resistance. However, often reductions in vegetation result in increases in albedo, decreases in LAI and decreases in minimum stomatal resistance, which reduces the amount of solar energy absorbed at the surface as well the amount of soil moisture transported to the atmosphere (therefore decreasing latent heat fluxes and increasing sensible heat fluxes). In the absence of rainfall (less solar radiation and increasing latent heat fluxes) this often leads to increasing surface temperatures, especially in arid regions.

3.3 Further investigations

Given that most of these feedbacks have their largest effects under subsiding anticyclonic conditions, it is not surprising that early spring, when these atmospheric conditions are more common, is a period when these antecedent conditions are simulated to have the greatest influence on regional climate. Therefore this period is potentially the best for observing when antecedent conditions affect rainfall patterns, though due to the complexity of the underlying atmospheric circulation anomalies it is not clear how rainfall could be related to antecedent conditions via a statistical forecasting approach. It is therefore recommended that the current approach to forecasting these relationships is to use General Circulation Models or Regional Climate Models, perhaps perturbing the initial conditions or periodically updating aerosols and vegetation as forecasts are made.

4 Potential for developing a forecast model which utilises information on antecedent conditions

One of the objectives of this project was to develop a forecast model which would incorporate measured quantities of pre-season (e.g. measured in August for a forecast made in September) antecedent conditions to predict the future characteristics of early-season rainfall and temperature. The original suggested method of doing this was to adopt an ANN (Artificial Neural Network) approach, which would capture the linear and non-linear relationships between antecedent conditions of soil moisture, vegetation and aerosols and rainfall/temperature at a particular location.

However, much of the regional climate model experiments undertaken in this project have only started to reveal consistent messages of change towards the end of the project, leaving little time to investigate the potential of developing a forecast model using the ANN approach. It was also expected that until there were clearly observable relationships between the antecedent conditions and surface climate variables in the modelling then pursuing an ANN approach would be difficult. Additionally any forecast model should be developed using only antecedent conditions shown to have a clearly demonstrated physical relationship with the surface climate. This was in part to make sure any forecast model was based on sound physical principals and therefore to avoid problems with overtraining and cross validation with predictor variables that may only be related to surface climate by chance i.e. training a forecast model which produces good forecasts for the training period but not at other times.

Even given the relationships demonstrated in the modelling experiments so far there are still important questions that should be answered before embarking on a approach using an ANN:

- The experiments so far have taken several approaches to modelling the anomaly of antecedent conditions: either raising/lowering antecedent conditions over the whole land surface (e.g. soil moisture experiments) or simulating an observed anomaly (e.g. vegetation and aerosol experiments). This raises the question of whether it is the absolute change in the fields or changes in the gradients that are mostly responsible for the simulated changes in climate;
- The relative contribution of the different antecedent conditions to surface climate variability is not clear i.e. for a particular period or location does soil moisture, vegetation or aerosols have a greater influence. Furthermore it is not clear to what extent interactions between the different components will be nonlinear, potentially leading to greater impacts than the sum of the different components;
- The impact of these antecedent conditions is clearly dependent on the large-scale synoptic conditions and it is not clear how to incorporate this dependence in an ANN training.

The implication of the last point is that it is necessary to include some measure or index of synoptic variability in the training of an ANN. In a simple sense this may be an index that captures the annual cycle; the modelling results suggest that the frequency of synoptic systems associated with strong land surface feedbacks is associated with the seasonality of the regional climate. However, this will not capture feedbacks that may be promoted when either the annual cycle deviates from its climatological norm (e.g. the start/end of the summer season is early/late) or when particular synoptic patterns are prevalent due to teleconnections with remote forcings e.g. ENSO, AAO etc. A further potential complication to this approach would be how to handle changes in circulation due to climate change; it may be possible to include say a temperature dependent variable that would resolve this, but it would have to be assumed that there is enough historical data to be able to resolve the components of change due to anthropogenic forcing and that this component will continue to change in a similar manner in the near future.

One way of handling changes in synoptic state which come about through remote teleconnections and climate change would be to use a GCM, forced by forecast or persisted SSTs, to make the forecast of the atmospheric fields. This approach is currently implemented within the group and so, given its ability to handle changes in synoptic state as well as its current implementation, is the preferred method for making forecasts. However, it is still not clear how to incorporate the changes in antecedent conditions within this forecasting scheme.

One option would be to run an RCM within the GCM forecast fields, incorporating changes to antecedent conditons in the same manner that the RCM experiments were conducted in this project. However, this is a computationally demanding process (though feasible given current computing resources) and potentially very complicated given uncertainties regarding the appropriate RCM configuration (e.g. which physics schemes are appropriate) and that no one RCM can accommodate or is set up to run with the varied and different antecedent forcings; that is partly why we have used 3 RCMs to test the range of antecedent forcings. Given these considerations it was decided not to implement forecasts using an RCM.

The latest implementations of GCM forecasts at UCT include a downscaling of the GCM output to local (station) observations via a statistical technique developed by Professor Hewitson at UCT. This technique utilises Self Organising Maps (SOMs) to relate changes in synoptic state to changes in local climate variables such as rainfall and temperature. Incorporating changes in the response of the local climate variable within this 'post-processing' of the GCM data is a feasible option, though it would not include feedbacks on the large-scale synoptic circulation simulated by the GCM. Even so, given its current implementation and ability to disaggregate changes based on the synoptic forcing it is the preferred option.

4.1 Current GCMs used for seasonal forecasting at UCT

Seasonal forecasts at UCT are currently undertaken using 3 GCMs which along with their configuration characteristics are:

- CAM3 Community Atmospheric Model (NCAR, USA); currently 2° x 2.5° (in the future 1° x 1°, 26 vertical levels)
- HadAM3P (Met Office, UK); 1.25° x 1.875°, 19 vertical levels
- CAM-EULAG (Iowa State University, USA); in the future 1° x 1°, 26 vertical levels

All three models are run globally though CAM-EULAG is currently only run for research purposes. The motivation behind utilising many GCMs for the seasonal forecasts has not been to pick the best GCM but to know best way of combining the models' results for making multi-model ensemble forecasts, as well as looking for ways to improve the performances of the GCMs over Africa

Different SST boundary forcing methods are also being investigated for seasonal forecasts, including:

- Statistical SST Forecasts
- Using persisted SST Anomalies
- Slab Ocean Model
- Coupled-Ocean Model

For the purpose of the following discussion it will be assumed that a persisted SST (the simplest approach and therefore providing the lower boundary on predictability) approach is taken.

These models have been installed both on the computational cluster at CSAG and at the Centre for High-Performance Computing (CHPC). Several areas of work are progressing wrt these models, their implementation and their validation:

- Monthly production of the seasonal forecast using HadAM3P has been continuing. The method uses persisted SSTs to run a 10-member ensemble for 6 months into the future, the results of which are fed into the seasonal forecasts produced by the LRF group at SAWS. A 10 member ensemble using observed SSTs (AMIP type run for the 1960-2005 period) has been produced on the local cluster. Due to the increase in resolution (and appropriate change in the timestep) resulting in an 8 fold increase in computation these runs take approximately 45 days. Further hindcast forecasts using persisted SSTs are currently being generated for 4 seasons (SON, DJF, MAM, JJA) for the same 1960-2005 period. These will form the basis for deriving skill scores for the seasonal forecast;
- A 27-year (1980-2006) baseline simulation with CAM3 has been completed on the CHPC machines at low (2^o x 2.5^o) and high (0.9^o x 1.25^o) horizontal grid resolutions. For each resolution we produced 10 member ensembles. Similar simulations with CAM-EULAG will be completed.
- Development of skill and validation procedures. Climate forecasts on the UCT system before converting forecasts to a common format which are used by UKZN in their agrohydrological models (e.g. ACRU);
- Further development of methods for treating multi-model large ensembles to identify signal versus noise, and to develop probabilistic projections. This is the subject of several student theses;
- Statistical downscaling methods have been further refined. Development has focused on maintaining the spatio-temporal coherence of downscaled estimates of precipitation and temperature, which is particularly important for modelling of downstream hydrological impacts;

4.1.1 Sensitivity to horizontal resolution

Initial experiments with CAM3 were undertaken to determine the sensitivity of the model to horizontal resolution and a preliminary analysis (Figure 48) shows that CAM3 is only moderately sensitive to these changes. In terms of surface wind changes appear to be mostly associated with wind speed and less so with wind direction. Even so, this indicates changes in convergence which can result in slight changes in rainfall (Figure 48).

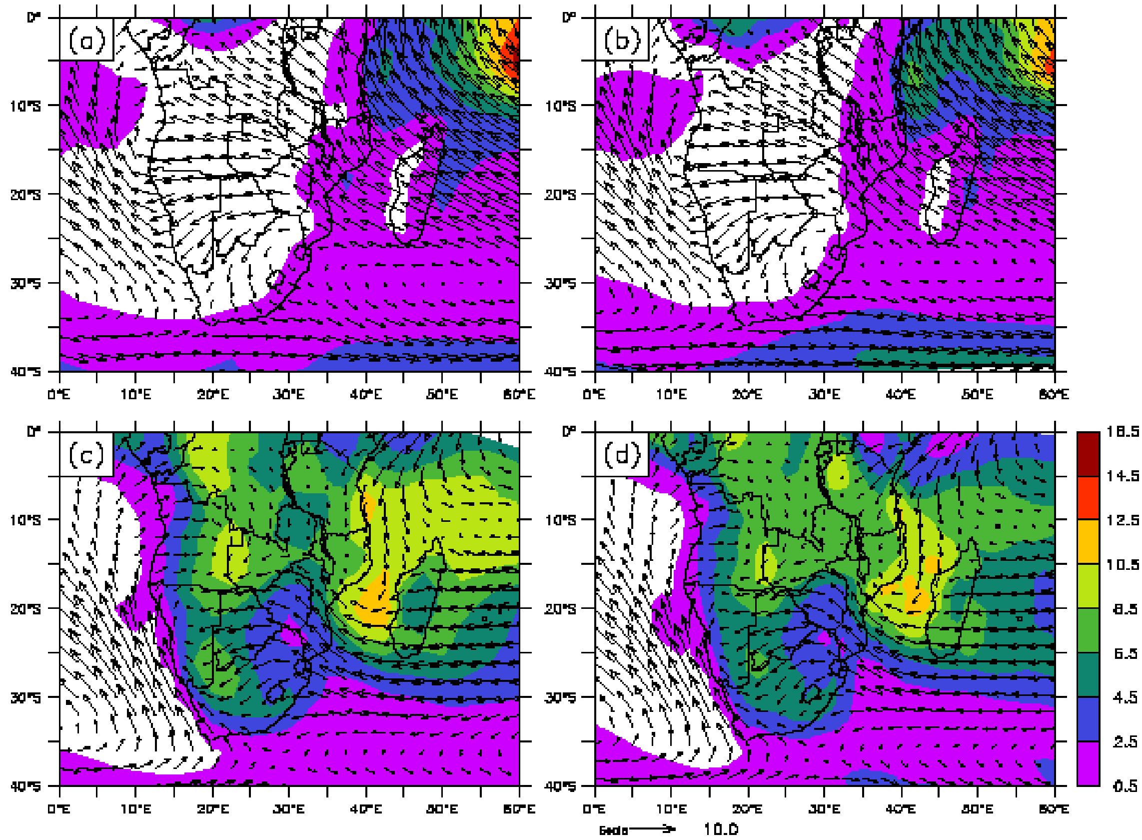

Figure 48: CAM3 Simulated (1980-1990) mean rainfall (shaded) and surface wind vectors (arrows) over Southern Africa at Low (2 x 2.5, latitude x longitude) and High (2 x 2.5, latitude x longitude) horizontal grid resolutions for June-August (JJA) and December-February (DJF) months. The left and right panels are for Low and high resolutions simulations, respectively, while the upper and lower panels are for JJA and DJF simulations, respectively.

4.1.2 Interannual variability

It is also important that the HadAM3P and CAM3 models simulate the observed interannual variability so the AMIP runs are being analysed to see how well each model simulates the annual and seasonal cycles. As an example Figure 49 below shows how the two models simulate the position of the anticyclones and sub tropical jet in relation to the observations;

4.2 <u>The statistical downscaling procedure</u>

The statistical downscaling procedure is applied to the GCM as a post-processing step. It takes the GCM predictor fields and uses them to define the synoptic circulation types found at a particular location where station observations of climate exist. The GCM predictor fields for defining the synoptic state are:

- 10 m U winds
- 10 m V winds
- 700 hPa U winds
- 700 hPa V winds
- 850-500 hPa lapse rate

- 2mtemperature anomaly
- 850 hPa relative humidity
- 850 hPa specific humidity

The first step is to use these same fields from the NCEP reanalysis (defining the observed state of the atmosphere), for training the statistical downscaling model; a Self Organising Map (SOM), which is a type of Artificial Neural Network (ANN), is used to decompose the 1979-2005 period into 99 archetype daily synoptic circulations at a particular location. The observed rainfall and temperature for each day is then used to define a probability density function (PDF) of rainfall/temperature for each synoptic type. The GCM predictor fields can then be used to map each day of the GCM data to a particular synoptic type and a value for rainfall/temperature can be sampled from the PDF associated with that synoptic type. This is achieved for both the GCM control climate (1960-2005, from the AMIP type runs)) and the GCM forecast fields and the forecast anomaly is taken as the downscaled GCM forecast minus the average of the downscaled GCM control climate.

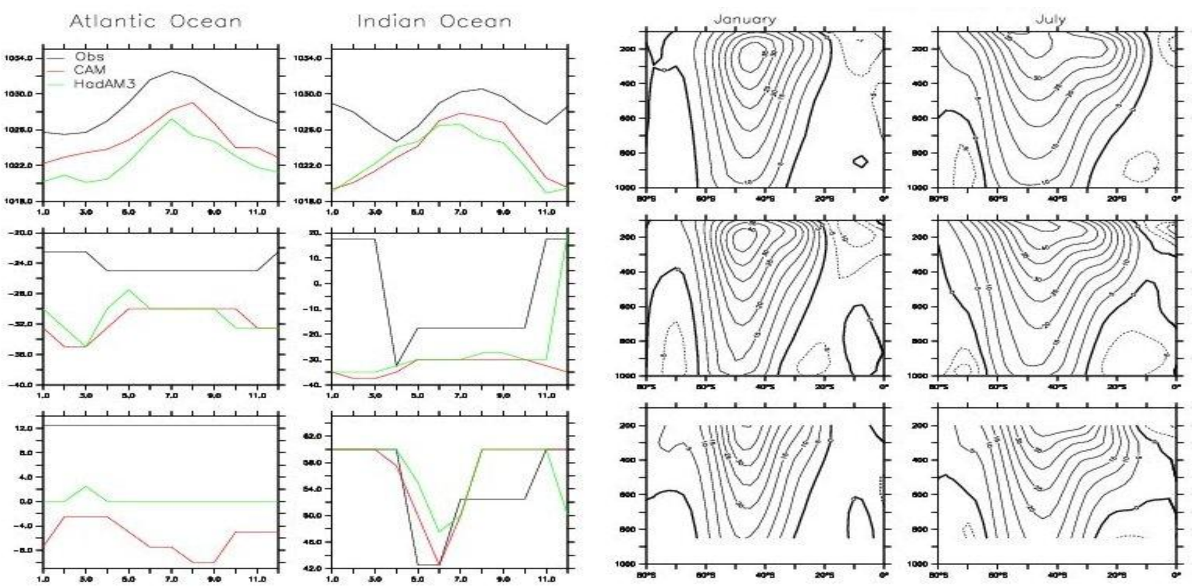

(a) (b)

Figure 49: CAM and HadAM3 position of (a) the anticyclones [rows are central pressure, latitude and longitude] and (b) sub-tropical jet [rows are NCEP, CAM3 and HadAM3]

There are several positive aspects of this procedure which have a bearing on the objectives of this project:

- The projected changes in rainfall and temperature are realistic when compared with observations;
- The method explicitly addresses the dependence on the daily synoptic state;
- Downscaled rainfall and temperature are produced for each day.

4.2.1 Using downscaled data to suggest changes in the start of the rains

The last aspect is important in that it allows the development of rainfall indices related to agricultural decision making e.g. the start of the rains. These indices have now been developed to include changes in potential evapotranspiration (see Figure 50 for an example related to changes in seasonal boundaries e.g. start, end and duration of the rainfall season – this example is for climate change but can be applied to seasonal forecasts as the procedure is the same).

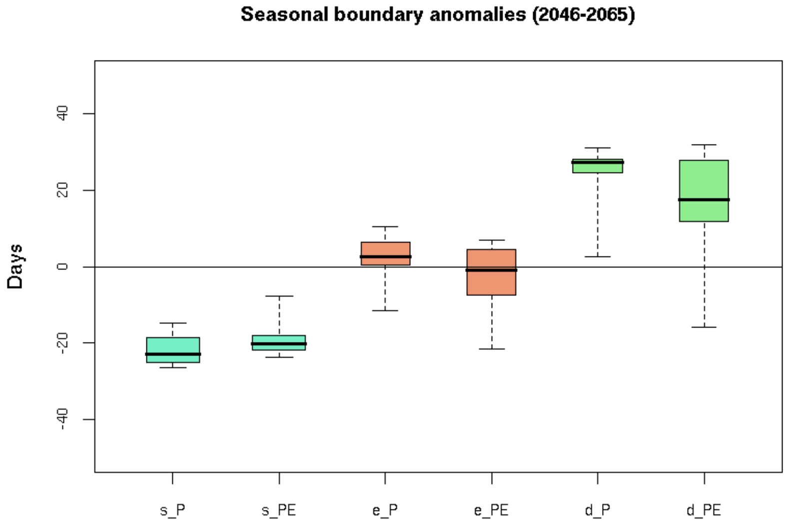

Figure 50: Changes in the start (s_*), end (e_*) and duration (d_*) of the season from 7 downscaled GCMs under anthropogenic climate change.

Other work related to this explores how planting dates (as defined by the start of the rains) can affect crop yields and how changes in the definition of the planting date can be used to offset forecast yields. The work is currently undertaken as part of a climate change project to understand how changes in rainfall and temperature affect water allocations in the Berg River. Whilst the focus is climate change the methods can easily be applied to seasonal forecasts. This work explores how planting dates and other management decisions, which are parameterised within crop models, can be used to maximise expected yields, which can lead to a prioritisation of management decisions given a climate forecast.

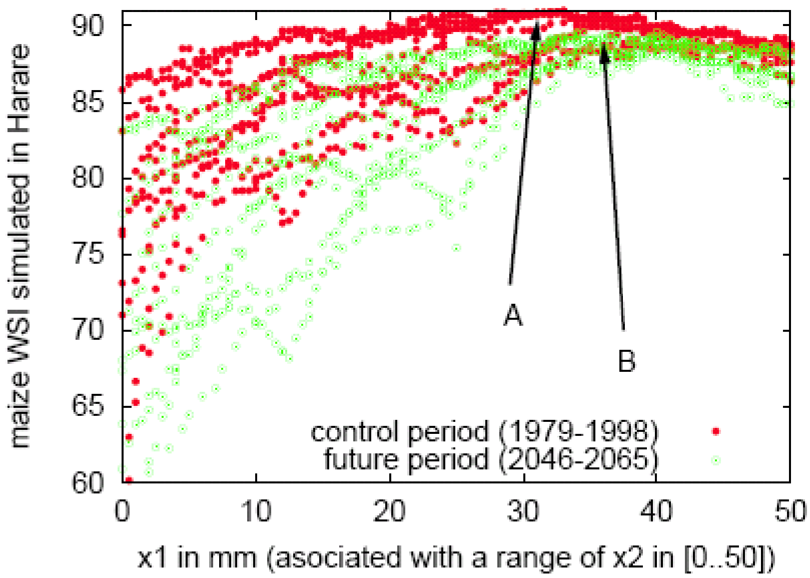

Figure 51: Simulated maize Water Satisfaction Index (WSI) given x1 (amount of rainfall before planting) for a range of downscaled climates during a control period (1979-1998) and future period (2046-2065). A and B show the change in optimal x1 for the control and future periods respectively.

Figure 51 shows the simulated maize Water Satisfaction Index (WSI) given x1 (amount of rainfall before planting) for a range of downscaled climates during a control period (1979-1998) and future period (2046-2065). A and B indicate the change in optimal x1 for the control and future periods respectively, which suggests that the criteria for planting (rainfall before planting) should be increased in a future climate in order to maximise WSI (used as a proxy for yield).

4.3 Including antecedent conditions of soil moisture, vegetation and aerosols in the current seasonal forecasting scheme

Section 4.2.1 shows how the start of the rains (and potentially other sub-seasonal and agriculturally relevant information) can be derived from the seasonal forecast. This will be implemented as part of the development of seasonal forecasts at CSAG in an effort to make the forecast information more relevant to end users and farmers. Note, however, that the skill of the forecast model also needs verification and will form part of the thesis of a PhD and an MSc student. Verification will be undertaken using a variety of skill scores including root mean square error, anomaly correlations and the Brier skill score.

The main problem to overcome is how to include the changes suggested by antecedent conditions in the current forecasting scheme. One way would be to develop transfer functions that alter the PDFs used in the statistical downscaling, based on known relationships between the antecedent conditions and the climate variable. This is not a simple task but could be achieved if the rainfall/temperature PDF is parameterised via a distribution function e.g. a Gamma/Weibull function for rainfall. Parameterising the PDF would then reduce the description of the PDF to 1 or 2 parameters e.g. mean and skew. Any transfer function that would allow these parameters to be estimated from antecedent conditions could then form an intermediate step in the current seasonal forecasting process. However, the only feasible method for estimating these transfer functions is to use the RCM data from the perturbation experiments; it would not be feasible to use observed data as it would not be possible to disaggregate changes due to other processes (e.g. changes in SST and other antecedent conditions), besides that due to a particular antecedent condition.

Unfortunately the limited set of experiments and the limited time span of these experiments may prove unfeasible for this purpose; given that a PDF is required for each of the 99 synoptic types this implies that with 10 years of simulation there will be approx 3650 days of simulation (which will be approx 37 days per synoptic type and less for some). This is likely a minimum and ideally we should have more. One alternative would be to derive the transfer function for a smaller set of synoptic types that span the continuum of possible states e.g. find transfer functions for say 12 synoptic types. More simply, it may even be more feasible to find a transfer function for each month of the year, which relates the mean monthly change in rainfall/temperature to the anomaly in antecedent conditions. This problem, while tractable, nevertheless requires a dedicated researcher to undertake the necessary steps and currently there is no one available on the project team. Therefore it is recommended that this form the basis of an MSc or PhD topic in the future.

5 Summary and future work

The project has successfully completed a range of modelling experiments, more than was originally envisaged. These experiments have clearly shown that antecedent conditions of soil moisture, vegetation and aerosols affect the southern African regional climate; more directly influencing surface temperature and indirectly rainfall. The resulting changes in climate are, however, dependent on the large-scale synoptic circulation and there is evidence that large-scale subsidence promotes the effect of the antecedent anomaly on the climate. Given that large-scale subsidence is associated with dry conditions, it is perhaps not surprising that antecedent anomalies that promote dry conditions demonstrate the most convincing changes in regional climate. This has implications for modelling extremes in climate, particularly dry extremes. It is also not surprising then that changes promoting dry conditions are more evident during spring (when anticyclonic circulations are more frequent) than later in the season when wetter synoptic conditions tend to dominate the regional climate response.

Even given these new insights into the regional climate and potential non-linear interactions there remain a number of unanswered scientific questions regarding the effect of antecedent conditions. Of particular immediate relevance are:

- the effect of spatial gradients in these antecedent fields;
- understanding how changes in antecedent conditions alter the distribution of energy and consequent development of convective rainfall systems;
- understanding to what extent the interaction between the large-scale and local perturbations is non-linear.

Additionally there is a need to develop a forecast methodology that can use observed changes in these antecedent conditions to improve current forecasts. This was not achieved in this project but we have suggested a way in which it could be achieved within the current forecast framework at CSAG and should be a goal within any future projects. Additionally we cannot discount the original suggestion of an ANN approach, though this should be clearly informed by well defined physical relationships.

5.1 Suggestions for further work

Given the findings of this project and the potential for improving climate forecasts several further avenues of exploration are considered potentially fruitful:

- Continue the current suite of modelling experiments, concentrating on the effects of these antecedent conditions on simulating the variability of the climate, particularly extremes and especially droughts. How do these antecedent conditions contribute to the frequency with which particular drought (or flood) thresholds are crossed ?
- Further experiments to determine the primary factors which affect the residence time of aerosols in the atmosphere. How do the different aerosol components respond and contribute to the localised changes in circulation ?
- Incorporating additional knowledge into current seasonal forecasting schemes and climate change projections. In particular, when should these factors be considered and when can they be largely ignored.

The overarching goal of this work would be to improve current forecasting schemes and to lead to better forecasts which will benefit society at large.

6 References

Anthes, R.A. 1977. A cumulus parameterization scheme utilizing a one-dimensional cloud model. *Mon. Wea. Rev.*, 105, 270–286.

Abel, S.J., Highwood, E.J., Haywood, J.M., Stringer, M.A. 2005. The direct radiative effect of biomass burning aerosols over southern Africa. *Atmospheric Chemistry & Physics*, 5, 1999–2018.

Ackermann, I.J., Hass, H., Memmesheimer, M., Ebel, A., Binkowski, F.S., Shankar, U. 1998. Modal aerosol dynamics model for Europe: Development and first applications. *Atmos. Environ,* 32, 2981–2999.

Alfaro, S.C., Gomes, L. 2001. Modeling mineral aerosol production by wind erosion: Emission intensities and aerosol size distributions in source areas. *J. Geophys. Res.* 106 (D16), 18075-18084.

Binkowski, F.S., Shankar, U. 1995. The Regional Particulate Matter Model 1. Model description and preliminary results. *J. Geophys. Res*., 100 (D12), 26,191–26,209.

Betts, A.K., Miller, M.J. 1993. The Betts-Miller scheme. Chapter in *The representation of cumulus convection in numerical models of the atmosphere*. Eds. Emanuel, K.A., Raymond, D.J. American Meteorological Society.

Bond, W.J., Midgley, G.F., Woodward, F.I. 2003. What controls South African Vegetation – climate or fire? *South African Journal of Botany*, 69(1), 1-13.

Caya, D., Biner, S. 2004. Internal variability of RCM simulations over an annual cycle. *Climate Dynamics,* 22, 33-46.

Charney, J.G. 1975. Dynamics of deserts and drought in the Sahel. *Quarterly Journal of the Royal Meteorological Society,* 101, 193-202.

Charney, J.G., Quirk, W.J., Chow, S., Kornfield, J. 1977. A comparative study of the effects of albedo change on drought in semi-arid regions. *Journal of the Atmospheric Sciences,* 34, 1366-1385.

Chen, F., Dudhia, J. 2001. Coupling an advanced land surface-hydrology model with the Penn State-NCAR MM5 modeling system. Part I: Model implementation and sensitivity. *Monthly Weather Review,* 129, 569-585.

Christensen, O.B., Gaertner, M.A., Prego, J.A., Polcher, J. 2001. Internal variability of regional climate models. *Climate Dynamics,* 17, 875-887.

Cramer, W., Bondeau, A., Woodward, F.I., Prentice, C.I., Betts, R.A., Brovkin, V., Cox, P.M., Fisher, V., Foley, J.A., Friend, A.D., Kucharik, C., Lomas, M.R., Ramankutty, N., Sitch, S., Smith, B., White, A., Young-Molling, C. 2001. Global response of terrestrial ecosystem structure and function to CO2 and climate change: results from six dynamic global vegetation models. *Global Change Biology,* 7, 357-373.

Crutzen, P.J., Andreae, M.O. 1990. Biomass Burning in the Tropics: Impact on Atmospheric Chemistry and Biogeochemical Cycles. *Science*, 250(4988), 1669–1678. doi:10.1126/science.250.4988.1669.

Deardoff, J.W. 1978. Efficient prediction of ground surface temperature and moisture with inclusion of a layer of vegetation. *J. Geophys. Res.,* 83, 1889-1903.

Dickinson, R.E., Kennedy P.J., Henderson-Sellers, A., Wilson, M. 1986. Biosphere-Atmosphere Transfer Scheme (BATS) for the NCAR Community Climate Model, *Tech. Rep. TN-275+STR*, National Center for Atmospheric Research, Boulder, Colorado, US.

Dickinson, R.E., Henderson-Sellers, A., Kennedy, P.J. 1993. Biosphere-atmosphere transfer scheme (BATS) version 1e as coupled to the ncar community climate model, *Tech. rep.*, National Center for Atmospheric Research, Boulder, Colorado, US.

Dickinson, R.E., Henderson-Sellers, A. 1988. Modeling tropical deforestation: A study of GCM land-surface parameterizations. *Quarterly Journal of the Royal Meteorological Society,* 114. 439-462.

Dirmeyer, P.A., Shukla, J. 1994. Albedo as a modulator of climate response to tropical deforestation. *Journal of Geophysical Research,* 99(D10), 20, 863-20,877

Emanuel, K.A. 1991. A scheme for representing cumulus convection in large-scale models. *J. Atmos. Sci.*, 48(21), 2313–2335.

Giorgi, F., Chameides, W.L. 1986. 'Rainout Lifetimes of Highly Soluble Aerosols', *J. Geophys. Res*., 91, 14367–14376.

Giorgi, F. 1989. ‘Two-Dimensional Simulations of Possible Mesoscale Effects Nuclear War Fires. I: Model Description’, *J. Geophys. Res*., 94, 1127–1144.

Giorgi, F., Bates, G.T., Nieman, S.J. 1993a. The multi-year surface climatology of a regional atmospheric model over the western united states. *J. Climate*, 6, 75–95.

Giorgi, F., Marinucci, M.R., Bates, G.T. 1993b. Development of a second generation regional climate model (RegCM2) I: Boundary layer and radiative transfer processes. *Mon. Wea. Rev.*, 121, 2794–2813.

Giorgi, F., Bi, X.Q., Qian, Y. 2003a. Indirect vs. direct effects of anthropogenic sulfate on the climate of east asia as simulated with a regional coupled climate-chemistry/aerosol model. *Climatic Change*, 58, 345–376.

Giorgi, F., Francisco, R., Pal, J.S. 2003b. Effects of a subgrid-scale topography and land use scheme on the simulation of surface climate and hydrology. part 1: Effects of temperature and water vapor disaggregation. *Journal of Hydrometeorology*, 4, 317–333.

Giorgi, F, Bi X. 2000. A study of internal variability of a regional climate model. *Journal of Geophysical Research,* 105(D24), 29503-29521.

Grell, G. 1993. Prognostic evaluation of assumptions used by cumulus parameterizations. *Mon. Wea. Rev.*, 121, 764–787.

Grell, G.A., Dudhia, J., Stauffer, D.R. 1994. A description of the fifth-generation Penn State/NCAR Mesoscale Model (MM5). *NCAR Technical Note NCAR/TN-3981STR*, 117 pp.

Gutman, G., Ignatov, A. 1998. The derivation of the green vegetation fraction from NOAA/AVHRR data for use in numerical weather prediction models. *International Journal of Remote Sensing,* 19, 1533–1543.

Hachigonta, S., Reason, C.J.C., Tadross, M. 2008. An analysis of onset date and rainy season duration over Zambia. *Theoretical & Applied Climatology*, 91, 229-243. doi: 10.1007/s00704-007-0306-4.

Haywood, J.M., Roberts, D.L., Slingo, A., Edwards, J.M., Shine, K.P. 1997. ‘General Circulation Model Calculations of the Direct Radiative Forcing by Anthropogenic Sulfate and Fossil-Fuel Soot Aerosol’. *J. Climate*, 10, 1562–1577.

Haywood, J.M., Shine, K.P. 1997. ‘Multi-Spectral Calculations of the Direct Radiative Forcing of Tropospheric Sulphate and Soot Aerosols Using a Column Model’, *Quart. J. R. Meteorol. Soc*., 123, 1907–1930.

Haywood, J.M., Osborne, S.R., Francis, P.N., Keil, A., Formenti, P., Andreae, M.O., Kaye, P.H. 2003. The mean physical and optical properties of regional haze dominated by biomass burning aerosol measured from the C-130 aircraft during SAFARI 2000. *J. Geophys. Res.*, 108(D13), 8473–. doi:10.1029/2002JD002226.

Helas, G., Pienaar, J.J. 1996. The influence of vegetation fires on the chemical composition of the atmosphere. *S. Afr. J. Sci.*, 92(3), 132–136.

Hewitson, B., Crane, R. 2002. Self-organizing maps: Applications to synoptic climatology. *Climate Research*, 22, 13–26.

Holtslag, A.A.M., de Bruijn, E.I.F., Pan, H-L. 1990. A high resolution air mass transformation model for short-range weather forecasting. *Mon. Wea. Rev.*, 118, 1561–1575.

Hong, S-Y, Pan, H-L. 1996. Nonlocal boundary layer vertical diffusion in a mediumrange forecast model. *Monthly Weather Review,* 124, 2322-2339.

Hsie, E.Y., Anthes, R.A., Keyser, D. 1984. Numerical simulation of frontogenisis in a moist atmosphere. *J. Atmos. Sci.*, 41, 2581–2594.

Kalnay, E. and 21 others. 1996. The NCEP/NCAR 40-year reanalysis project. *Bulletin of the American Meteorological Society,* 77(3), 437–471.

Kiehl, J.T., Hack, J.J., Bonan, G.B., Boville, B.A., Breigleb, B.P., Williamson, D., Rasch, P. 1996. Description of the ncar community climate model (CCM3), *Tech. Rep. NCAR/TN-420+STR*, National Center for Atmospheric Research, Boulder, Colorado, US.

Keil, A., Haywood, J.M. 2003. Solar radiative forcing by biomass burning aerosol particles during SAFARI 2000: A case study based on measured aerosol and cloud properties. *J. Geophys. Res.*, 108(D13), 8467–. doi:10.1029/2002JD002315.

Lin, X, Randall, D.A, Fowler, L.D. 2000. Diurnal variability of the hydrologic cycle and radiative fluxes comparisons between observations and a GCM. *J. Climate*, 13**(**23), 4159-4179.

Marticorena, B., Bergametti, G. 1995. Modeling the atmospheric dust cycle. Part 1: Design of soil-derived dust emission scheme. *J. Geopys. Res., 100*(D8), 16415-16430.

Martiny, N., Richard, Y., Camberlin, P. 2005. Interannual persistence effects in vegetation dynamics of semi-arid Africa. *Geophys. Res. Lett.*, 32, L24403, doi:10.1029/2005GL024634.

Matsui, T., Lakshmi, V., Small, E. 2005. The effects of satellite-derived vegetation cover variability on simulated land–atmosphere interactions in the NAMS. *Journal of Climate,* 18, 21-40.

Maynard, K., Royer, J-F. 2004. Effects of “realistic” land-cover change on a greenhousewarmed African climate. *Climate Dynamics,* 22, 343-358.

Myhre, G., Stordal, F., Restad, K., Isaksen, I.S.A. 1998. ‘Estimation of the Direct Radiative Forcing Due to Sulfate and SSO Aerosols’. *Tellus*, 50B, 463–477.

New, M.G., Hulme, M., Jones, P.D. 1999. Representing twentieth century space-time climate variability. Part I: Development of a 1961-1990 mean monthly terrestrial climatology. *Journal of Climate,* 12, 829-856.

New, M.G., Hulme, M., Jones, P.D. 2000. Representing twentieth century space-time climate variability. Part II: development of 1901-96 monthly grids of terrestrial surface climate. *Journal of Climate,* 13, 2217-2238.

Odum, J.R., Hoffmann, T., Bowman, F., Collins, D., Flagan, R.C., Seinfeld, J.H. 1996. Gas/particle partitioning and secondary organic aerosol yields. *Environ. Sci. Technol.*, 30, 2580–2585.

Pal, J.S., Small, E.E., Eltahir, E.A.B. 2000. Simulation of regional-scale water and energy budgets: Representation of subgrid cloud and precipitation processes within RegCM. *J. Geophys. Res.*, 105(D24), 29579–29594.

Pal, J., Eltahir, E.A.B. 2001. Pathways Relating Soil Moisture Conditions to Future Summer Rainfall within a Model of the Land-atmosphere System. *Journal of Climate*, 14(6), 1227-1242.

Pal, J.S, and Co-authors. 2007. The ICTP RegCM3 and RegCNET: Regional Climate Modeling for the Developing World. *Bull. of the Amer. Met. Soc*. 88**,** 1395-1409.

Pitman, A.J., Durbidge, T.B., Henderson-Sellers, A., McGuffie, K. 1993. Assessing climate model sensitivity to prescribed deforested landscapes. *International Journal of Climatology,* 13, 879-898.

Pöschl, U., Fehrenbach, T., Franze, T., Mikhailov, E., McKeon, U., Schauer, C., Zerrath, A. 2005. Carbonaceous aerosol components: chemical composition, reactivity, and hygroscopicity (CARBAERO). *Geophys. Res. Abs.*, 7(05164), 1607–7962.

Privette, J.L., Roy, D.P. 2005. Southern Africa as a remote sensing test bed: SAFARI 2000 Special Issue overview. *Int. J. Rem. Sens.*, 19, 4141-4158.

Qian, Y., Giorgi, F., Huang, Y., Chameides, W.L., Luo, C. 2001. 'Simulation of Anthropogenic Sulfur over East Asia with a Regional Coupled Chemistry-Climate Model'. *Tellus*, 53B, 171–191.

Randerson, J.T., van der Werf, G.R., Giglio, L., Collatz, G.J. Kasibhatla, P.S. 2007. Global Fire Emissions Database, Version 2 (GFEDv2.1). Data set. Available on-line [http://daac.ornl.gov/] from Oak Ridge National Laboratory Distributed Active Archive Center, Oak Ridge, Tennessee, U.S.A. doi:10.3334/ORNLDAAC/849.

Reason, C.J.C., Hachigonta, S., Phaladi, R.F. 2005. Interannual variability in rainy season characteristics over the Limpopo region of southern Africa. *Int J Climatol*, 25(14), 1835–1853.

Richard, Y., Martiny, N., Fauchereau, N., Reason, C., Rouault, M., Vigaud, N., Tracol, Y. 2008. Interannual memory effects for spring NDVI in semi-arid South Africa, *Geophys. Res. Lett.*, 35, L13704, doi:10.1029/2008GL034119.

Rosenfeld, D., Feingold, G. 2003. Explanation of discrepancies among satellite observations of the aerosol indirect effects. *Geophys. Res. Lett.*, 30(14), L1776. doi:10.1029/2003GL017684.

Saxena, P., Hudischewskyj, A.B., Seigneur, C., Seinfeld, J.H. 1986. A comparative study of equilibrium approaches to the chemical characterization of secondary aerosols. *Atmos. Env.*, 20, 1471-1483.

Schell, B., Ackermann, I.J., Hass, H., Binkowski, F.S., Ebel, A. 2001. Modeling the formation of secondary organic aerosol within a comprehensive air quality model system. *J. Geophys. Res.*, 106, 28275-28293.

Schmid, B. 2003. Coordinated airborne and spaceborne and ground-based measurements of massive thick aerosol layers during the dry season in southern Africa. *J. Geophys. Res.*, 108(D13), 8496–. doi:10.1029/2002JD002297.

Scholes, R.J., Annegarn, H., Marufu, L. 2001. Emissions From Fires in Southern Africa. *AGU Fall Meeting Abstracts*, pages C5+. Provided by the SAO/NASA Astrophysics Data System.

Scholes, R.J., Kendall, J., Justice, C.O. 1996. The quantity of biomass burned in southern Africa. *J. Geophys. Res.*, 101(D19), 23667–23676. doi:10.1029/96JD01623.

Stockwell, WR., Middleton, P., Chang, J.S., Tang, X. 1990. The second generation regional acid deposition model chemical mechanism for regional air quality modeling. *J. Geophys. Res.*, 95, 16343-16367.

Stockwell, W.R., Kirchner, F., Kuhn, M., Seefeld, S. 1997. A new mechanism for regional atmospheric chemistry modeling. *J. Geophys. .Res.*, 102, 15847-25879.

Swap, R., Garstang, M., Macko, S.A., Tyson, P.D., Maenhaut, W., Artaxo, P., Kallberg, P. Talbot, R. 1996. The long-range transport of southern African aerosols to the tropical South Atlantic. *J. Geophys. Res.*, 101, 23777-23791.

Swap, R.J., Annegarn, H.J., Suttles, J.T., King, M.D., Platnick, S., Privette, J.L., and Scholes, R.J. 2003. Africa burning: A thematic analysis of the Southern African Regional Science Initiative (SAFARI 2000). *J. Geophys. Res.*, 108(D13), 8465–. doi:10.1029/2003JD003747.

Tadross, M., Hewitson, B.C., Usman, M.T. 2005. The inter-annual variability of the onset of the growing season over southern Africa. *J. Climate*, 18(16), 3356–3372.

Tadross, M.A., Gutowski, W.J., Hewitson, B.C., Jack, C., New, M. 2006. MM5 simulations of interannual change and the diurnal cycle of southern African regional climate. *Theoretical and Applied Climatology,* 86, 63-80.

Woodward, F.I., Smith, T.M., Emanuel, W.R. 1995. A global land primary productivity and phytogeography model. G*lobal Biogeochemical Cycles,* 9, 471-490.

Woodward, F.I., Lomas, M.R. 2004. Vegetation dynamics – simulating responses to climatic change. *Biological Reviews,* 79, 643-670.

WRF model. *Atmospheric Environment*, 39(37):6957–6975. doi:10.1016/j.atmosenv.2005.04.027.

Zeng, X., Zhao, M., Dickinson, R.E. 1998. Intercomparison of bulk aerodynamic algorithms for the computation of sea surface fluxes using toga coare and tao data. *J. Climate*, 11, 2628–2644.

Zunckel, M., Robertson, L., Tyson, P.D. Rodhe, H. 2000. Modelled transport and deposition of sulphur over Southern Africa. *Atmos. Env.*, 34, 2797-2808.

Appendix A: Student involvement, theses and capacity building

There has been extensive student involvement within this project, particularly with respect to setting up and running the RCMs (WRF and MM5). Tasks included:

- Setting up and installing the models on both the local computing cluster at CSAG and the Centre for High Performance Computing (CHPC);
- Writing computer code to manipulate the boundary conditions (vegetation, aerosol and sea surface temperature distributions) with which the RCMs are forced in the experiments;
- Running the RCMs and quality control of the model output;
- Coding analyses of the model output and figure plotting;
- Physical interpretation of the model output, figures and implications for the regional climate;

This has led to the development of programming skills across a range of languages, including: C, FORTRAN, Python and R. The interpretative component of the work required skill development in meteorology, climatology, the interpretation of international research papers and projects, as well as scientific writing and comprehension.

Additionally much of the analyses presented in this report was conducted by these students, under the supervision of the project PI, and will or have formed the basis for several PhD theses. These theses and the corresponding students are listed in the table below:

Igor Oliveira, Marshall Mdoka, Fiona Tummon, Genito Maure, Neil MacKellar, Nana Browne, Oliver Crespo, Sepo Hachigonta

Student name	Registered degree	Thesis title	Contribution to report	Status
Igor Oliveira	PhD	Vegetation influences on southern African climate	Section 2.5.2 and 2.5.3	Writing up
Marshall Mdoka	PhD	Soil moisture-atmosphere dynamics over southern Africa	Section 2.4.2	Writing up
Fiona Tummon	PhD	Aerosol and land-use change feedbacks on southern African climate	Section 2.6.2	Writing up
Genito Maure	PhD	The effect of biomass burning on southern African climate	Section 2.6.1	Data analyses
Neil MacKellar	PhD	Simulating the effects of land-surface change on southern Africa's climate	Section 2.4.1	Finished
Nana Browne	PhD	Multi-model seasonal forecasting of climate over southern Africa	Section 4.1	Writing up
Sepo Hachigonta	PhD	Changes in maize water requirements in a future climate	Section 4.2.1	Submitted

All these students, and the project PI, have presented these findings at international and local conferences. Many of the findings are currently in submission or published as journal papers, including:

Mackellar, NC, Tadross MA, Hewitson BC (2009). Effects of vegetation map change in MM5 simulations of southern Africa's summer climate. International journal of climatology. 29. 885-898. DOI: 10.1002/joc.1754

Mackellar, NC, Tadross MA, Hewitson BC (2009). Synoptic-based evaluation of climatic response to vegetation change over southern Africa. International journal of climatology. DOI: 10.1002/joc.1925

Tadross M., Suarez P., Lotsch A., Hachigonta S., Mdoka M., Unganai L., Lucio F., Kamdonyo D., Muchinda M. (2009) Growing-season rainfall and scenarios of future change in southeast Africa:

implications for cultivating maize. Climate Research. Vol. 40. 147-161. DOI: 10.3354/cr00821.

Hachigonta S., Reason C.J.C., Tadross M. (2008) An analysis of onset date and rainy season duration over Zambia. Theoretical & Applied Climatology. 91. p 229-243. doi: 10.1007/s00704-007-0306-4.

Simulation of the climatic impacts of the natural aerosol loading over southern Africa during the biomass burning season using RegCM3. F. Tummon, F. Solmon, C. Liousse and M. Tadross. Submitted Journal of Geophysical Research.

Seasonal forecasting over southern Africa: Simulation of General Circulation features. Nana A. K. Browne, Babatunde J. Abiodun, Mark Tadross, Bruce Hewitson. Submitted international journal of climatology

Appendix B: Workshop answers to the question "How does the onset vary spatially, and according to sectors?" and "Does anything other than rainfall determine/affect the start of a growing season?"

Sector	Sub-region	Typical onset date	planting dates	Earliest onset date	Latest onset date	Amount of rainfall during onset	Other important onset variables
Water Resources	Catchment Management Areas -DWAF						Extreme events are important, can carry over 4-5 years so onset mostly important after long droughts, planning purposes and scheduling
Maize	Highveld	earlier in the east	Bloemfontein - late Nov/early Dec - avoid January drought (potential with short cultivar to plant in Jan). September-December (earlier in the east)	October/November	10th January - second half too late	frequency +intensity depends on aridity of region	Heat units
	Lowveld		Mpumalanga	no frost - can plant in September	10th January - second half too late		
	Eastern Seaboard			September	end of December		Heat units during late planting
	Northwest (Highveld)		November-December(later than rest of highveld)	15 September - further north gets later	10th January - second half too late		
						heavy storms are undesirable e.g. getting farm equipment into field and large runoff	Farmers like to plant after 15th September when 2+ days of general rainfall - useful to categorise 2 soil categories - sandy/clay
Sugar							Mostly around equipment - rainfall at end of season is more important
Livestock							Fire risk, when to move stock between winter and summer regions. Parasites on livestock after rain (quite a bit later in the season). Wet and cold combinations for Angora goats.
Savanna/eco-systems	Arid	20 mm					Similar to water resources - not so important for indigenous plants and systems not providing resources. Savanna systems have on average 9 mm per event - moist savanna such as kruger). Potential importance for fire risk - dependent on biomass and fuel load
	Moist (east of Thabazimbi)	20 mm =170 mm penetration - dry in 4-5 days		see above		400 mm soil wetting dry in 5-10 days - very soil dependent. Trees and grasses green at very different rates. Greenup of grass keeps getting higher to maximum in February. LAI in trees maximises earlier REALLY DOESN'T DEPEND SO MUCH ON THE AMOUNT	